NASA TM X-53598

FACILITY FORM 602

N67-30160

(ACCESSION NUMBER)

(THRU)

98

(PAGES)

(CODE)

TMX-53598

(NASA CR OR TMX OR AD NUMBER)

14

(CATEGORY)

# DEVELOPMENT OF MECHANIZED ULTRASONIC SCANNING SYSTEM

By Raymond Evans and J. A. MacDonald
   Quality and Reliability Assurance Laboratory

**NASA**

*George C. Marshall*

*Space Flight Center,*

*Huntsville, Alabama*

# DEVELOPMENT OF MECHANIZED
# ULTRASONIC SCANNING SYSTEM

By

Raymond Evans
and
J. A. MacDonald

George C. Marshall Space Flight Center

Huntsville, Alabama

## ABSTRACT

This report presents data related to the development and testing
of a mechanized ultrasonic scanning system for testing butt welds in large
aluminum tanks. A significant phase of the project was the design and
development of a water column probe. The employment of the water
column probe in conjunction with an electronic pulser and recording unit
permitted welds to be tested in the same relative time as required for
semiautomatic radiography as utilized at the Marshall Space Flight
Center. The results of the ultrasonic scan are recorded for the detection
and evaluation of flaw content. The basic configuration of the system
along with recordings of various types of flaws are presented and correlated
with radiographic and metallographic data. Basic ultrasonic equations are
used to demonstrate the practicability for using the technique in testing
butt welds.

**NASA - GEORGE C. MARSHALL SPACE FLIGHT CENTER**

NASA - GEORGE C. MARSHALL SPACE FLIGHT CENTER

TECHNICAL MEMORANDUM TM X-53598

# DEVELOPMENT OF MECHANIZED
# ULTRASONIC SCANNING SYSTEM

By

Raymond Evans
and
J. A. MacDonald

## TABLE OF CONTENTS

# TABLE OF CONTENTS (Continued)

## LIST OF ILLUSTRATIONS

## LIST OF ILLUSTRATIONS (Continued)

# LIST OF ILLUSTRATIONS (Continued)

LIST OF ILLUSTRATIONS (Continued)

LIST OF TABLES

# UNUSUAL TERMS

A-SCAN PRESENTATION - A presentation on a cathode ray tube (CRT)
representing the sound energy reflected back to the transducer
by a material surface or discontinuity.  The presentation is in
terms of amplitude of sound level reflected versus time for
sound to travel from the front surface of the part to the reflecting
surface or discontinuity (flaw).  This presentation is graphically
expressed in figure 1.

At a given sensitivity (gain) setting, the amplitude of the sound
reflection indication (pip) on the CRT is determined by the
strength of the signal generated by the reflected sound wave.
The larger the discontinuity, the higher (greater the amplitude)
the pip.  Thus, the A-scan presentation on the CRT screen dis-
plays two types of information; the depth of the discontinuity
in the test part and the relative size of the discontinuity.  The
A-scan presentation (figure 1) may then be interpreted as shown
in figure 2, where dimensions A, B, and C are defined as follows:

(1)     A is the material (test part) thickness.

(2)     B is the  depth of flaw.

(3)     C is the relative size of flaw.

Relative size is determined by comparing the magnitude of flaw
(pip) to the magnitude of the pip obtained from a known artificial
defect at a known depth in a reference block of like material.

A-SCAN RECORDING - The recording of an A-scan presentation on a
Brush Recorder chart.

ANGLE OF INCIDENCE - The angle of incidence is the beam angle with
respect to a normal to the surface.  (See figure 3.)

ANGLE OF REFRACTION - The angle of refraction is the beam angle
in the material with respect to a normal to the surface.  (See
figure 3.)

BOUNCE SHOT - An angle beam reflection technique in which the shear wave beam is bounced off the bottom surface of the test plate and then up to the weld. (See figure 4.)

CALIBRATION BLOCK - The International Institute of Welding (IIW) calibration block (figure 5) provides known distances and angular relationships for determining the unknown beam characteristics of a probe or transducer. The centerline of the beam, when leaving from the probe or transducer, can be determined and calibrated by properly utilizing the calibration block. The calibration block is also used to determine and calibrate the angle of refraction of the ultrasonic beam after entering the material.

CONCENTRATED BEAM - The principal sound beam. The zone of maximum sound intensity located in the center of the ultrasonic beam. (See figure 6.)

COUPLANT - A material, usually a liquid, placed between the probe and the test surface which acts as a media for transmitting ultrasonic energy. Water, oil, and glycerine are commonly used as couplants.

DIRECT SHOT - An angle beam reflection technique in which the shear waves are transmitted, at an angle to the surface, directly to the weld area.

ELECTRONIC GATING - The fixing of a specific area on the horizontal axis of the CRT so that different depth increments of the weld may be tested and recorded individually. Gating is also used to eliminate the spurious effect of surface scratches and weld bead edges.

LACK-OF-PENETRATION - The failure of weld material to fully penetrate and fuse two pieces of metal together. The thickness (T) and width (W) are shown in figure 7.

LONGITUDINAL WAVES - An ultrasonic wave in which particle displacement is in the same direction as the wave is traveling.

REFERENCE PLATE FOR BEAM SIZE - An aluminum plate, as shown in figure 8, 0.800-inch thick with a 0.060-inch diameter by 0.030-inch deep flat-bottomed hole drilled in the bottom surface. The distance the probe moves is measured in both the X and Y directions as the beam is moved across the hole in the plate by observing the pulse-echo return from the hole on the CRT presentation.

SHEAR WAVE - An ultrasonic wave in which the particle displacement is at right angles to the direction of propagation of the wave.

SQUARE BUTT WELD - A butt weld made where two pieces of metal are joined and the mating surfaces have been machined square, or at right angles to the surface.

STANDARD ANGLE BEAM REFERENCE BLOCK - The reference block (figure 9) is made of the same material as the test specimen. A series of flat-bottomed test holes are drilled in the reference block at graduated depths at the correct angle so that the flat bottoms of the holes are perpendicular to the ultrasonic beam. The flat-bottomed holes, 0.067 inch in diameter, are used to set up the CRT display in terms of depth in the material, whereas the flat-bottomed holes, 0.047 inch in diameter, are used to set the system's sensitivity level. Separate blocks having all holes the same size are used for each setup requirement.

U-JOINT BUTT WELD - A butt weld made along a U-shaped groove, machined out of two pieces of metal, at the point of their joining. (See figure 10.)
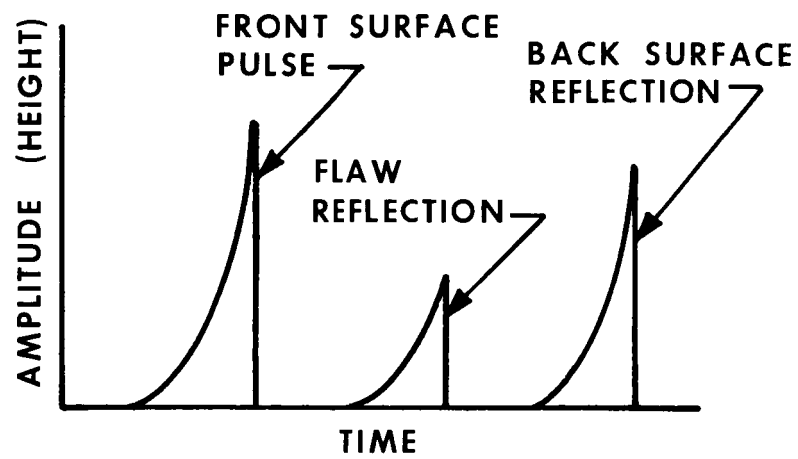
Figure 1.  A-Scan Presentation
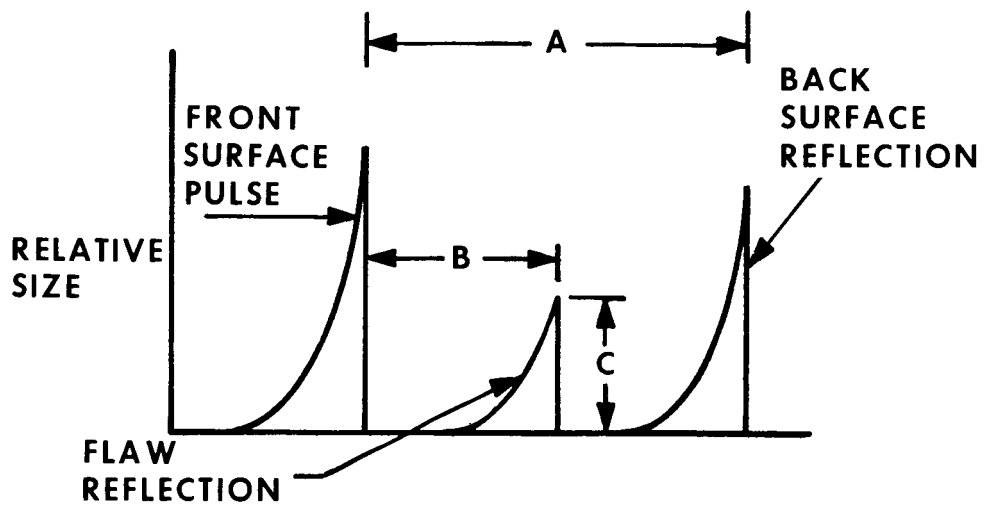


Figure 2.  A-Scan Presentation Interpretation

CENTER OF
EFFECTIVE BEAM

-ANGLE OF INCIDENCE

- LINE NORMAL
  TO SURFACE

ANGLE OF REFRACTION
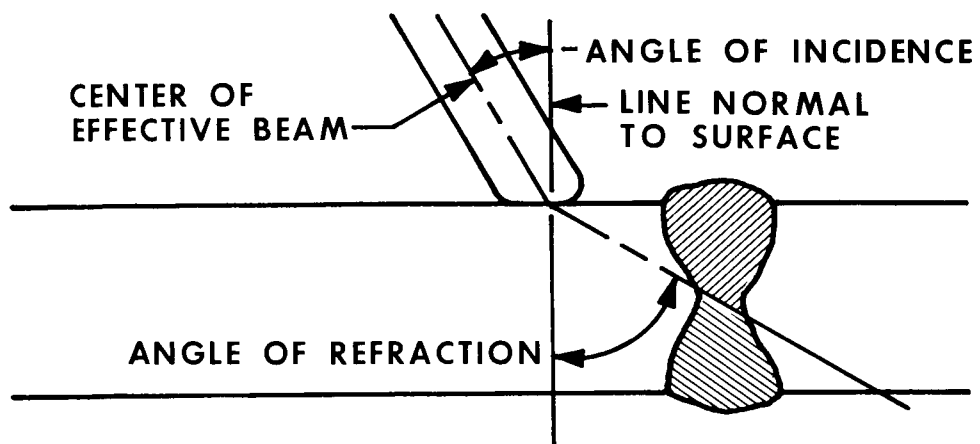
Figure 3.  Angular Relationships



TOP SURFACE
OF PLATE

BOTTOM SURFACE
OF PLATE
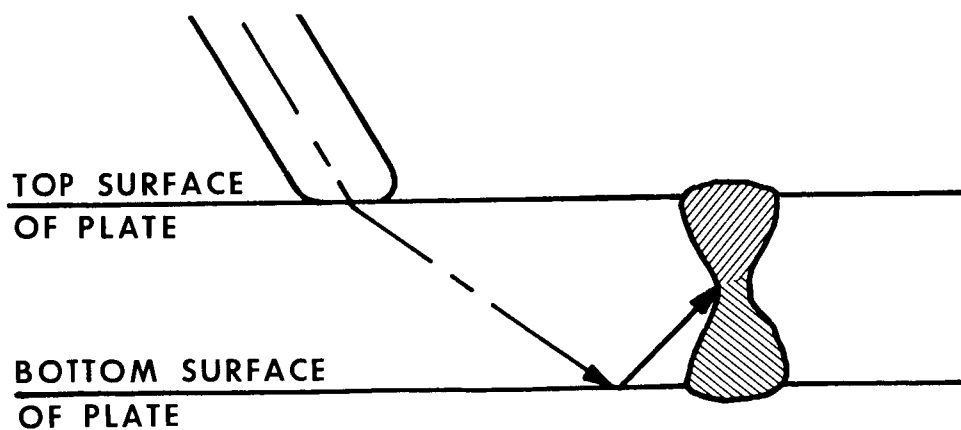
Figure 4.  Bounce Shot
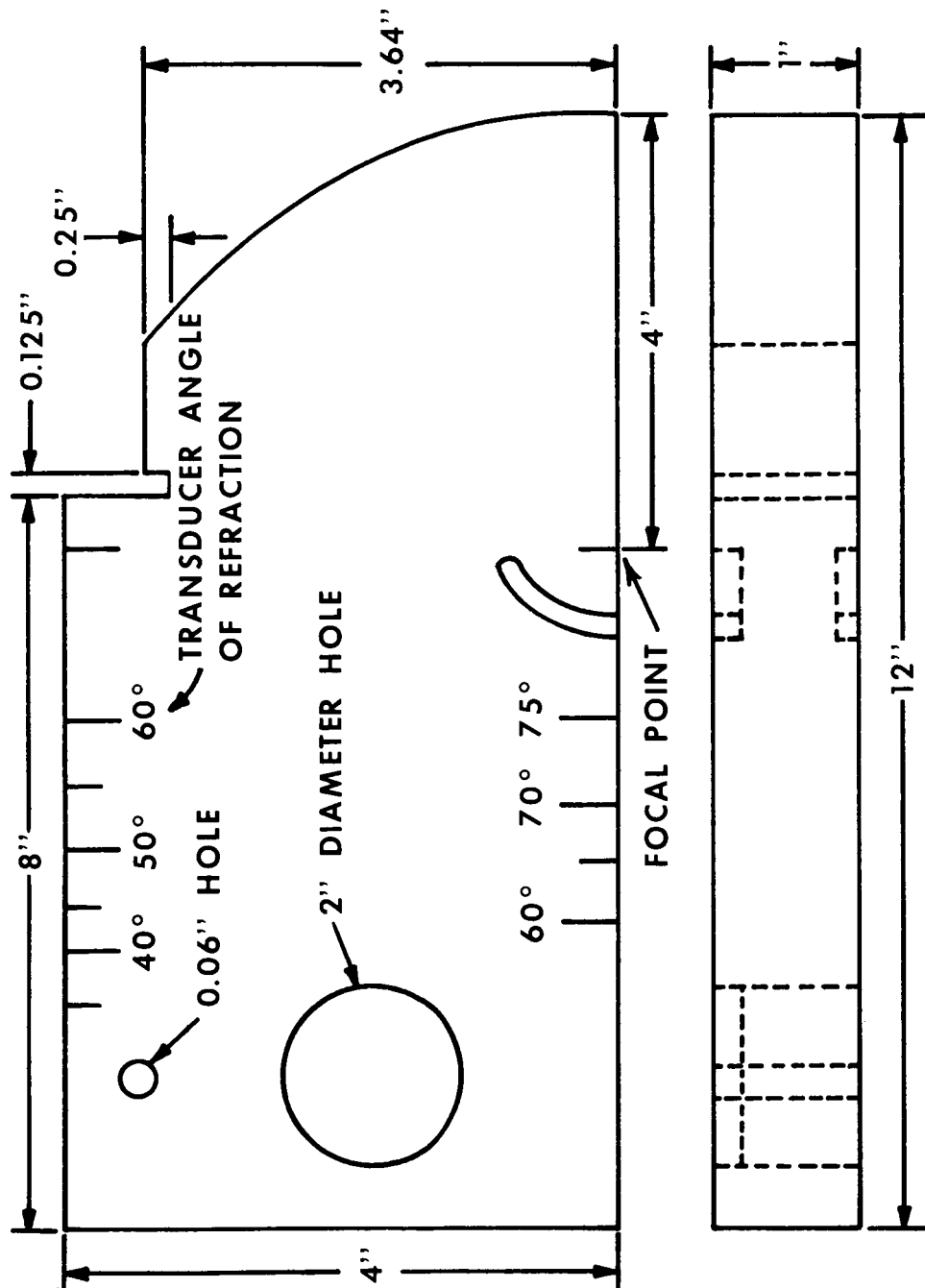
Figure 5. Calibration Block
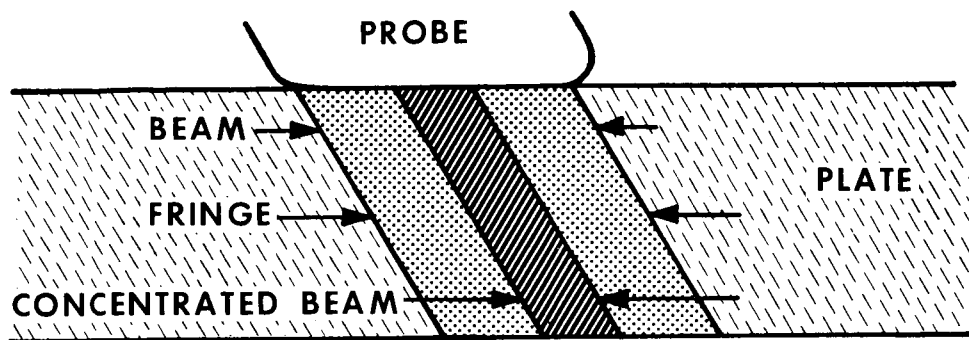
Figure 6.   Concentrated Beam
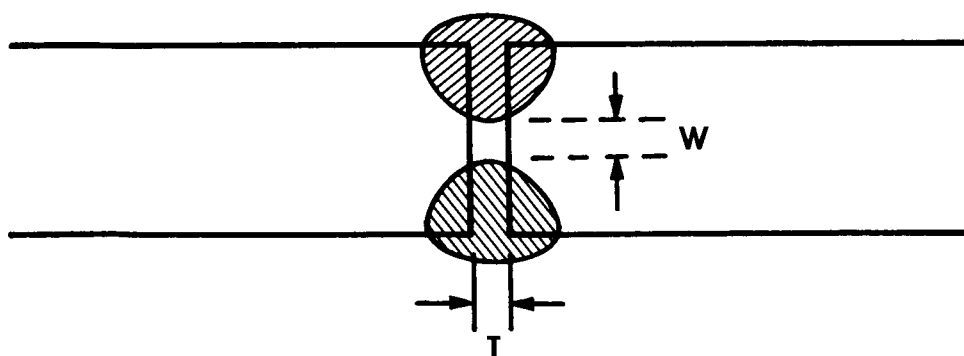


Figure 7.   Lack-of-Penetration Dimensions
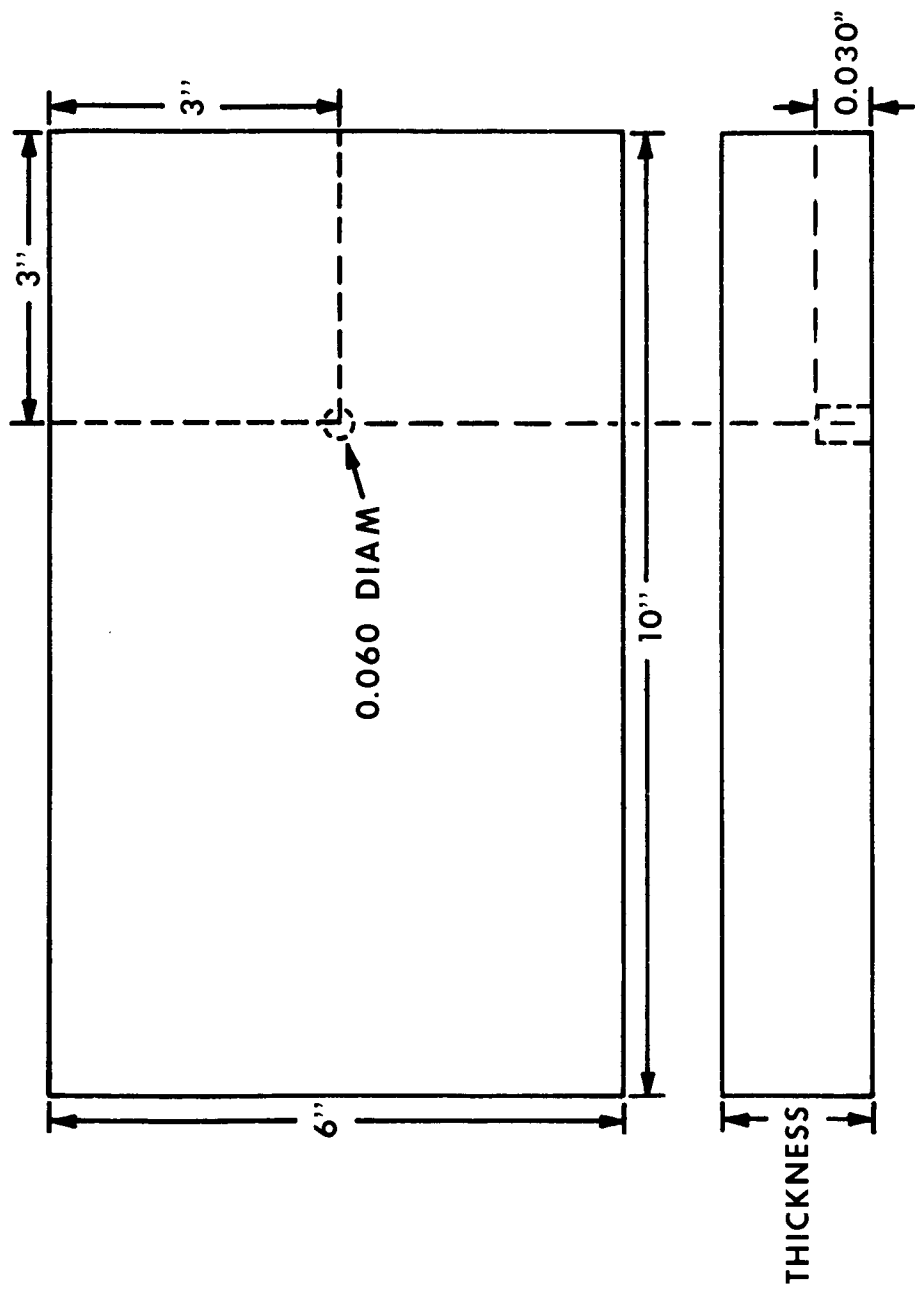
Figure 8.  Reference Plates for Beam Size

3"

3"

6"

10"

0.060 DIAM

0.030"

THICKNESS

HOLES TO DEPTH .200 INCH

HOLES TO DEPTH .400 INCH

HOLES TO DEPTH .600 INCH

HOLES TO DEPTH .800 INCH
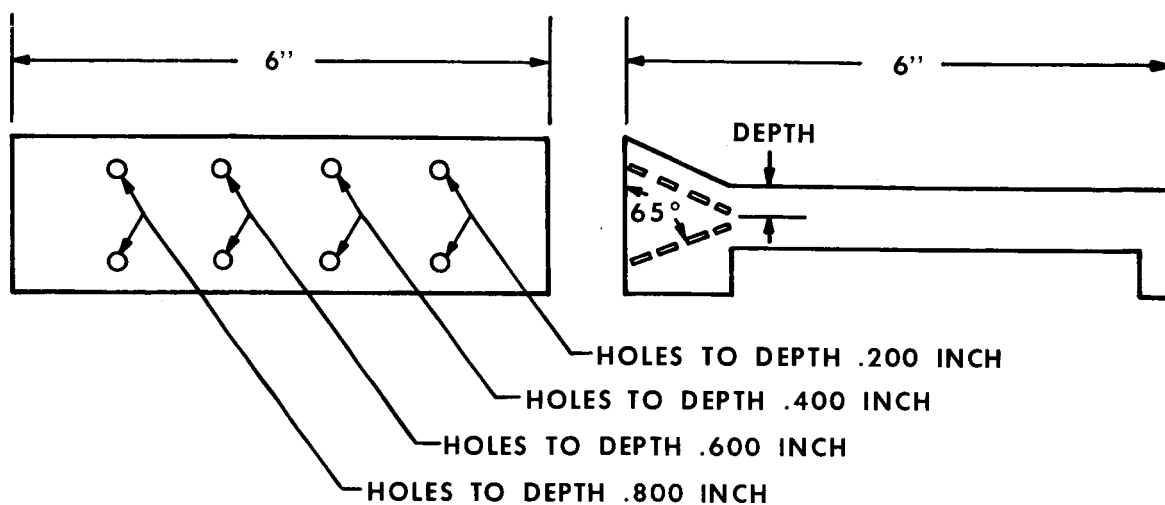
Figure 9.   Standard Angle Beam Reference Block
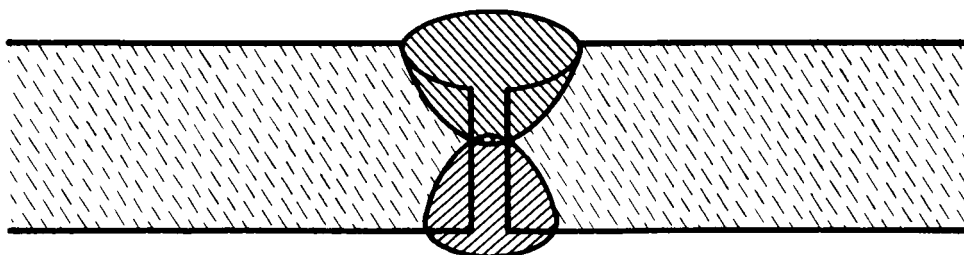


Figure 10.   U-Joint Butt Weld

DEVELOPMENT OF MECHANIZED

ULTRASONIC SCANNING SYSTEM

By

Raymond Evans
and
J. A. MacDonald

SUMMARY

The first in-house production mechanized ultrasonic scanning system has been developed and designed. This system was developed for inspecting the flaw content in the welds of the Saturn V Booster Stage S-IC propellant tanks. The system will provide, for the first time, the capability to 100 percent ultrasonically inspect welds within a time frame compatible with stage fabrication schedules.

The most significant achievement of the project in terms of equipment was the development of a water column probe which eliminates the necessity of submerging the weld being tested in water or providing a water flush over the inspection surface. The mechanized ultrasonic scanning system was proven to be capable of scanning welds at speeds greater than 1 inch per second. These scanning rates permit entire welds to be ultrasonically tested in approximately the same amount of time as required for radiographic testing.

The evaluation of the system included the determination of the beam characteristics of the water column probe by utilizing the angle beam calibration blocks and other standard reference blocks. The results of these tests were comparable with the data obtained from theoretical calculations.

After due consideration, it was decided that an angle of incidence of 26 degrees would be used for the probe tip. This angle will produce shear waves at the optimum angle to detect lack-of-penetration and lack-of-fusion.

A study of complete test data for selected panels used in this evaluation has shown that the mechanized ultrasonic scanning system is feasible for use as:

(1) A complete inspection system to supplement radiographic methods in the detection of subsurface weld flaws through a precise interpretation of the A-scan recordings.

(2) A fast survey scanning system to detect weld flaw areas which can then be inspected for flaw definition using the manual scanning method.

# SECTION I.  INTRODUCTION

The objective of the project was to develop a nonimmersion ultrasonic inspection system which could be mechanized to inspect butt-welds in aluminum.  The system was conceived for use in inspecting butt welds on the booster stage S-IC and other Saturn V vehicle propellant tanks.  Overall considerations included the achievement of:

    (1)    A system capable of detecting and locating subsurface, minute weld flaws.

    (2)    A system capable of scanning welds at speeds in excess of 1 inch per second.

Radiographic (X-ray) techniques for testing butt welds on space vehicle components have been in use for some time.  This technique has contributed greatly to the reliability of space vehicle performance. In the range of material thicknesses used in the S-IC propellant tanks, radiography is limited in the detection of lack-of-fusion and lack-of-penetration due to insufficient density changes.  Thus, a method was desired that was capable of a higher degree of reliability in the detection of flaws, and would provide improved butt-weld analysis within the manufacturing schedule.  It was established that the technique of ultrasonic inspection of butt welds could provide increased capability for the detection of weld defects, especially lack-of-fusion and lack-of-penetration, over present radiographic methods.

A manually operated commercial ultrasonic system was used to supplement radiography on the early S-IC hardware.  However, to insure more complete coverage of testing welds on the propellant tanks and similar large items, a mechanized ultrasonic scanning system was developed to facilitate the nondestructive testing of large butt welds, such as Y-ring-to-skin, Y-ring to-bulkhead, skin-to-skin, and gore-to-gore meridian welds.

In evaluating the complete system, all weld beads were scarfed to a height of less than 1/32 inch and porosity in the weldments was given very little consideration because this flaw is readily detectable by radiographic methods.  The following parameters were given prime consideration:

3

(1)    The optimum technique for testing butt welds
       with the specially designed water column probe.

(2)    The optimum angle of incidence to best satisfy
       weld coverage in various thicknesses of material
       using shear waves exclusively.

(3)    The evaluation and definition of the calibration
       methods for the water column probe as applied to
       butt welds.

(4)    The establishment of some basic correlations and
       interpretations between radiographs, metallographic
       surveys, and brush recordings for interpreting
       various flaw indications.

This report presents theoretical bases, test setups, and test results that comprised the project necessary to develop the water column probe, improvements in the water column probe after system evaluation, mechanized tooling, and other elements of the mechanized ultrasonic scanning system.

SECTION II.   SYSTEM DESCRIPTION

A.    GENERAL INFORMATION

A mechanized ultrasonic scanning system is a system for detecting weld flaws.  The mechanized system consists of:

(1)    The ultrasonic flaw detection instrument.

(2)    A recording system.

(3)    A transmitting and receiving unit.

(4)    The special tooling required to move the transmitting
       and receiving unit along the part being inspected.

The ultrasonic technique utilized by the mechanized ultrasonic scanning system is a simulated immersion angle beam pulse-echo technique.  A schematic  of the system covered in this report is shown in figure 11.

4

TRANSMITTING AND
RECEIVING UNIT

TEST PLATE

ULTRASONIC FLAW
DETECTION UNIT

RECORDER
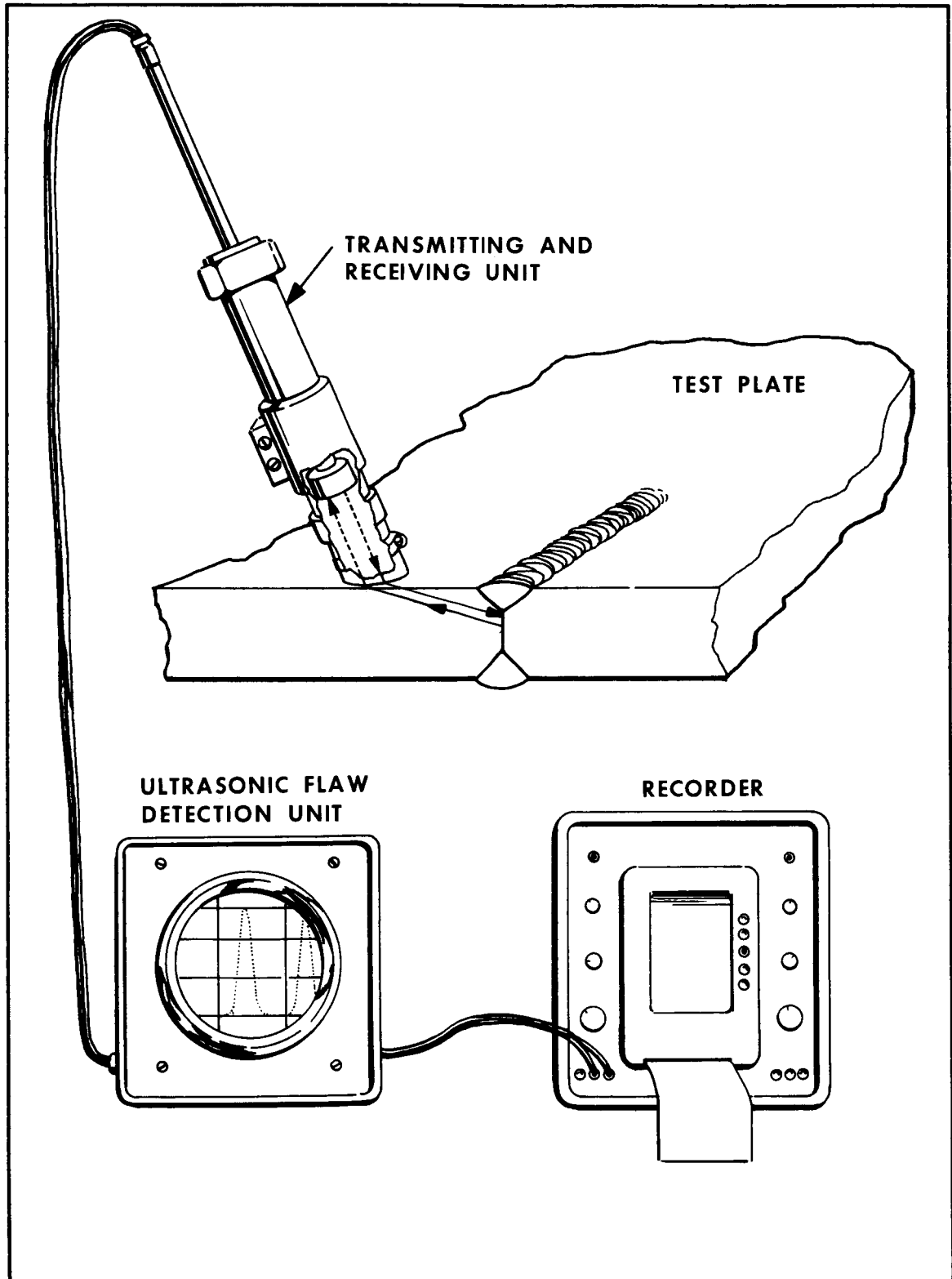
Figure 11.   Mechanized Ultrasonic Scanning System Schematic

5

B.    EVALUATION SYSTEM

1.    Basic Functional Units.  The mechanized scanning
evaluation system consists of four basic functional units as shown in
figure 12.  These are:

(1)    Electronic Pulse Generator and Receiving
Unit (Reflectoscope).

(2)    A-Scan Recording Unit (Brush Recorder).

(3)    Transmitting and Receiving Unit (Water
Column Probe Assembly).

(4)    Support and Translation Unit for the Trans-
mitting and Receiving Unit (X-Y Scanner).

2.    Electronic Pulse Generator and Receiving Unit.
The electronic pulse generator and receiving unit is a standard off-the-
shelf instrument and will not be described or discussed in detail.  The
instrument used is a Sperry UM-700 reflectoscope as shown in figure 13.

3.    A-Scan Recording Unit.  The A-scan recording
unit is a standard off-the-shelf instrument and will not be described
or discussed in detail.  The instrument used is a Brush Mark II Recorder
as shown in figure 14.

4.    Transmitting and Receiving Unit.  The transmitting
and receiving unit, hereinafter designated  water column probe, consists
of an ultrasonic transducer enclosed within a water filled cylinder as shown
in figure 15.  The transducer is connected to a coaxial rod that is routed
through the upper end of the sealed cylinder and connected to a coaxial
cable, which is connected to the reflectoscope.  The lower end of the
cylinder is covered with a rubber diaphragm that serves as a water seal
and contact surface  and permits transmission of the ultrasonic beam to
the weldment being inspected with a minimum loss of energy.  The
transducer used in the probe is a Sperry, 2.25 megacycle, 1 3/4-inch
diameter, straight beam immersion type.  The probe body is an aluminum
cylinder with a 2-inch inside diameter and a 2 1/4-inch outside diameter.
The body is 11-inches long, and the contact end is cut on a 26-degree
angle.  The rubber diaphragm or probe tip is molded of polyurethane
rubber; the contact surface of the diaphragm is 0.020-inch thick.  The
water column probe is considered to be the heart of the entire system and

RECORDER

REFLECTOSCOPE

PROBE

TEST PLATE

X-Y SCANNER
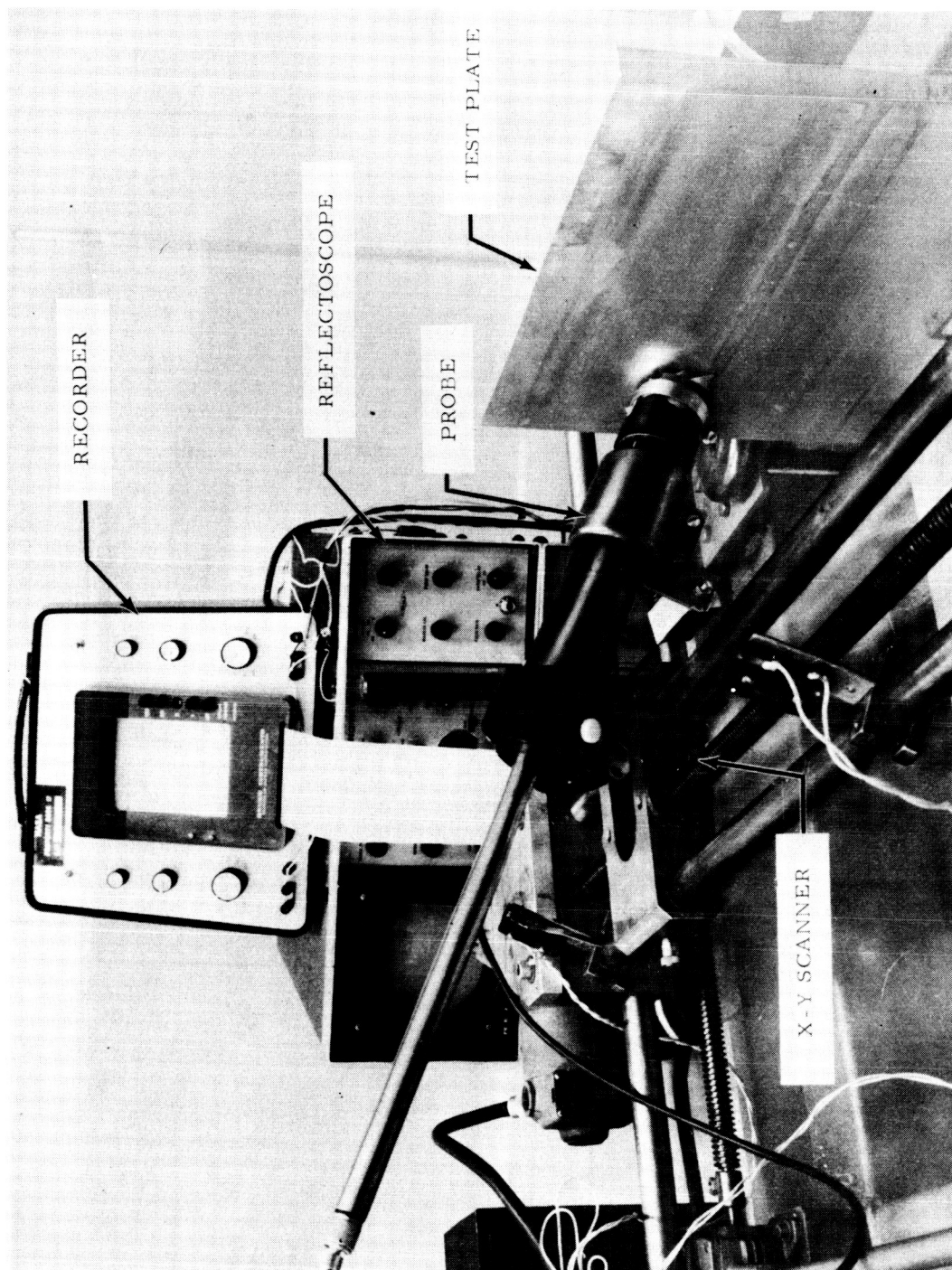
Figure 12.  Evaluation System

7
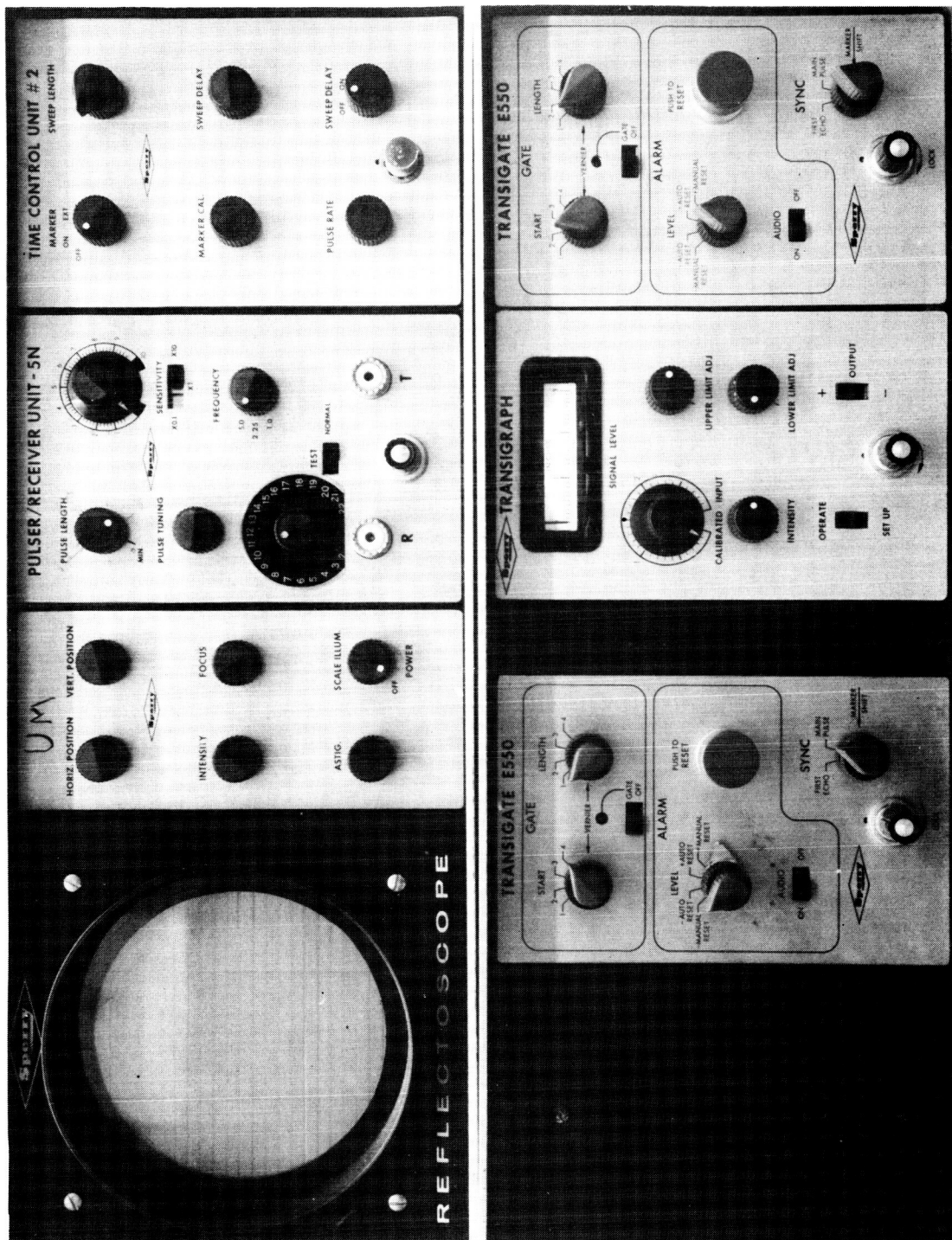
Figure 13. Sperry UM-700 Reflectoscope

Figure 14.  Brush Mark II Recorder
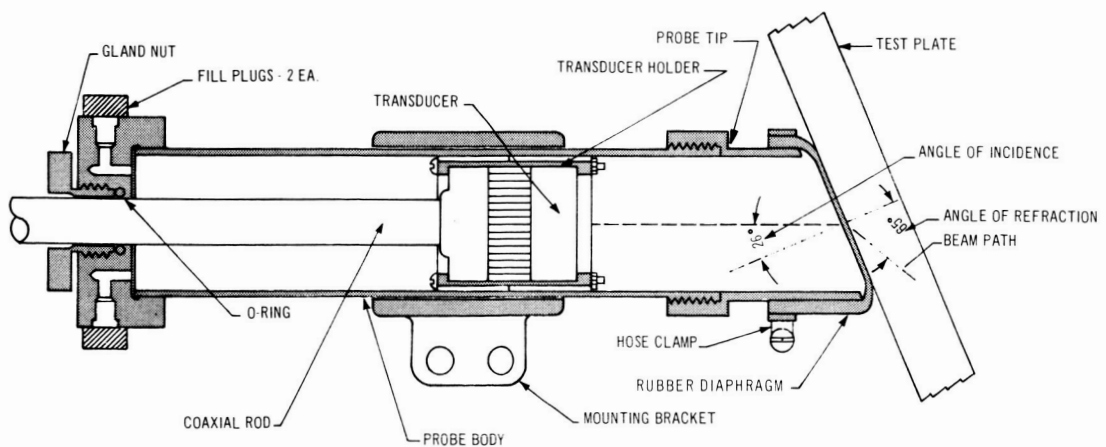


Figure 15.   Water Column Probe

provides the following advantages over other available ultrasonic probes used in mechanized scanning:

(1) The ease of changing tips. By changing tips the angle of incidence can be changed such that the angle of refraction can be varied from 45 to 90 degrees.

(2) The ability to confine the ultrasonic near field within the water column.

(3) Minimum couplant requirements; only a damp surface is required.

5. Support and Translation Unit. The support and translation unit used was the laboratory X-Y scanner as shown in figure 16. The X-Y scanner moved the probe at a uniform speed from one end of the plate to the other. The scanning speed was adjustable to permit matching the scanner to a recorder in order to produce a recording of the same length as the weld being tested.

C. PRODUCTION SYSTEM

1. Basic Functional Units. The mechanized scanning production system consists of two basic functional units as shown in figure 17. These units are:

(1) The instrument console.

(2) The scanning head.

2. Instrument Console. The instrument console, as shown in figure 18, consists of standard off-the-shelf items and will not be described or discussed in detail. These items are:

(1) Branson Sonoray 301 Ultrasonic Instrument.

(2) Brush Mark 280 Recorder for A-Scan Recording.

(3) A commercial instrument cart with power cord reel and isolation transformer.

10
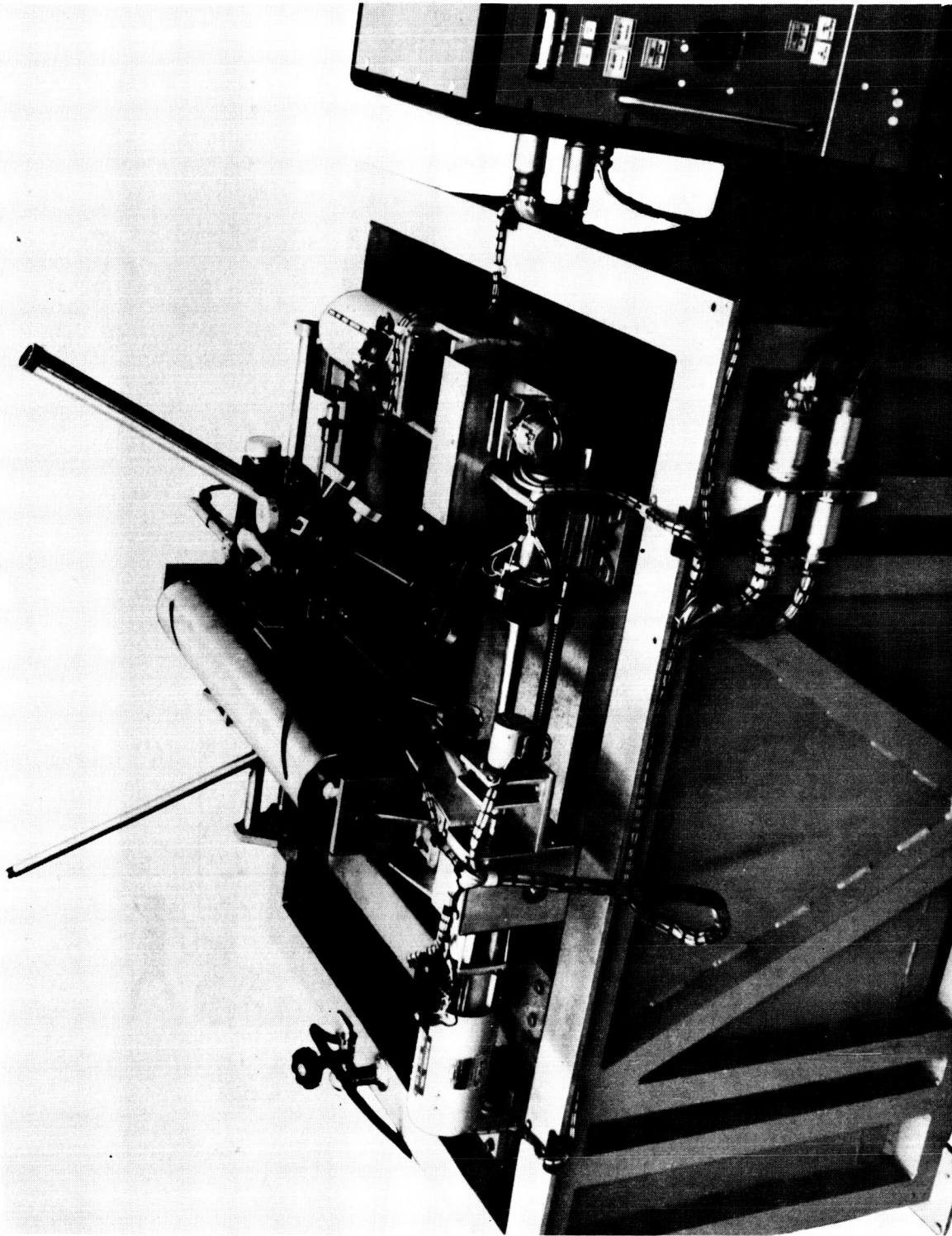
Figure 16. Laboratory X-Y Scanner

11

SCANNING HEAD
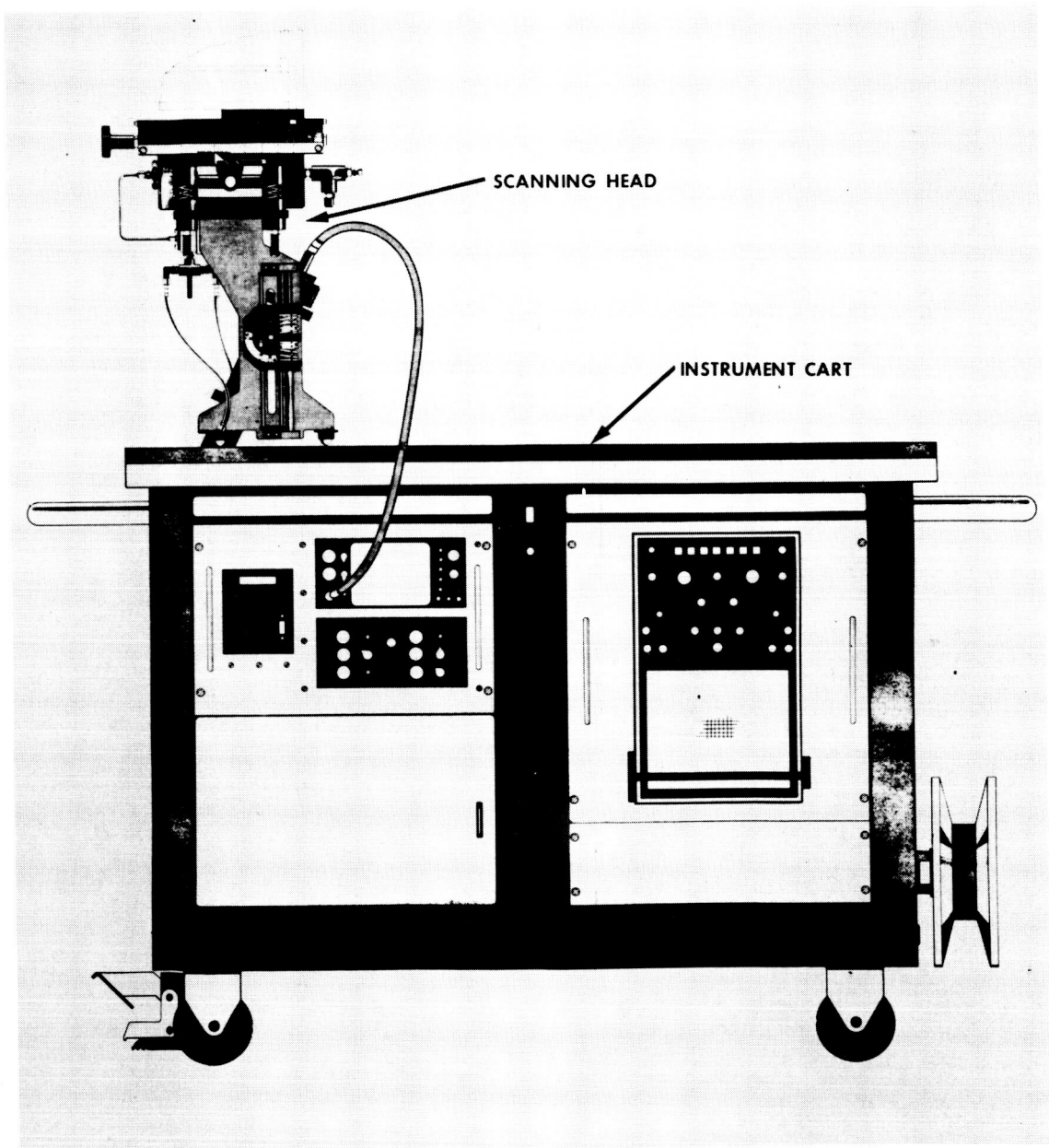
INSTRUMENT CART

Figure 17. Production System
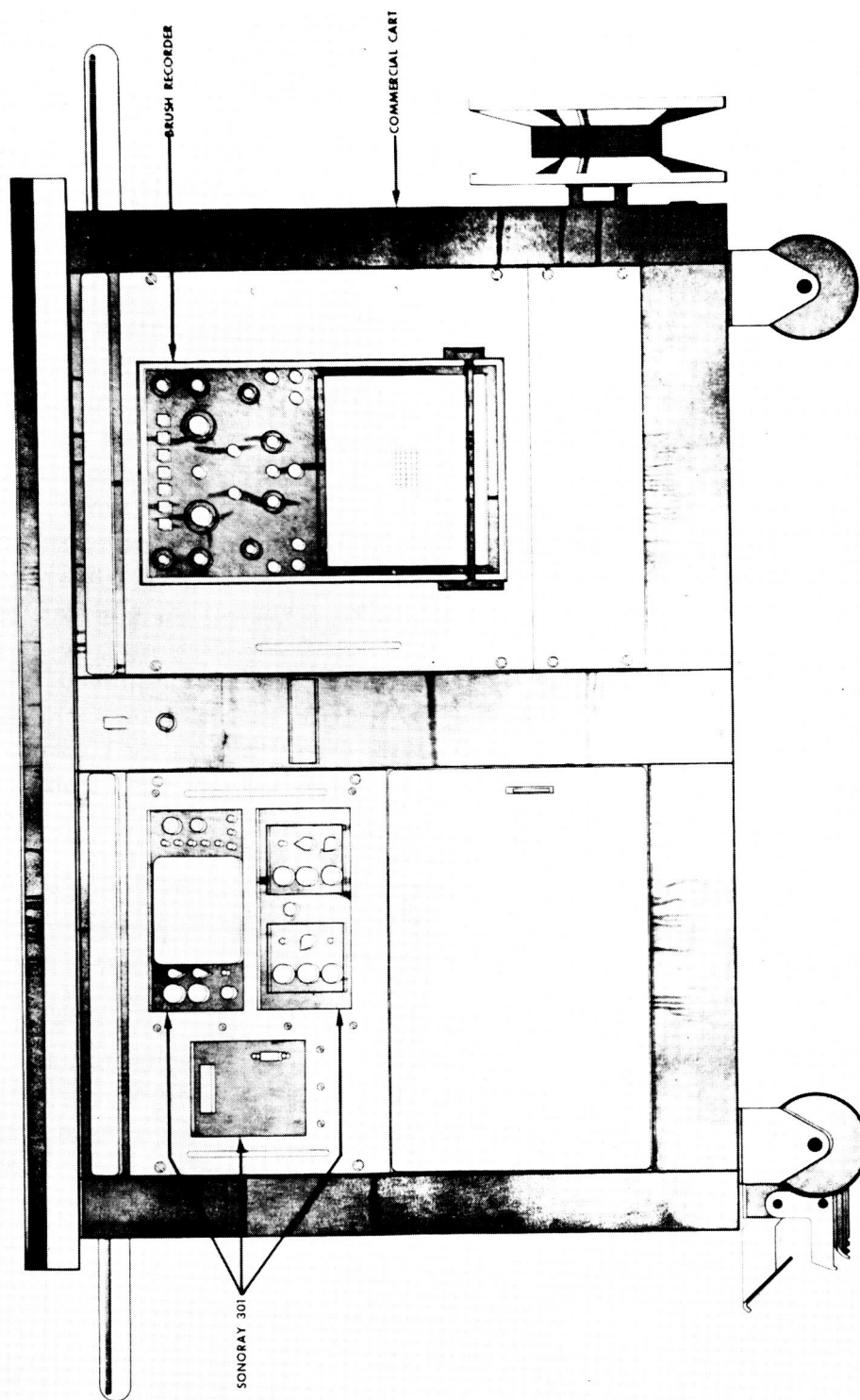
Figure 18.   Instrument Console

13

3. Scanning Head. The scanning head, as shown in figure 19, consists of two basic assemblies described in the following paragraphs.

a. Water column probe. Reference paragraph B, 4 of this section for a description of the water column probe.

b. Contour following tool. The contour following tool is a specially designed device that cradles the water column probe. The tool design incorporated a basic universal joint (figure 19, reference 1) that permits 7 1/2 degrees of tilt in all directions relative to the tool mounting surface. The three spherical balls (reference 2) are positioned around the probe tip for orientation to the plane of the weld surface. In this manner, proper alignment of the probe to the weld, with respect to angularity and position, can be obtained. The secondary suspension system (reference 3) was provided to permit probe movement in a completely fixed relationship perpendicular to the plane established by the three spherical balls. This feature will not change the alignment of the probe angularity and positioning in any way, but will compensate for any surface curvature irregularity up to ± 1/16 inch. The water reservoir or accumulator (reference 4) will contain a sufficient quantity of water that, when pressurized by air, will supply the couplant necessary for scanning for approximately four hours. The couplant control valve (reference 5) will allow the couplant to be shut off, spray on either side of the probe tip, or spray on both sides simultaneously. Single spray nozzles (reference 6) are mounted on each side of the probe tip. These nozzles provide a fine water mist to dampen the surface of the material being tested in order to couple the ultrasonic beam to the material. The probe angle indicator (reference 7) shows the angularity of the probe to the plane established by the three spherical balls. The position indicator (reference 8) allows the pointer to be moved to the zero position after the probe is first aligned on the center of the weld bead. When additional passes are made at different distances from the weld bead, the position of the probe from the center of the weld may be readily determined. The handwheel (reference 9) is used to vary the position of the probe from the center of the weld without changing the original test setup. The adapter plate (reference 10) permits mounting of the tool on any type of surface.

14

REF. NO. 8
POSITION INDICATOR

REF. NO. 9
HAND WHEEL

REF. NO. 1
UNIVERSAL

REF. NO. 5
COUPLANT CONTROL
VALVE

REF. NO. 7
PROBE ANGLE
INDICATOR

REF. NO. 6
SPRAY NOZZLES

REF. NO. 2
SPHERICAL BALLS

REF. NO. 10
ADAPTER PLATE

REF. NO. 4
ACCUMULATOR

WATER
COLUMN PROBE

REF. NO. 3
SECONDARY SUSPENSION SYSTEM

CONTOUR
FOLLOWING TOOL
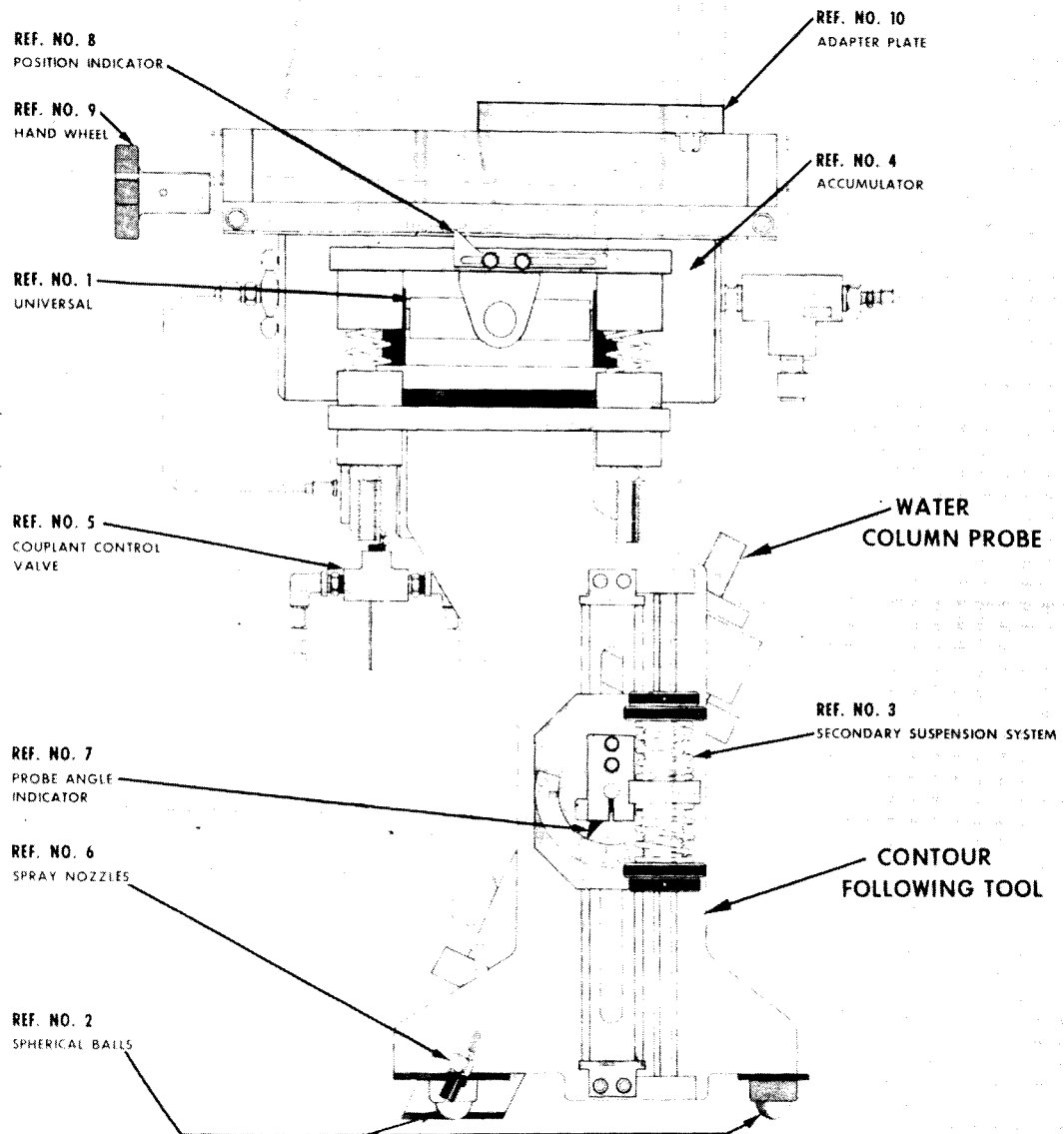
Figure 19.   Scanning Head

15

# SECTION III. WATER COLUMN PROBE

## A.    THEORY AND CALCULATIONS

The design and development of the water column probe encompassed several aspects of engineering theory and principles; the most important of which will be discussed in detail within this section. In order to grasp the applied theory, it is necessary to understand the physical relationships of the ultrasonic sound beam propagation. As shown in figure 20, the sound wave is emitted from the transducer, through the water column along path A, and into the metal. Upon intersection with the weld flaw, the sound wave reflects and returns to the transducer along path B, coincident with path A. The following paragraphs present the engineering principles, theoretical considerations, and calculations relating to the behavior of the sound beam.
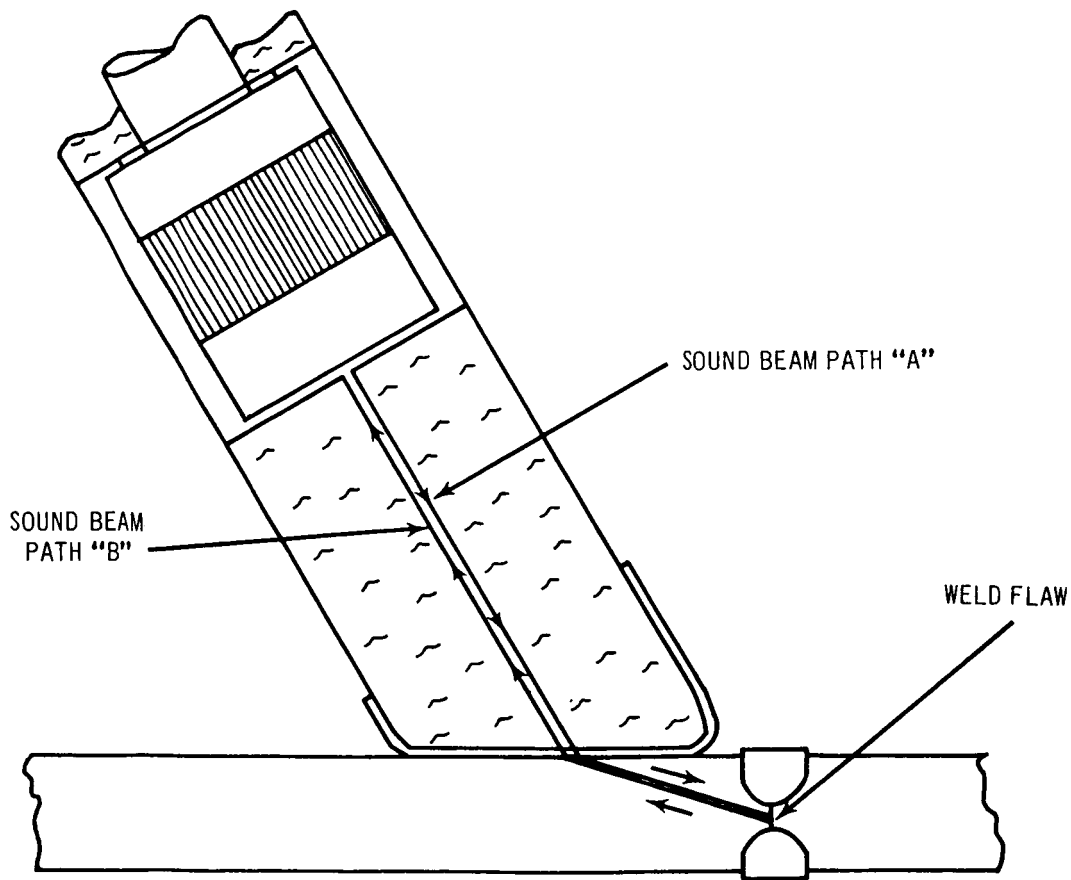
Figure 20.   Ultrasonic Sound Beam Propagation

16

1.    Angles of Sound Refraction.  As stated in the Nondestructive Testing Handbook:* "When sound travels from a liquid into a solid, the impedance change at the liquid-metal interface results in reflection of a large portion of the incident energy.  Only a small portion of the sound is transmitted into the metal.  When the incident energy is directed at an angle other than normal to the surface of the metal, the transmitted sound divides into both longitudinal and shear modes as shown in figure 21.  Each of these waves travel in a different direction and at differing velocities.  At an interface between two solids (for example, bonded metals), both reflected and refracted longitudinal and shear waves occur."

2.    Angular Relationship Calculations.  The angular relationships of the angle of incidence to the angle of refraction is determined by using Snell's law.

INCIDENT PLANE WAVE

$V_L$

REFLECTED PLANE WAVE

r

i

REFRACTED
LONGITUDINAL WAVE

LIQUID

METAL

$$\frac{SIN\ i}{SIN\ \theta_{LM}} = \frac{V_L}{V_{LM}}$$

$\theta_{SM}$

$\theta_{LM}$

$V_{SM}$  $V_{LM}$

$$\frac{SIN\ i}{SIN\ \theta_{SM}} = \frac{V_L}{V_{SM}}$$

REFRACTED  SHEAR  WAVE
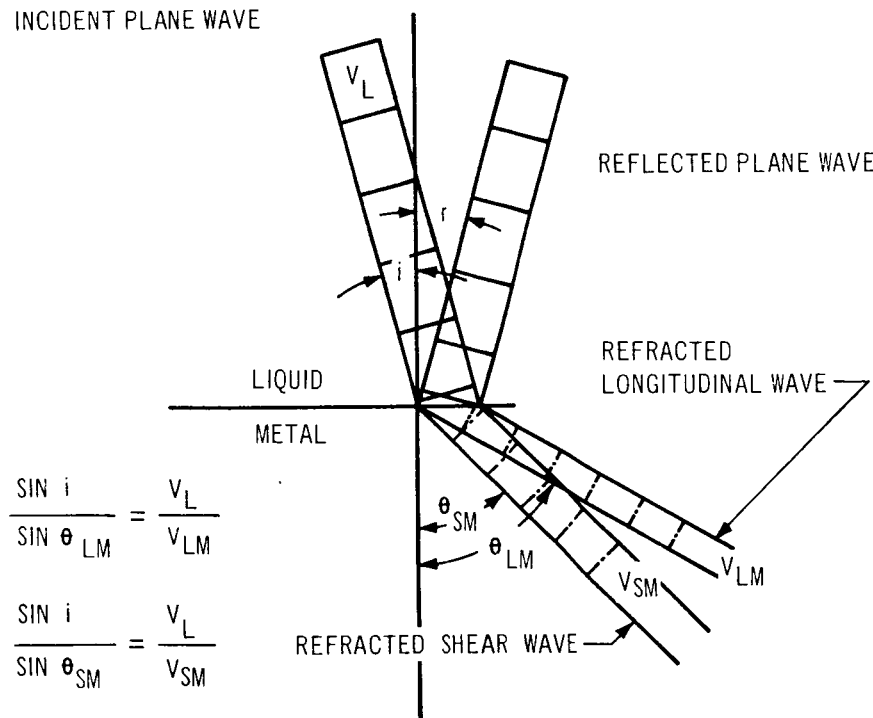
NONDESTRUCTIVE TESTING HANDBOOK

Figure 21.   Relationships for The Sound Beam at Angular Incidence
to The Metal Surface

*McMaster, Robert C., Nondestructive Testing Handbook, Ronald Press Company, New York, New York, 1959.

17

Snell's Law $\quad \dfrac{\text{Sine } I}{V_1} = \dfrac{\text{Sine } R}{V_2}$

Where:
- I = Angle of incidence
- $V_1$ = Velocity in water - $1.49 \times 10^5$ centimeters per second
- R = Angle of refraction
- $V_2$ = Velocity in aluminum -

   (a) Shear wave - $3.1 \times 10^5$ centimeters per second

   (b) Longitudinal Wave - $6.35 \times 10^5$ centimeters per second

By selecting values of I and solving Snell's Law the angle of refraction can be determined as shown in table 1.

Table 1. Relation of Angle of Incidence to Angle of Refraction

| ANGLE OF INCIDENCE (DEGREES) | ANGLE OF REFRACTION | |
|---|---|---|
| | SHEAR WAVE (DEGREES) | LONGITUDINAL WAVE (DEGREES) |
| 9 | 23 | 41 |
| 14 | 30 | 91 |
| 18 | 40 | -- |
| 26 | 65 | -- |
| 28 | 78 | -- |

Analysis of the data in table 1 shows that an angle of incidence in excess of 18 degress is desirable. At angles greater than 18 degrees there are no longitudinal wave components of the sound beam remaining in the material to give erroneous signals. Therefore, the shear wave components are utilized to provide weld flaw indications.

It is known that the weld flaws, lack-of-penetration, and lack-of-fusion lie in a plane normally perpendicular to the surface of the plate. In addition, ultrasonic inspection is known to be most effective when the sound beam is perpendicular to the plane of the weld flaws. By

utilizing these facts, plus the data in table 1, it was determined that 26 degrees would be the optimum angle of incidence for shear waves. This provided an angle of refraction of 65 degrees in the material, thus permitting sound beam intersection with the weld flaw plane as near to perpendicular as feasible. Angles of incidence in excess of 26 degrees result in excessive probe displacement from weld centerline. The selected angle of incidence, 26 degrees, was used throughout the evaluation of this project.

3.    The Near Field.*

a.    Characteristics of ultrasonic wave fronts. The most often neglected and misunderstood portion of a sound beam is the effect of the near field. Sound fields can usually be analyzed by some of the same methods used in the analysis of light beams. The one most often used, Huygens' principle, states that energy is radiated from a point source in all directions. The wave front is spherical in shape, and its intensity decreases as the square of the distance from the source. If two point sources of sound energy are placed beside each other, the resultant wave front will be a combination of the two, and will no longer be spherical.

b.    Maximum and minimum intensity points along the central axis. A transducer can be considered as a large group of sound energy point sources next-to each other. Figure 22 shows a graphic construction of the sound field directly in front of a transducer. The parallel lines represent the resultant plane-wave front across the face of the transducer. The circular lines represent the wave front from a single point source at the edge of the transducer. Solid lines represent pressure maxima, and dashed lines the pressure minima. When two maxima intersect, a point of high intensity occurs. When a maxima and a minima intersect, a point of low intensity occurs.

If the transducer is approached from infinity with a point detector along the central axis of the transducer, the signal will gradually increase up to the point where the plane wave is intersected by the cylindrical waves from the edges. This is the point of first central-axis maximum. The next central-axis maximum is caused by the intersection of the maximum from the edges and the maximum from the center. When the transducer is an idealized plane piston, the position of the point of maxima and minima on the central axis can be predicted.

*McMaster, Robert C., Nondestructive Testing Handbook, Ronald Press Company, New York, New York, 1959.

If:   Y+ = A maximum,
      Y- = A minimum,
      D  = The distance across a piston (transducer) in centimeters,
      R  = The radius of a circular piston (transducer) in centimeters,
      $\lambda$  = The acoustical velocity of sound waves in a material,
           the frequency of the transducer,
      M  = A maximum point, and
      N  = A minimum or null point,

Then for a circular piston, the equations are:

$$Y_{+m} = \frac{4R^2 - \lambda^2 (2M + 1)^2}{4_\lambda (2M + 1)} \qquad (M = 0, 1, 2 \ldots) \qquad (1)$$

$$Y_{-n} = \frac{R^2 - \lambda^2 N^2}{2N_\lambda} \qquad (N = 1, 2, 3 \ldots) \qquad (2)$$
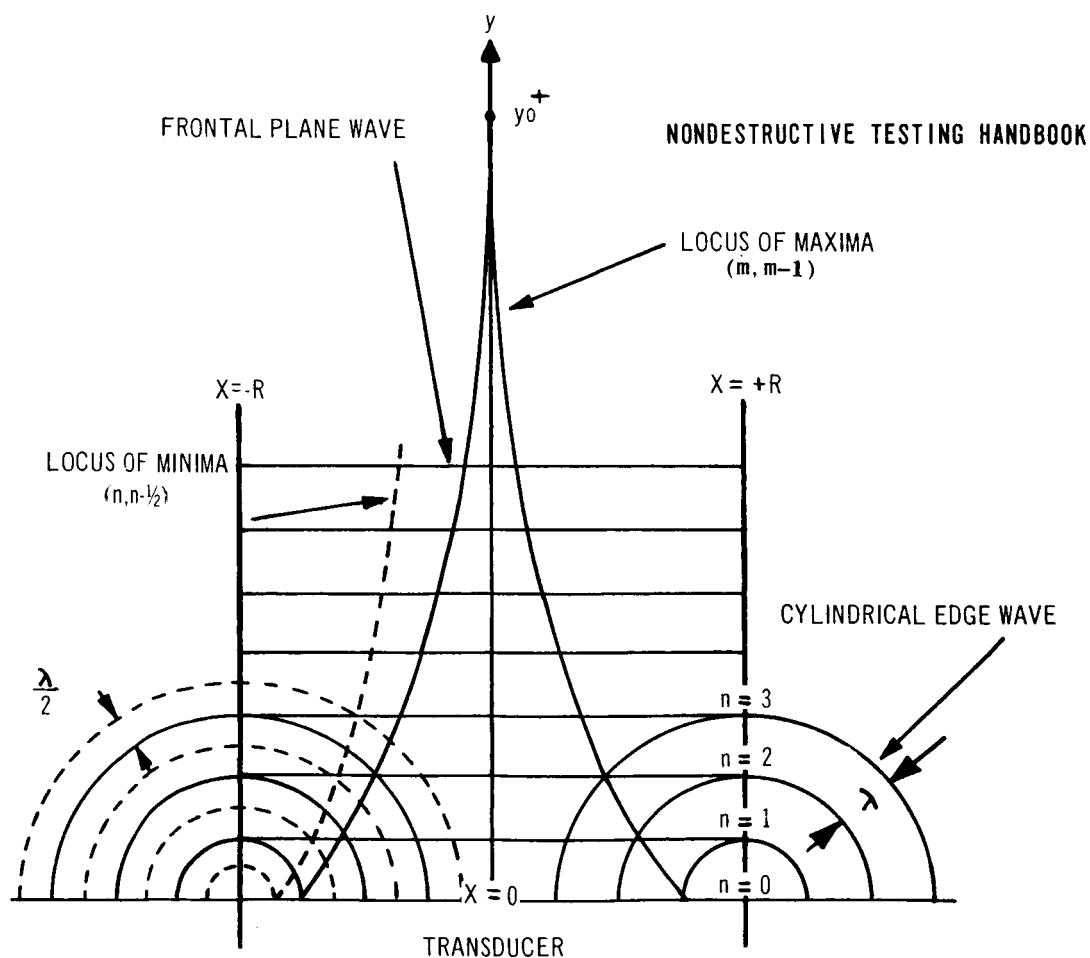


Figure 22.  Graphic Representation of Near Field

If the transducer is driven with a continuous wave the maxima are all equal, and the minima are all zero on the central axis. In the pulse system, the output wave is a damped sinusoid; each succeeding maximum after the first maximum, when approached from infinity, will decrease and each succeeding minimum after the first minimum, when approached from infinity, will increase.

Although the transducers used in ultrasonic nondestructive testing only approximate the action of a plane-piston radiator, the results obtained from these equations are close enough to be used.

         c.    Near-field effects. Particular attention is called to the first maximum and the first minimum signal points because these are the points which determine the extent of the near field. The entire region between the transducer and a position between these two points is a zone of confusion. A Schlieren image of the sound beam near a transducer is shown in figure 23. The characteristics of an echo from a reflector in this region are very difficult to analyze.

The near field is comprised of discrete annular rings of energy converging toward the axis at the region of primary intensity. If a material in which the sound velocity increases is placed in the near field, the region of primary intensity will move toward the transducer and become shorter. This is caused by the refraction of energy from the edges of the transducer, which is not of the same material as that inserted.

The foregoing discussion of near-field phenomena describes their importance in ultrasonic nondestructive testing interpretations. When comparing test objects to standard test blocks, a single defect can appear to be multiple defects, or the echo amplitude can vary by more than a standard hole size from the true defect size. These circumstances can develop if the frequency, water-path length, and flaw depth in the material are not identical.

        4.    <u>Near Field Length Calculations</u>. Calculations for the length of the near field are as follows: (Reference figure 22 and equation (1) under paragraph A, 3 of this section.)

TRANSDUCER

(A) SCHLIEREN
IMAGE OF SOUND
BEAM NEAR
TRANSDUCER.

BEAM PATTERN

NONDESTRUCTIVE TESTING
HANDBOOK
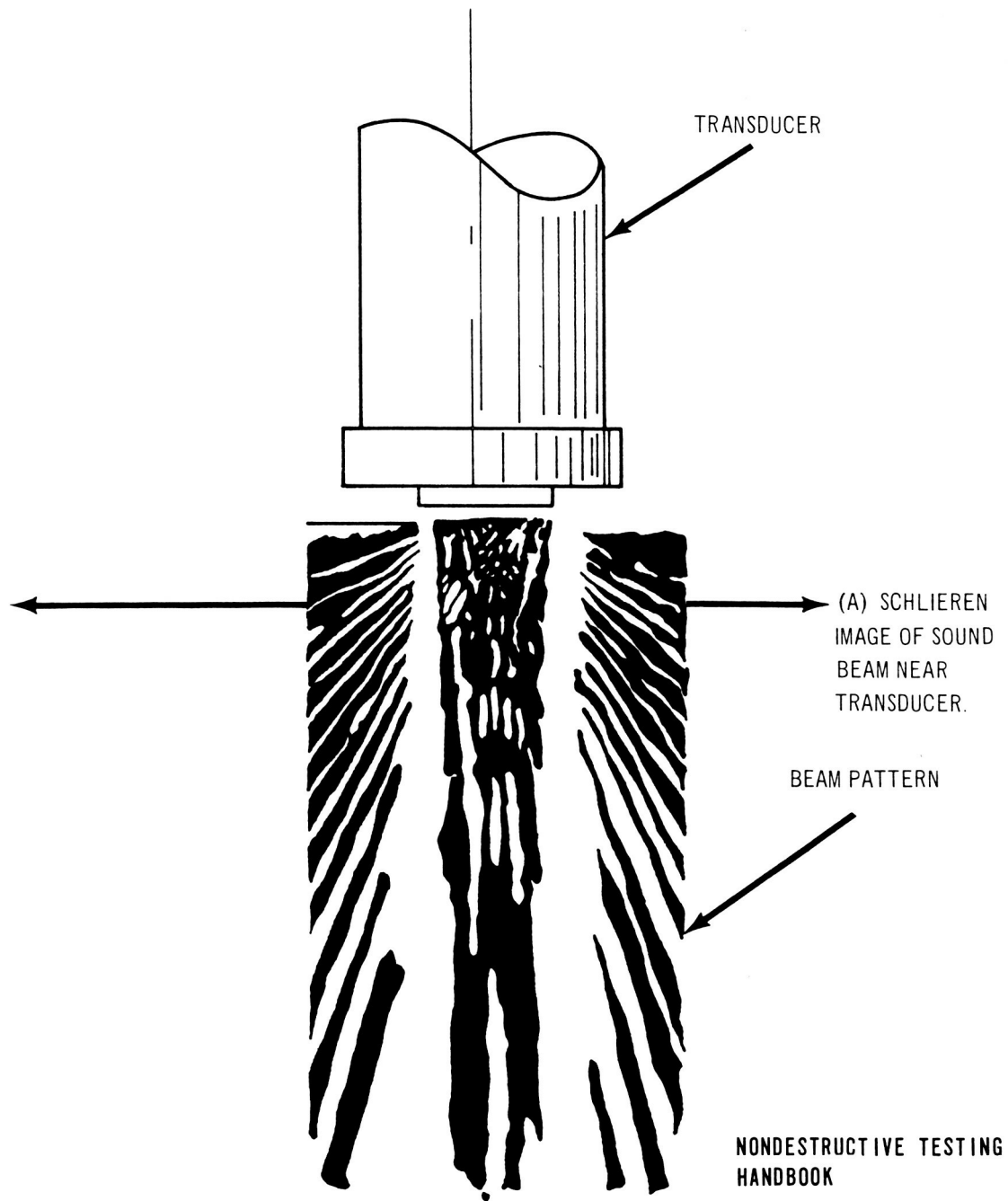
Figure 23.   Schlieren Image of Sound Beam

$$Y_{+m} = \frac{4R^2 - \lambda^2 (2m + 1)^2}{4 \lambda (2m + 1)} \qquad (1)$$

$$Y_{+m} = \frac{4R^2 - \lambda^2 - 4m\lambda^2 - 4M^2\lambda^2}{8m\lambda + 4\lambda} \qquad (2)$$

Then $m \longrightarrow 0$

Therefore $\quad Yo = \dfrac{4R^2 - \lambda^2}{4\lambda} \qquad (3)$

$$Yo = \frac{D^2 - \lambda^2}{4\lambda} \qquad (4)$$

and $\lambda = \dfrac{\text{velocity of sound in material}}{\text{frequency}} = \dfrac{V}{F}$

$$Yo = \frac{.25 \, D^2 F}{V} - \frac{.25 \, V}{F} \qquad (5)$$

Substituting known values in equation (5) gives:

$$Yo = \frac{(.25)(1.9)^2 (2.25 \times 10^6)}{1.49 \times 10^5} - \frac{(1.49 \times 10^5)(.25)}{2.25 \times 10^6} \qquad (6)$$

Where 1.9 centimeters is the diameter of the transducer (D), $2.25 \times 10^6$ is the frequency of the transducer (F), and $1.49 \times 10^5$ is the velocity of sound waves in water (V).

$$Yo - 13.612 \text{ centimeters or } 5.4 \text{ inches} \qquad (7)$$

This computed length represents the distance from the face of the transducer to the end of the near field of the sound waves for 2.25 megacycles.

## B.    DETERMINATION AND EVALUATION OF THE WATER COLUMN PROBE BEAM CHARACTERISTICS

1.    Calibration.    There are two features of the ultrasonic beam emerging from the water column probe tip, which need to be calibrated.    These are described in the following paragraphs.

a.    Beam centerline.    It is necessary to determine the exact center of the ultrasonic beam when leaving the rubber diaphragm that is covering the probe tip.    The setup shown in figure 24 is used for this purpose.    The surface A-B of the calibration block is coated with a thin film of water, which serves as a couplant.    The probe is then aligned in contact on surface A-B of the block and moved along surface A-B until the point of maximum pulse amplitude on the reflectoscope is reached.    At this point, the probe movement is stopped and the edge of the probe is marked above the center of radius as shown on the calibration block in figure 24.    This locates the centerline of the ultrasonic beam when leaving the rubber diaphragm.

b.    Angle of refraction.    It is necessary to calibrate the water column probe to define the exact angle of refraction of the ultrasonic beam after entering the material.    The setup shown in figure 25 is used to determine the angle of refraction.    The surface C-D of the calibration block is coated with a thin film of water, which serves as a couplant.    The probe is then aligned in contact on surface C-D and moved along surface C-D until the point of maximum pulse amplitude is reached for the echo pulse from hole F.    At this point the calibration block is marked at a point in line with the beam centerline mark on the tip of the probe.    The angle of refraction is extrapolated from the scale on the calibration block using this mark.

2.    Ultrasonic Beam Size and Weld Coverage.

a.    Ultrasonic beam size.    It is necessary to determine the size of the ultrasonic beam in the material in order to establish the weld coverage of the beam for each scan.    To determine the beam size, the setup shown in figure 26 was used.    All of the testing for beam size was conducted with the near field confined entirely within the water column probe.    The beam size was determined by using reference plates for beam size (figure 8) of different thicknesses; one 0.224 inch, one 0.410 inch, and one 0.608-inch thick.
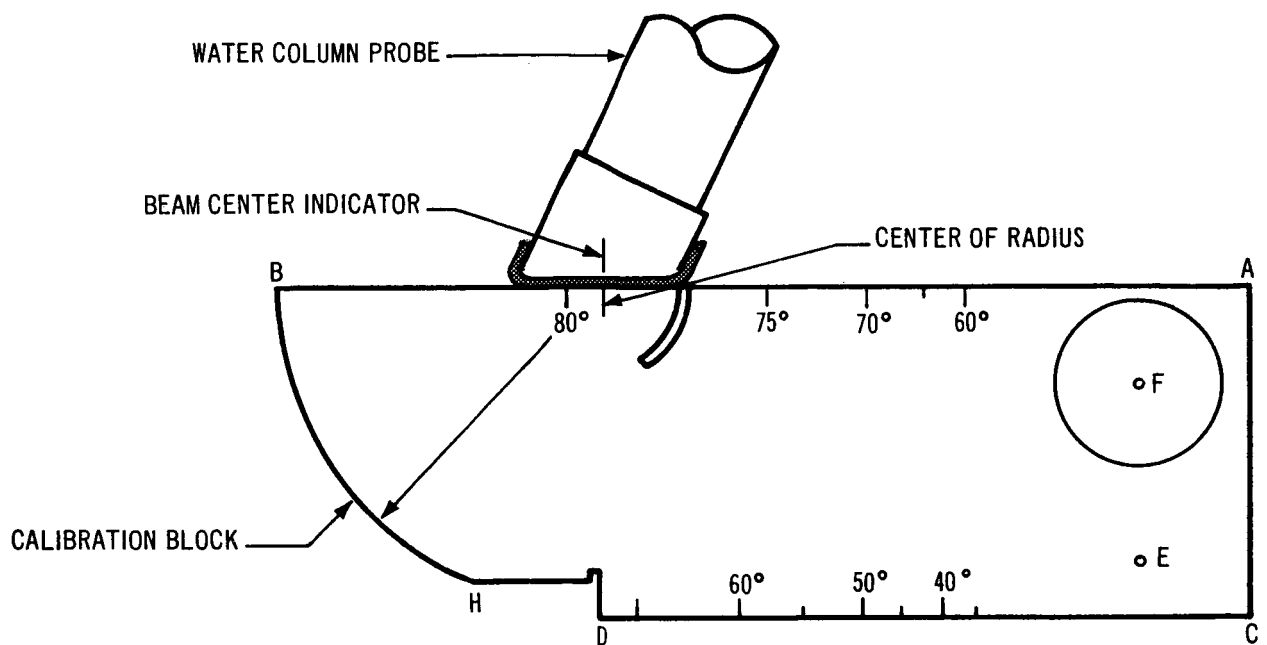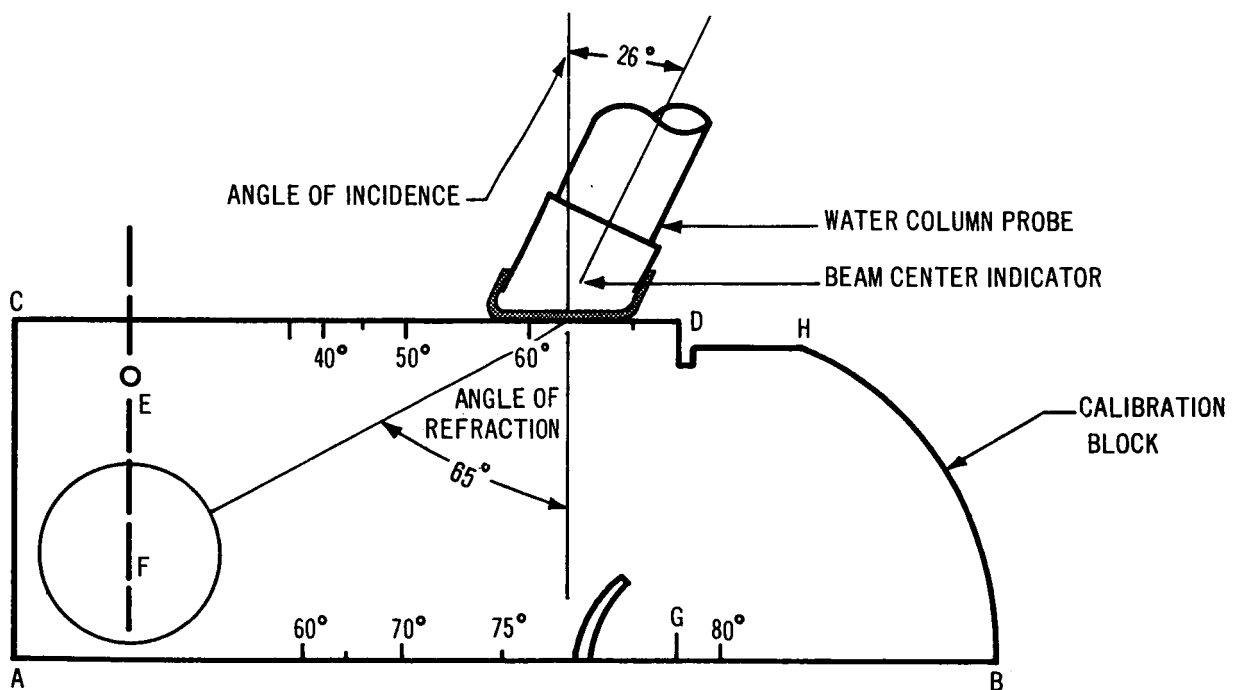
Figure 24. Calibration of Probe for Determination of Beam Centerline



ANGLE OF INCIDENCE = 26°

ANGLE OF REFRACTION = 65°

Figure 25. Calibration of Probe for Determination of The
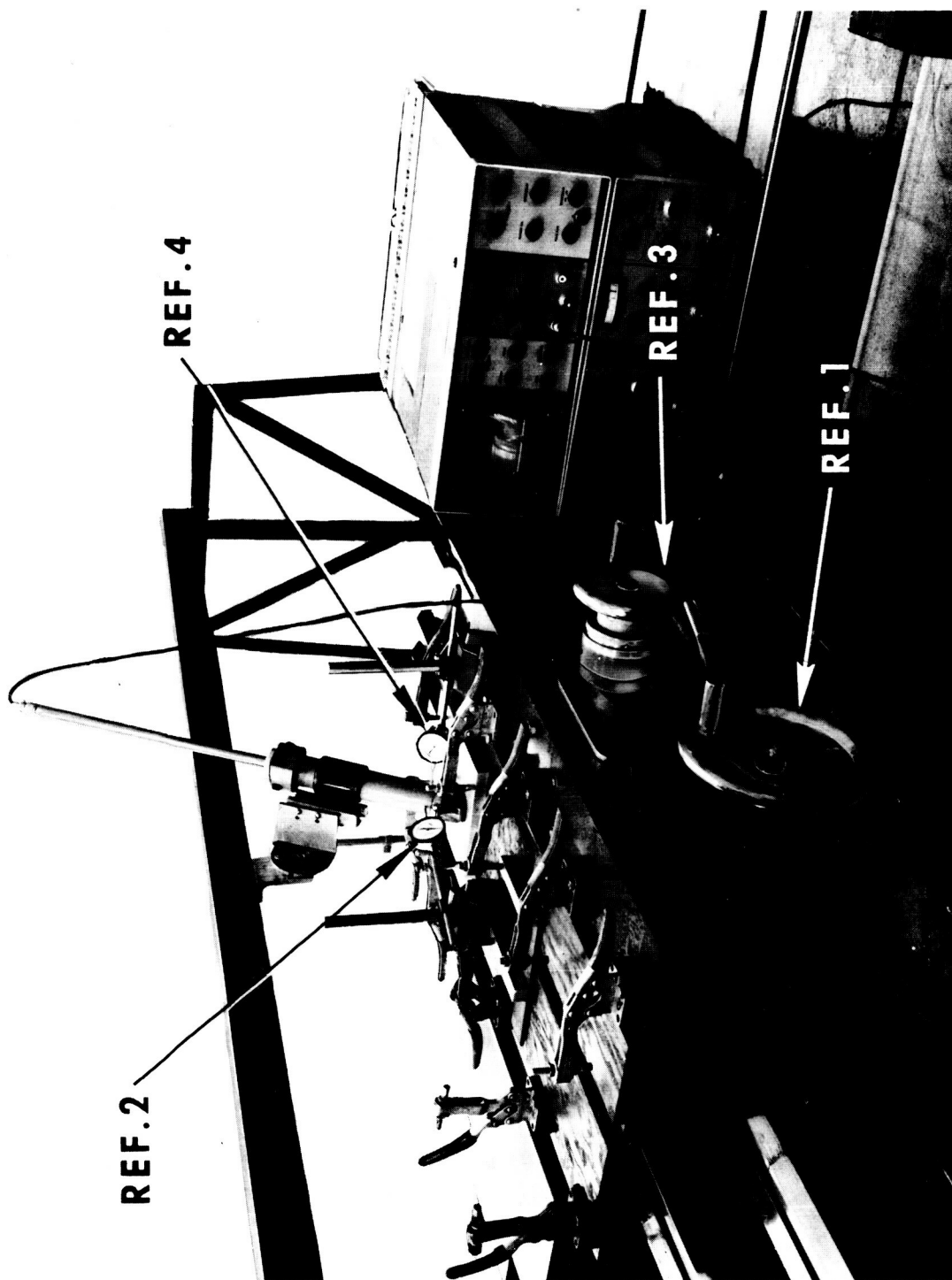Angle-of-Refraction

25

Figure 26. Test Setup to Determine Beam Size

The plate was moved in an X and Y axis relationship to the probe. By turning the handwheel (figure 26, reference 1), the lathe bed travel was effected and the plate was moved in the X-axis direction while observing the CRT display of the pulse echo from the hole in the plate. The readings for full beam width in table 2 were obtained by setting the dial indicator (reference 2) to zero at the point where the echo pulse on the CRT was two small divisions, or 10 percent of the maximum, above the baseline. The plate was then moved in the X direction until the pulse reached a maximum and was then returned to the starting level. The distance traveled, as shown by the dial indicator, represents the width of the beam. The readings for the width of the concentrated portion of the beam were taken in the same manner except that the starting and ending points were 10 percent below the maximum pulse amplitude shown on the CRT display. All tests for X-axis measurements were conducted with the beam centered over the hole in the Y-axis direction so that the beam width in the X direction was at a maximum.

Table 2. Beam Size Versus Depth Test Data

| TEST NUMBER | BEAM DEPTH IN MATERIAL | BEAM SIZE | | | |
|---|---|---|---|---|---|
| | | X-AXIS | | Y-AXIS | |
| | | FULL BEAM | CONCEN-TRATED BEAM | FULL BEAM | CONCEN-TRATED BEAM |
| 1 | 0.224 | 0.761 | 0.461 | 0.262 | 0.123 |
| 2 | 0.224 | 0.761 | 0.461 | 0.262 | 0.123 |
| 1 | 0.410 | 0.716 | 0.434 | 0.280 | 0.140 |
| 2 | 0.410 | 0.716 | 0.434 | 0.280 | 0.140 |
| 1 | 0.608 | 0.668 | 0.242 | 0.291 | 0.175 |
| 2 | 0.608 | 0.668 | 0.242 | 0.291 | 0.175 |
| ALL DIMENSIONS IN INCHES | | | | | |

The plate was moved in the Y-axis direction by turning the handwheel (figure 26, reference 3) to effect the lathe crossfeed movement, while observing the CRT display of the pulse echo from the hole in the plate. The readings for full beam width in table 2 were obtained by setting the dial indicator (reference 4) to zero at the point where the echo pulse on the CRT was 10 percent of maximum above the baseline. The plate was then moved in the Y direction until the pulse reached a maximum

and was then returned to the starting level. The distance traveled, as shown by the dial indicator, represents the width of the beam. The readings for the width of the concentrated portion of the beam were obtained in the same manner except the starting and ending points were 10 percent below the maximum pulse amplitude shown on the CRT display. All tests for Y-axis measurements were conducted with the beam centered over the hole in the X-axis direction so that the beam width in the Y direction was at a maximum.

A plot of the data in table 2, as shown in figure 27, shows that the beam decreases in size on the X-axis while increasing in size on the Y-axis as the beam depth in the material increases.

   b. Weld coverage by the ultrasonic beam. It is necessary to determine the number of scans required to completely cover the weld in a given thickness of material. By utilizing the size of the beam at a specified depth, the portion of the weld covered by each scan can be determined and the distance from the weld centerline (D) can be specified. The data in table 3 is extrapolated using the beam centerline, the beam angle of refraction in the material, the size of the beam at the specified depth in the material, and the thickness of the material containing the weld. Figure 28 depicts the number of scans required versus the thickness of the weld.

Table 3. D Measurement for Beam Centerline Depth in the Weld

| DISTANCE FROM CENTERLINE OF WELD (D) | DEPTH OF BEAM CENTERLINE IN MATERIAL |
|---|---|
| 0.2 | 0.1 |
| 0.4 | 0.2 |
| 0.6 | 0.3 |
| 0.8 | 0.4 |
| 1.0 | 0.5 |
| 1.2 | 0.6 |
| 1.4 | 0.7 |
| 1.6 | 0.8 |
| 1.8 | 0.9 |
| 2.0 | 1.0 |
| 2.4 | 1.2 |
| 2.8 | 1.4 |
| 3.2 | 1.6 |
| 3.5 | 1.8 |
| 4.0 | 2.0 |
| ALL DIMENSIONS IN INCHES | |
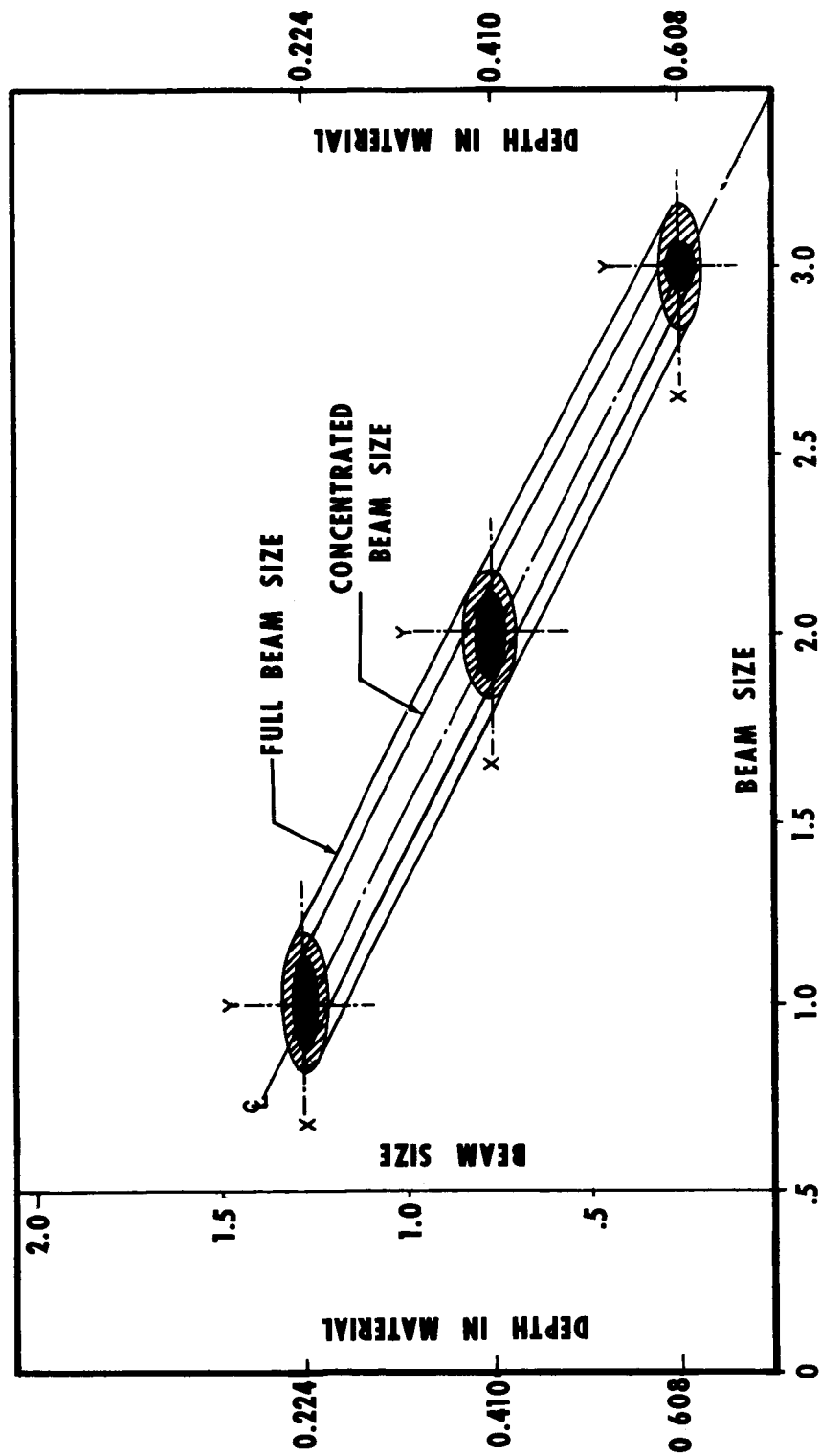
Figure 27.  Beam Size Versus Depth In Material

29

ANGLE OF INCIDENCE 26°
ANGLE OF REFRACTION 63°

.400 & DOWN

.400 TO .700

.700 TO 1.00
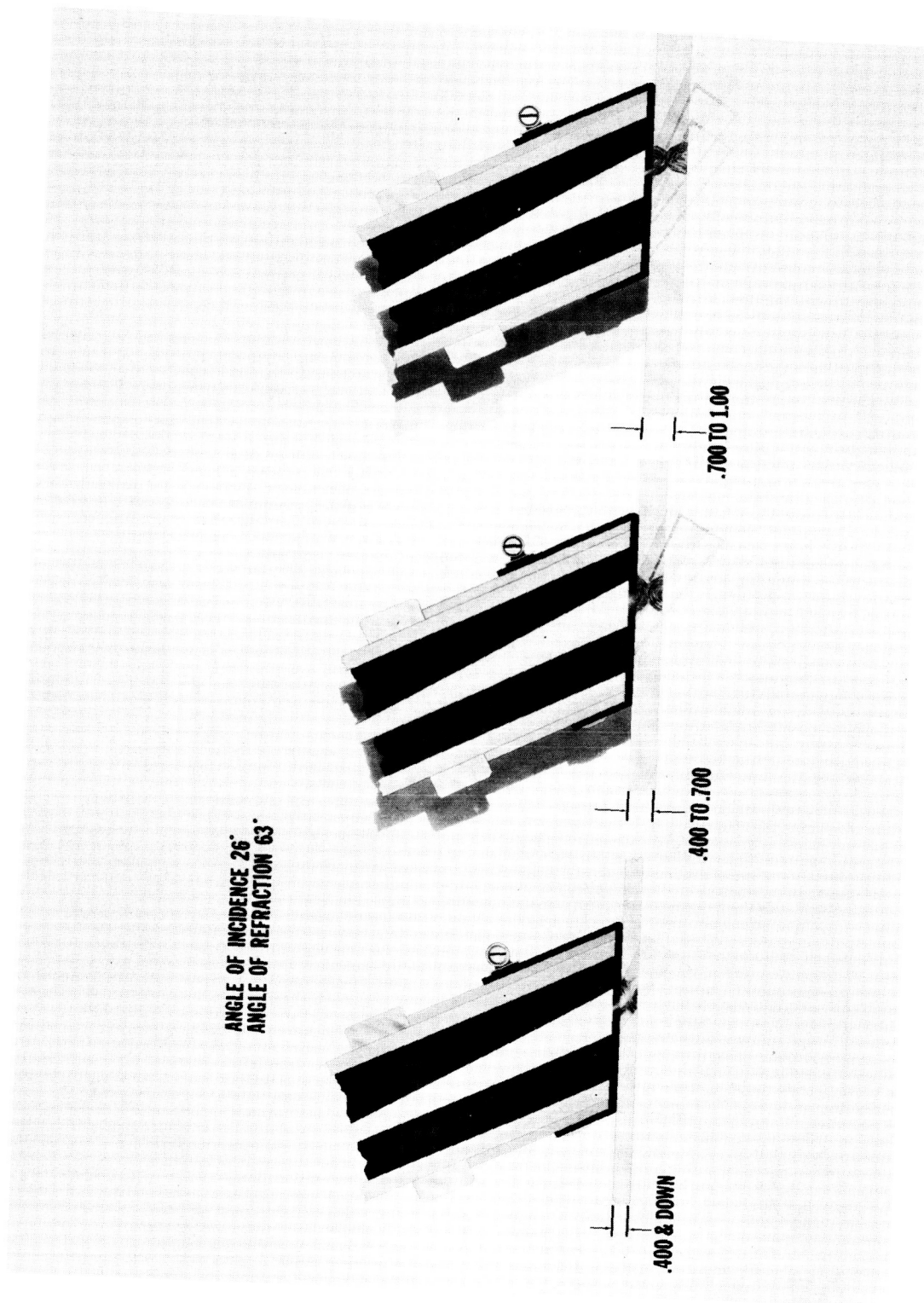
Figure 28. Thickness of Material Versus Number of Scans

30

# SECTION IV. SYSTEM EVALUATION

## A. SYSTEM SETUP

1. _Preliminary Testing._ Preliminary tests were con-- ducted using the test setup shown in figure 12. The vertical aluminum test plate contained a weldment that was tested radiographically and then mounted in the test jig for ultrasonic testing. Lack-of-penetration was simulated by segments of 0.005-inch diameter tungsten wire placed in the center of the weldment. When the water column probe was moved along the weldment, a permanent brush recording was made of the ultrasonic data. The probe scan speed was closely matched to the speed of the recorder during all tests. This insured that the recorder indication of flaw length and position would match the actual flaw length and position in the weldment. Figure 29 shows the correlation of data obtained both radiographically and ultrasonically. The difference in the three ultra- sonic scans is due to varying the sensitivity level of the reflectoscope. Scan I is the proper sensitivity level adjustment for reproducing the defects in the test plate.

A second series of tests were conducted to correlate the depth of a simulated defect in the weldment to the gating of the ultrasonic instrument. Figure 30 shows a typical series of these tests. The test specimen was a 1-inch thick aluminum plate with four holes drilled parallel to the surface at varying depths to simulate defects. For the first scan, the electronic gate of the reflectoscope was set to scan a material thickness greater than 1 inch. The recording labeled, FULL GATE, is the first scan and shows the reflection (indication) of each simulated defect (drilled holes) irrespective of depth. In the second scan, the electronic gate was set to scan from the plate surface to a depth of 1/2 inch. This recording labeled, GATE O - 1/2", shows the flaw indications for each of the three holes within the upper 1/2 inch of the plate. In the third scan, the electronic gate was set to scan from 1/2-inch below the plate surface to the bottom of the plate. The third recording labeled, GATE 1/2" - 1", shows the flaw indication from the single hole in the lower 1/2 inch of the plate. These tests established that it was feasible, by utilizing the electronic gate of the reflectoscope, to set up the system such that flaw indications would only be recorded from predetermined areas of the weld.
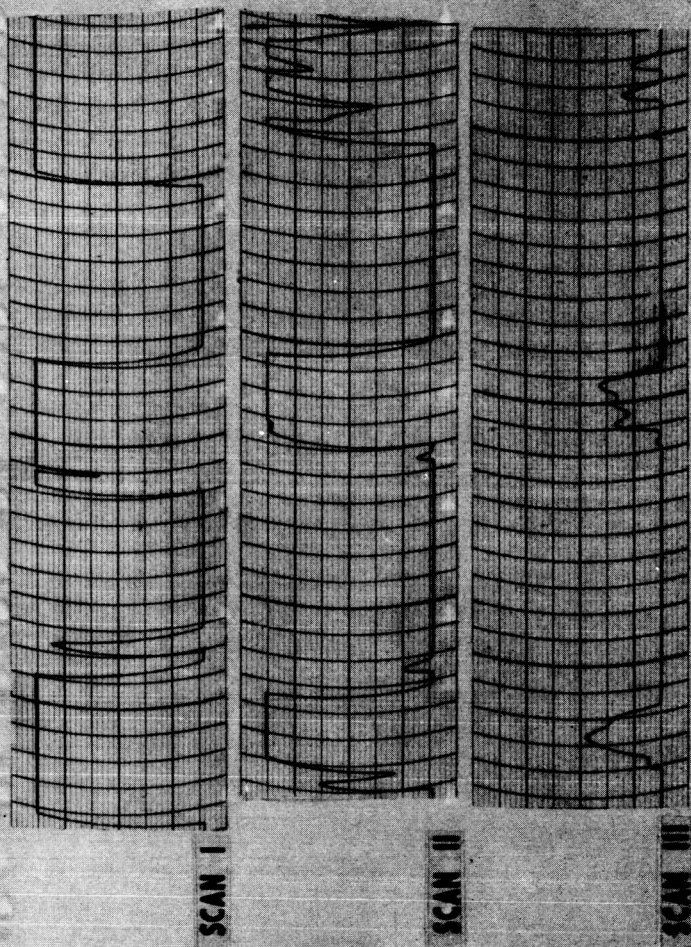
Figure 29. Tungsten Wire Test Plate Data

32
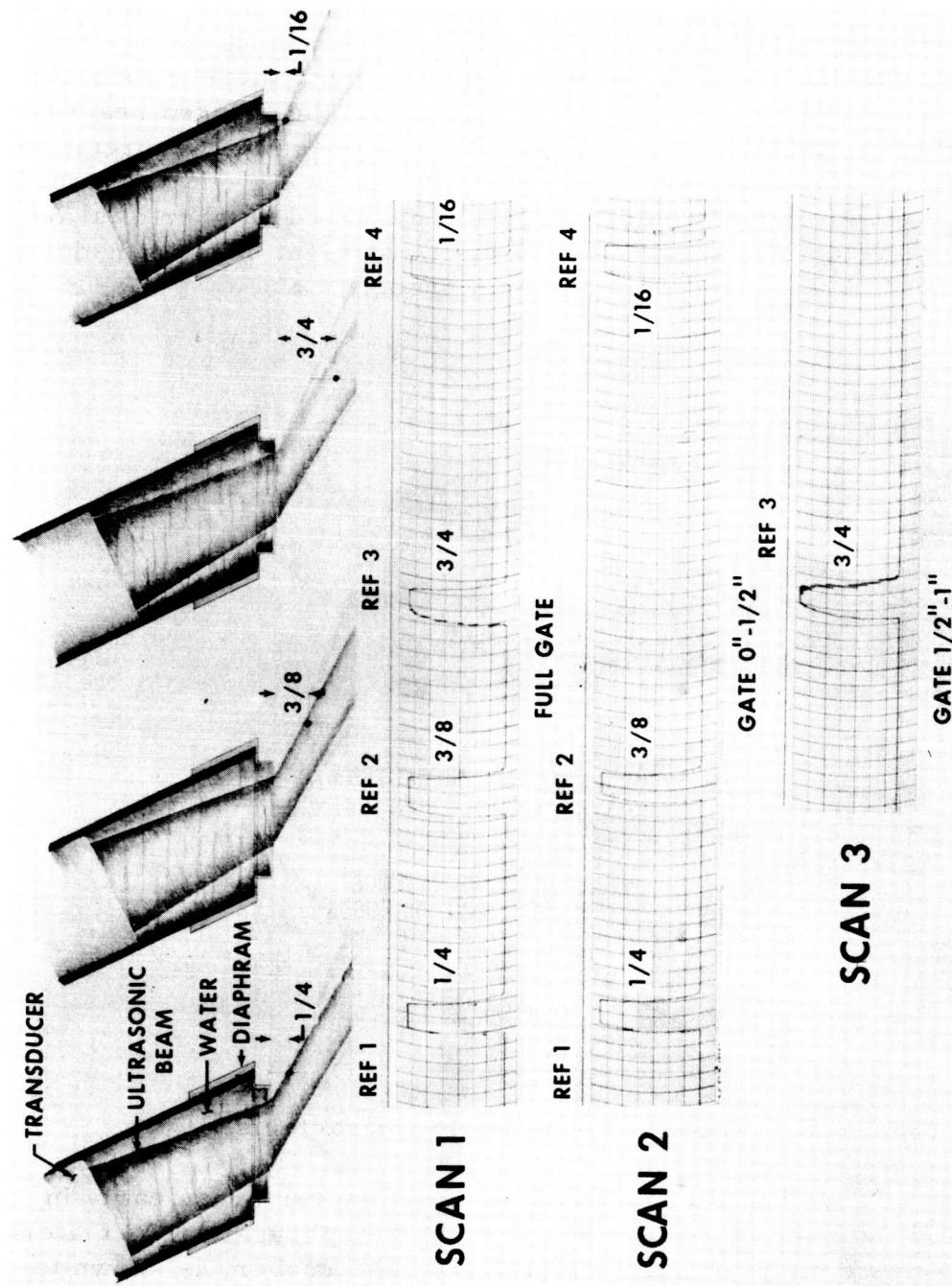
Figure 30. Gating Effects

33

2.    Transducer Selection.   Initially,  it was believed that
a focused beam transducer  would be the best for use in the water column
probe.  Subsequently,  it was established,  as shown in figure 31,  that
the metal of the test material acts as a second lens,  thereby focusing
the sound beam to a finite area.   This meant that the focused beam trans-
ducer would require adjustment for each scan to permit interpretation
of only the flaw content in the focused area of the beam.   In addition,  the
focused beam transducer would require an increased number of scans
for complete weld coverage.   Therefore,  the straight beam transducer
was selected for use in the water column probe.
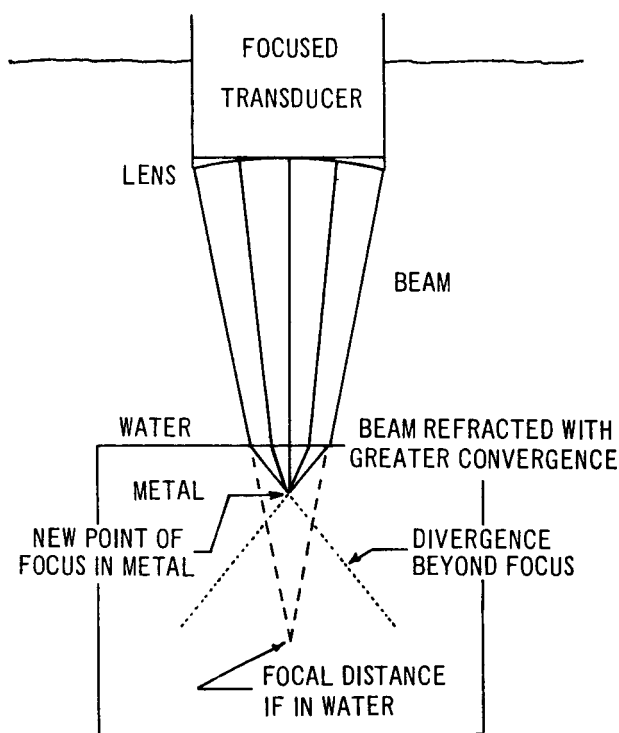


Figure 31.   Focused Sound Beam Characteristics

3.    The Rubber Diaphragm.   Concern arose early in
the program over the durability of the rubber diaphragm.   The material
chosen for this diaphragm,  molded polyurethane rubber,  is known to be
a  durable material that is highly resistant to damage by abrasive
materials.

34

4.   Standard Test Setup for Evaluation.   There are many items that require consideration when setting up the mechanized ultrasonic scanning system for the inspection of welds.   The most important and critical of these factors are the size of the beam in the material area being inspected and the angle of refraction of the sound beam in the material.   These factors, shown in figure 32, will be discussed, followed by a step-by-step electronics setup of the mechanized ultrasonic scanning system.

a.   Depth versus beam size.   By applying values of the angle of refraction and the dimension D, from sound beam centerline to weld centerline, the electronic gate of the ultrasonic instrument may be set up so that only the flaw indications from the weld area being inspected are recorded.

b.   Setting up the electronic gate.   The electronic gate has two controls that are necessary to preset.   Standard reference blocks are used to set the start and the end of the electronic gate.   By setting these controls properly, only the concentrated portion of the sound beam will be utilized.   This operation will eliminate the use of the beam fringe area which is unreliable for inspection purposes.   The standard reference blocks (figure 33) are designed so that one of the holes may be used at the specified depth in the material to set up the start and the end of the electronic gate.   A typical setup is as follows:

(1)   Start of electronic gate.   In this example, the chosen starting point for the electronic gate is at a depth of 0.200-inch below the top surface of the material.   First, the angle of incidence of the probe is set to produce the desired angle of refraction in the material.   The standard angle beam reference block is coated with a thin film of water to couple the sound beam to the material and then placed under the probe.   Then the reference block is moved around under the probe until the desired hole, at the proper depth, is shown by the pulse-echo amplitude on the scope of the ultrasonic instrument. The block is then moved in line with the probe until the amplitude of the return pulse is maximized.   Finally, the start of the electronic gate is positioned so that the pulse amplitude spike falls just within the gate start as shown in figure 34.

(2) End of electronic gate.   A beam width of 0.400 inch was chosen for this example; therefore, the end of the electronic gate would be located 0.600-inch below the top surface of the plate.

35
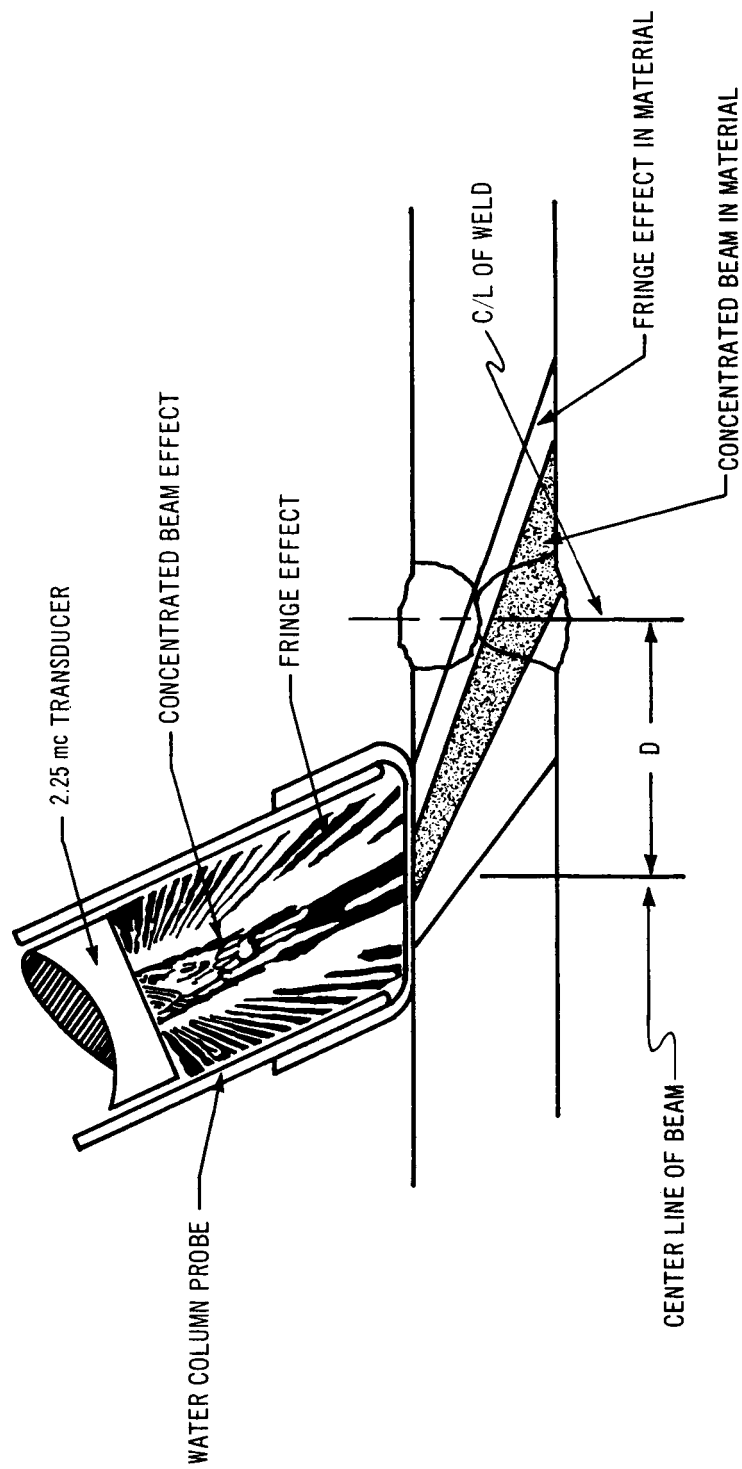
Figure 32.   Sound Beam Characteristics

36

HOLES TO DEPTH .200 INCH
HOLES TO DEPTH .400 INCH
HOLES TO DEPTH .600 INCH
HOLES TO DEPTH .800 INCH

**SECTION A-A**

**SECTION B-B**

**SECTION C-C**

**SECTION D-D**

Figure 33.    Standard Angle Beam Reference Blocks

37

SENSITIVITY CONTROL

GATE START

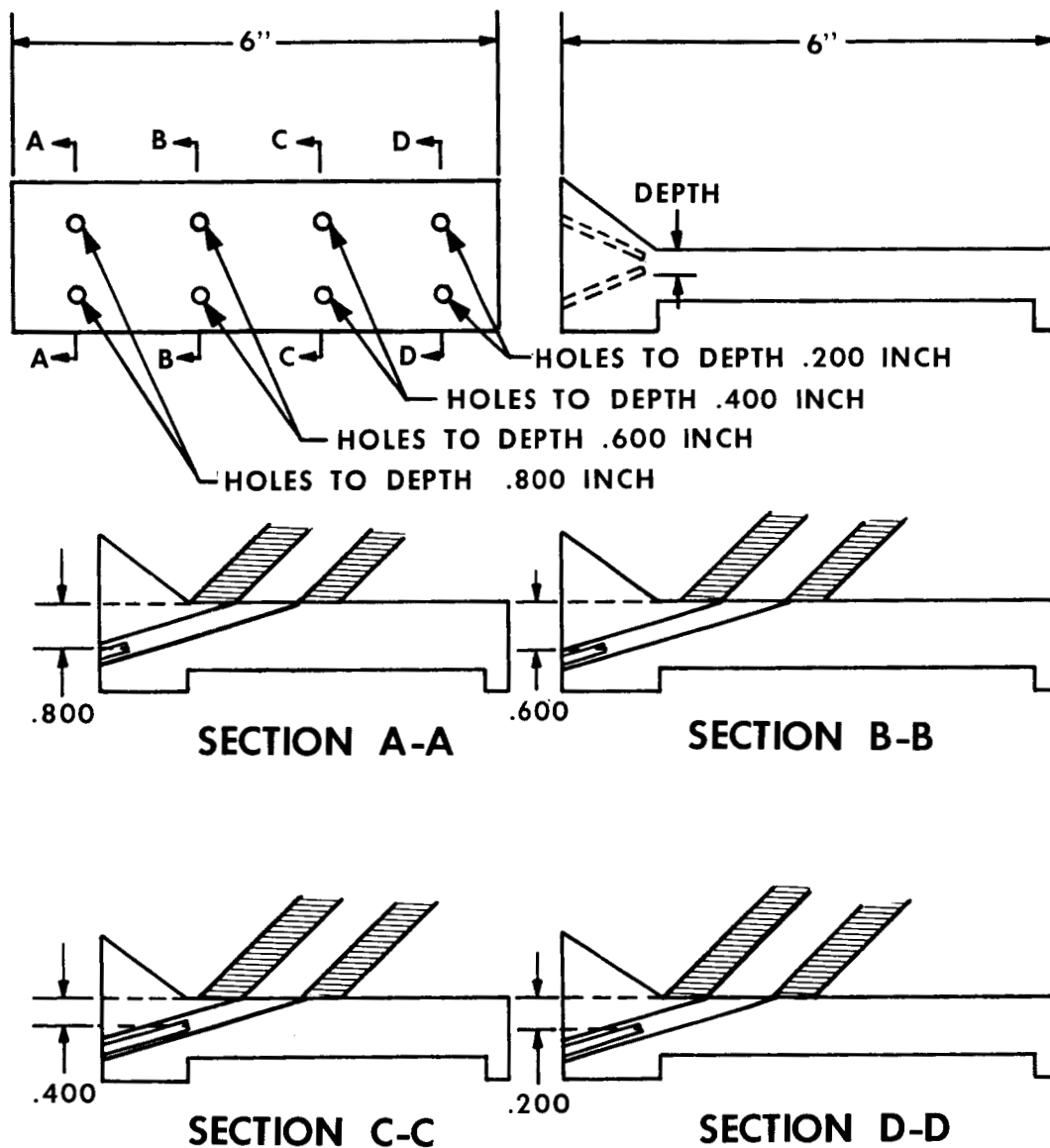GATE END
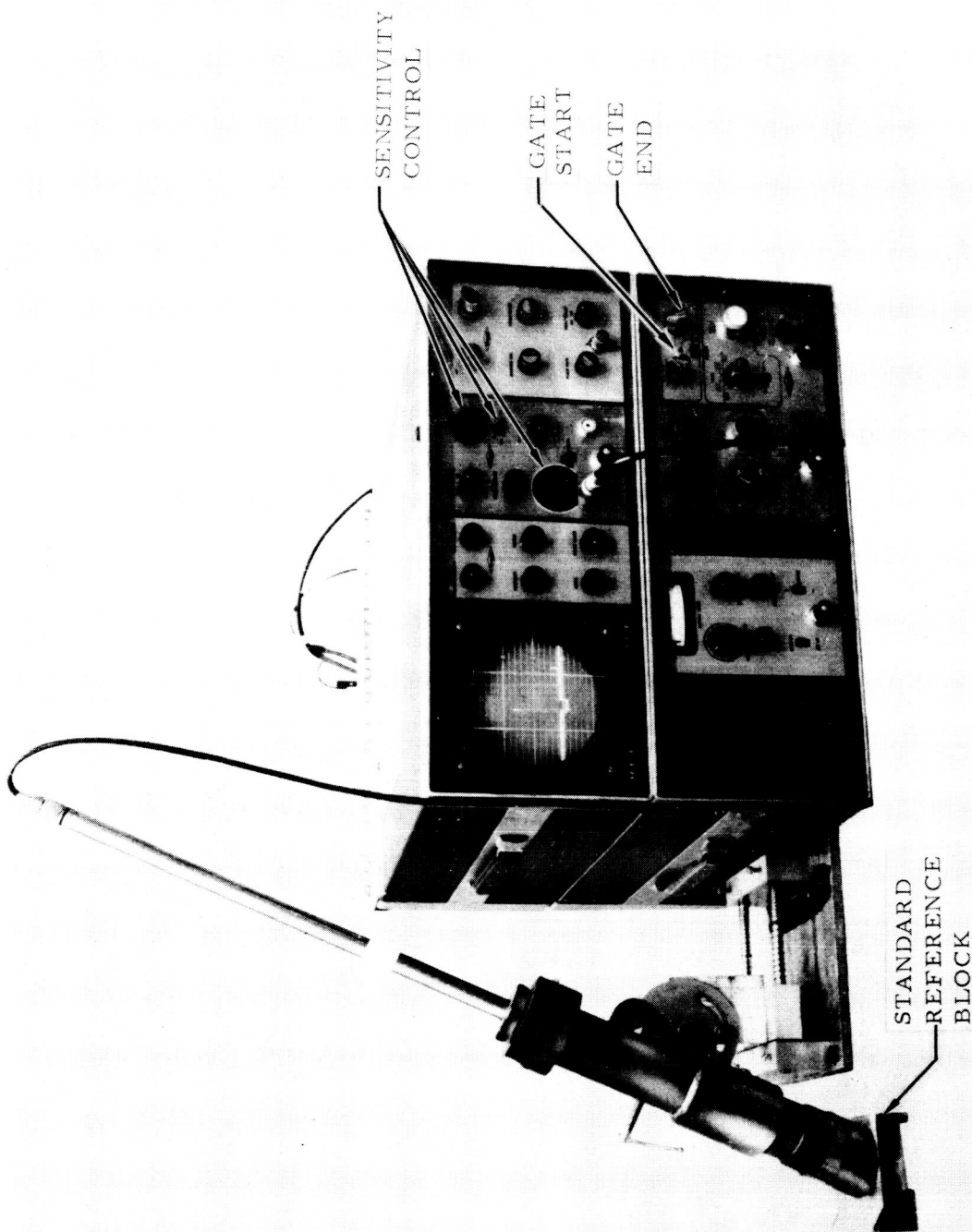
STANDARD REFERENCE BLOCK

Figure 34. Electronic Gate Setup

38

The standard angle beam reference block is used in the same manner as for the start of the gate except that the desired hole at the proper depth is used to end the electronic gate. After the pulse-echo amplitude has been maximized, the gate end is set so that the start of the amplitude spike is inside the gate. The gate end control is shown in figure 34.

(3) System sensitivity. The standard angle beam reference block, containing 0.047-inch diameter flat-bottomed holes ending at various depths, is used to set the system sensitivity so that the recording can be interpreted and marked as acceptable or rejectable flaw indication. A 0.047-inch diameter flat-bottomed hole of proper depth is used to establish the sensitivity level in the same manner used for setting the start of the electronic gate. In this typical setup, the electronic gate had been set for inspecting the weldment area from 0.200 to 0.600-inch below the surface of the plate. Thus, the proper depth flat-bottomed hole from the surface of the reference block would be at 0.400 inch. The reference block is then positioned to produce the maximum pulse amplitude and the sensitivity of the ultrasonic instrument is adjusted so that this amplitude rises only one large division of the grid above the baseline on the face of the scope. The recorder sensitivity level is then adjusted so that this amplitude causes a deflection of one and one-half large divisions or three small divisions above the baseline on the recording. The recorder baseline is established by moving the reference block to the point where there is no pulse-echo amplitude inside the electronic gate on the scope. System sensitivity controls are shown in figure 34.

## B.    LACK-OF-PENETRATION TESTS

1.    General. This series of panel tests were conducted before the standard sensitivity level, (0.047-inch diameter flat-bottom hole equals an amplitude of 1) for the system was established. Therefore, the lower sensitivity level used for the tests is a factor in the system's inability to detect certain sized defects.

The macrographs shown in this report were prepared by cutting the panels along a station line, metallographically polishing the surface, and finally etching the surface to bring out the granular structure and the flaw. The dimensions given relative to flaw size are slightly inaccurate because they were measured after the specimens were prepared for the macrographs.

2. <u>Lack-of-Penetration Data, Panel No. 1.</u> The first
lack-of-penetration panel tested was an 0.800-inch thick aluminum plate
that was machined prior to welding. This machining was performed
in steps varying from true steps 2 inches in length, 0.010-inch and
0.030-inch deep steps, to 3 inches in length. These steps provided a
variety of lack-of-penetration flaws when the machined surfaces were
butt welded. To achieve varying widths and varying thicknesses, the
welding amperage was programmed to increase from 280 amperes to
310 amperes. This test panel was then tested radiographically, scanned
with the manual ultrasonic system, and scanned with the mechanized
ultrasonic scanning system. A positive X-ray, a plot of the manual scan
data, plus the A-scan recording from the mechanized system is shown
in figure 35.

Analysis of the radiograph clearly revealed the predetermined
lack-of-penetration flaws at the 0.030-inch machined step. However, at
the 0.010-inch deep step, the flaw was barely discernible. In other areas
where high welding current reduced the number and size of lack-of-
penetration flaws, radiography failed to detect such flaws, but when
these same areas were manually scanned and then scanned with the
mechanized system, lack-of-penetration was evident.

The total weld area was mechanically scanned four times using
the water column probe. Each scan was made at different distances (D)
from the weld centerline to the probe centerline (figure 35) geometry
of weld coverage. Some variations between the four scans were attrib-
utable to the varying distances (D) which located the beam at different
depths in the weld. However, analysis of each scan recording revealed
that the water column probe readily detected the lack-of-penetration.
Areas designated by the letter B denote clear welds.

In scan IV of figure 35, note the bead effect caused by variations
in the weldment along the bead corner. An investigation of this bead
corner effect was made by physically rubbing the weld bead near the area
of the probe while noting any change in signal amplitude. This investi-
gation proved the system to be sensitive to bead corner effect and this
sensitivity must be considered when evaluating scan recordings. Scans
II and III indicate the variation in width and thickness of the lack-of-
penetration. In scan II, most of the concentrated beam was directed
on the lack-of-penetration, but in scan III, the beam was directed on a
lower portion of the weld. In scan III, the pulse amplitude of the flaw
has diminished indicating that the concentrated beam is not on the flaw;
thus, indicating that the beam has moved out of the flaw area.

# 0.800 AL. PLATE   BUTT WELD   1 PASS EACH SIDE

X—RAY

A-SCAN RECORDINGS

SCAN I   $D=\frac{1}{2}$

SCAN II   $D=\frac{3}{4}$

SCAN III   $D=1$

SCAN IV   $D=1\frac{1}{4}$

Scan I

Scan II

Scan III

Scan IV

GEOMETRY OF WELD COVERAGE

PLATE 85601
SENS.2

DIRECT

BOUNCE

AMPLITUDE

44 43 42 41 40 39 38 37 36 35 34 33 32 31 30 29 28 27 26 25 24 23 22 21 20 19 18 17 16 15 14 13 12 11 10 9 8 7
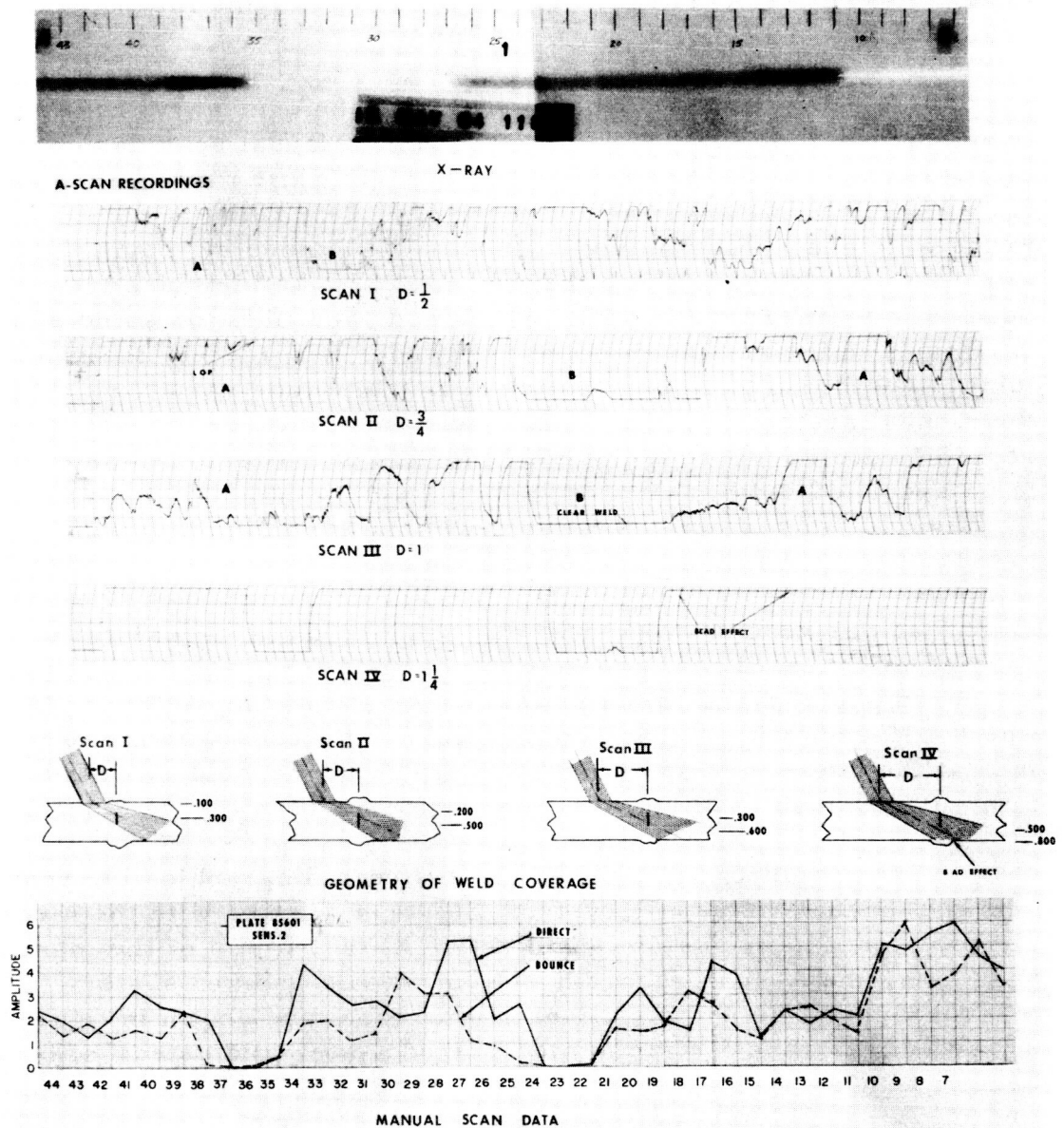
MANUAL SCAN DATA

Figure 35.   Test Data for Lack-of-Penetration, Panel No. 1

41

Considering the different weld coverage made by each scan, the water column probe scan data compared favorably with the manual scan data. Manual scan data includes information from both direct and bounce shots. The sensitivity setting selected depends upon the inherent characteristics of the individual system. No correlations were made between the sensitivity settings selected for the mechanized system and those selected for the manual system.

Manual scanning probe movement techniques vary from the technique used for the mechanized system. Manual scan data is obtained by rocking the probe from left to right while moving the probe back and forth on the surface of the material on a line at right angles to the weldment. Mechanized scan data is obtained by moving the probe along the surface parallel to the weldment at a set distance from the bead. This difference in scanning methods accounts for some of the variations in the maximum pulse amplitudes recorded by the two systems. Another factor contributing to the amplitude variations is that the manual system recorded only maximum amplitude signals without regard to depth, whereas the mechanized system recorded all signals for a specified depth.

3.   Lack-of-Penetration Data, Panel No. 2.   The second of the lack-of-penetration panels tested was of 0.900-inch thick aluminum plate that was welded to intentionally produce lack-of-penetration of varying thicknesses. The plate was designed for a square butt weld with a tapered gap separating the plates before and during welding. The gap was 0.070-inch wide at one end and closed at a constant rate to 0.000 inch at the other end, as shown in figure 36. The weld was made to obtain a 0.250-inch wide lack-of-penetration between the weld beads.

After welding, this panel was tested radiographically, scanned with the manual ultrasonic system, and then scanned with the mechanized ultrasonic scanning system. A positive X-ray, a plot of the manual scan data, the A-scan recordings from the mechanized system, and macrographs at selected stations of this panel are shown in figure 37. These results reveal that the mechanized system did detect lack-of-penetration in varying degrees. To evaluate the variation of scan data, the following analysis was made at various stations along the weld. In scan I, station 29, a maximum amplitude is indicated, but on scans II and III, station 29, reference B, the amplitude has diminished to zero. The macrograph of this area clearly revealed lack-of-penetration approximately 0.0008-inch thick at the top of the weld, reference A, and 0.0001-inch thick at the bottom of the weld, reference B.

42
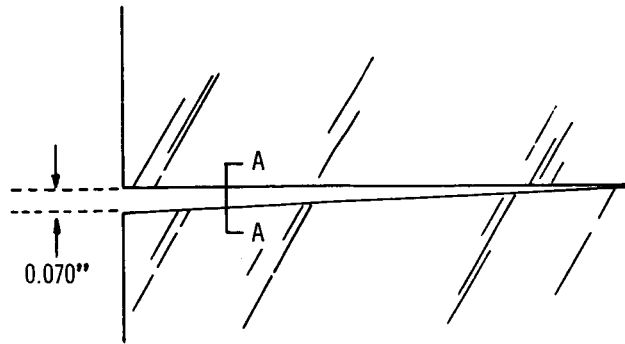
TOP VIEW OF PANEL BEFORE WELDING
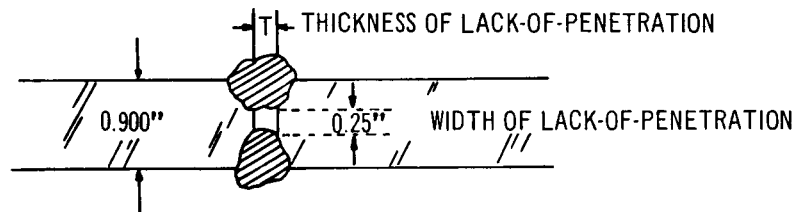


SECTION A-A AFTER WELDING

Figure 36.   Test Panel Design for Lack-of-Penetration, Panel No. 2

Similarly, a comparison at station 23 shows basically the same effect.
At station 20, reference E, the smallest thickness giving a lack-of-
penetration indication on the recording was approximately 0.0005 inch.
Both reference E and reference F show almost no signal amplitude for
these areas, yet the macrographs show lack-of-penetration.   The signal
amplitudes at stations 18 and 11 show the effect of flaw thickness on the
indication for this level of sensitivity.

       4.     Lack-of-Penetration Data, Panel No. 3.   The third
lack-of-penetration test panel was a 0.900-inch thick aluminum plate
welded to intentionally produce lack-of-penetration varying in width.
The panel was designed so as to produce a lack-of-penetration width
of 0.125 inch at one end and tapering to 0.000 at a point two-thirds of
the length down the panel, as shown in figure 38.   One of the disadvantages
encountered in tests on this panel was the extent of porosity in the weld.
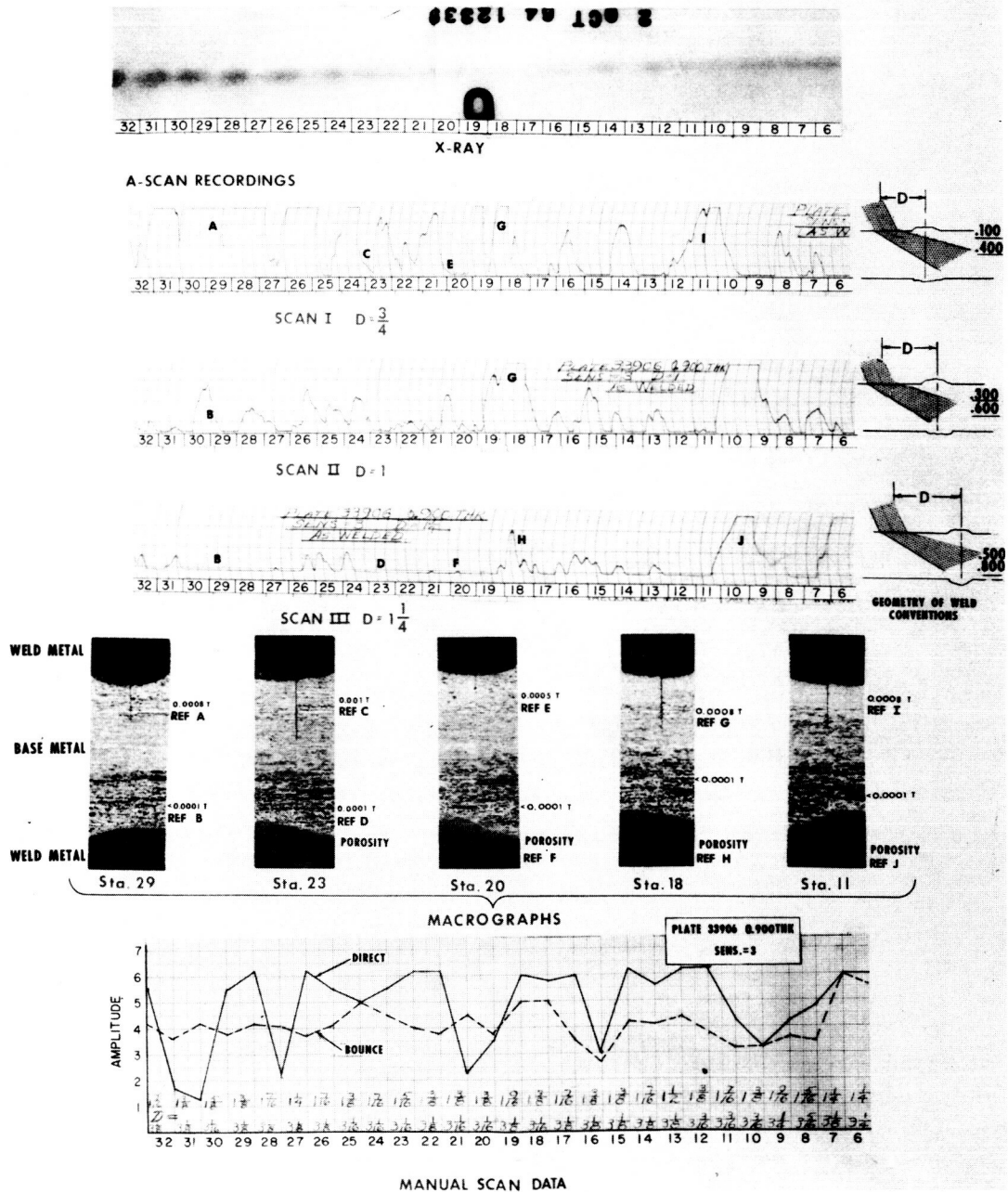
# 0.900 AL. PLATE   BUTT WELD   1 PASS EACH SIDE



Figure 37.   Test Data for Lack-of-Penetration, Panel No. 2
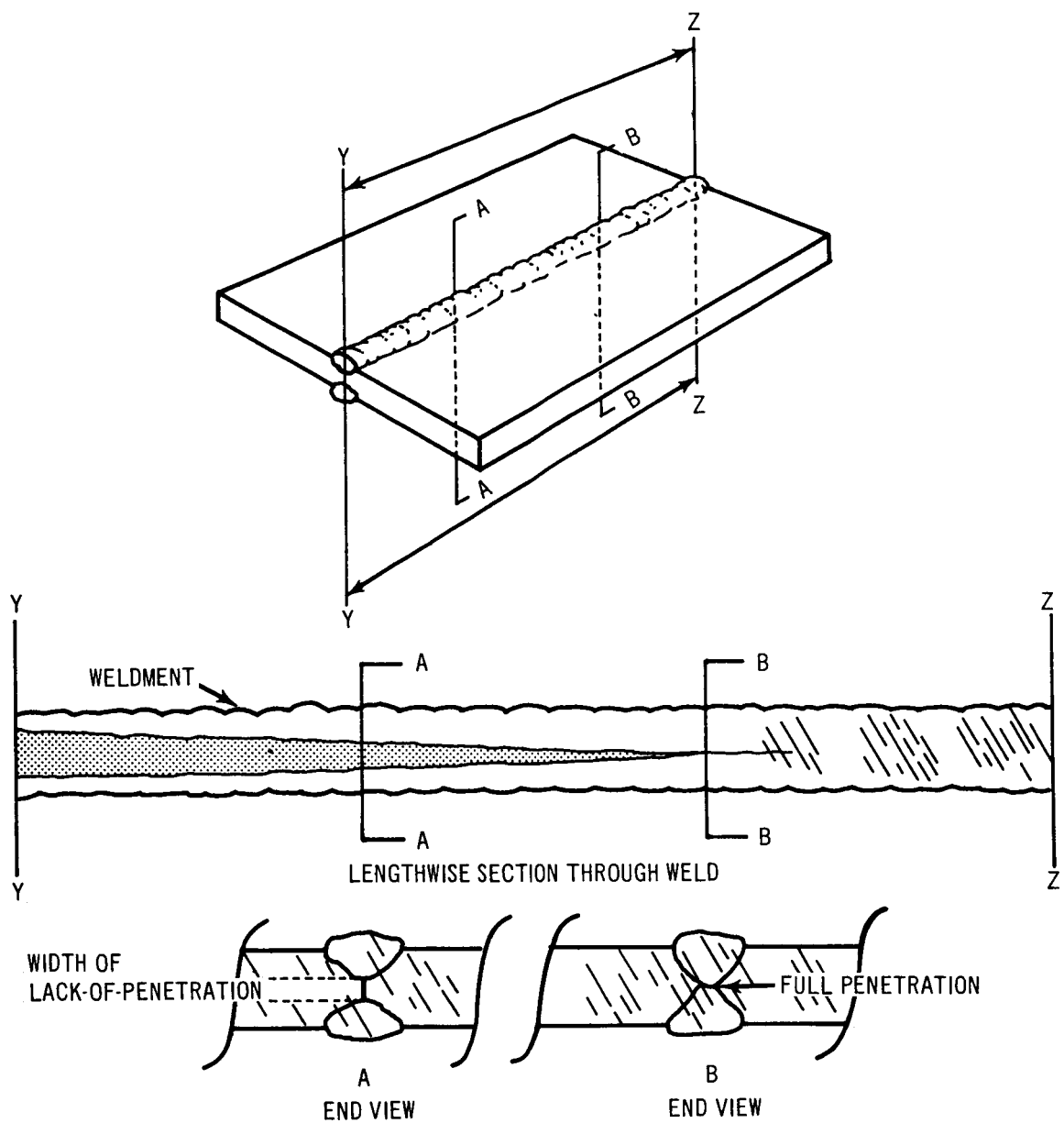
44

Figure 38. Test Panel Design for Lack-of-Penetration, Panel No. 3

This panel, after fabrication, was tested radiographically, scanned with the manual ultrasonic system, and scanned with the mechanized ultrasonic scanning system. A plot of the manual scan data, the A-scan recording from the mechanized system, and macrographs of certain stations along the weld are shown in figure 39. The porosity conditions in the weld required the selection of samples for comparison that were not affected by porosity. At station 28, the width of the flaw detected is approximately 0.030 inch and the thickness is about 0.0004 inch. This was the smallest flaw detectable at this sensitivity level.

5. <u>System Sensitivity Level Effects.</u> Variations in signal amplitude between scan recordings of a given area show the effect of flaw width, thickness, and length upon the system's capability to detect flaws at a specified sensitivity level. The detection of lack-of-penetration flaws less than 0.0005-inch thick, or where the joint approaches being a mechanical bond, requires an increase in the sensitivity level. However, when higher sensitivity levels are used, flaw indications caused by the crystalline structure of the material could adversely affect evaluation of the recordings.

C. LACK-OF-FUSION TEST DATA

Testing the mechanized ultrasonic scanning system for the detection of lack-of-fusion flaws proved most difficult since this type of flaw is not easily simulated. The test panel was designed for a U-joint butt weld since lack-of-fusion occurs most often in this type of weld. The U-joint butt weld consisted of a penetration pass followed by multiple filler passes. In this type of weld, lack-of-fusion most often occurs between the filler weldments.

Lack-of-fusion flaws are hard to detect by the radiographic method due to the difficulty in orienting the flaw plane with the radiographic plane. A radiograph of the test panel was obtained. The radiograph showed a clear weld except for two areas which indicated the possibility of lack-of-fusion. Scanning with the manual system provided definite flaw indications which correlated with the results of the mechanized ultrasonic scanning system. Four scans were made with the mechanized scanning system using different probe centerline-to-weld centerline distances for each scan. The results were:

| Distance (D) | Indication |
|---|---|
| 1/2 inch | Slight indication of a flaw in one area. |
| 3/4 inch | No flaw indication. |

# 0.900 AL. PLATE  BUTT WELD  1 PASS EACH SIDE
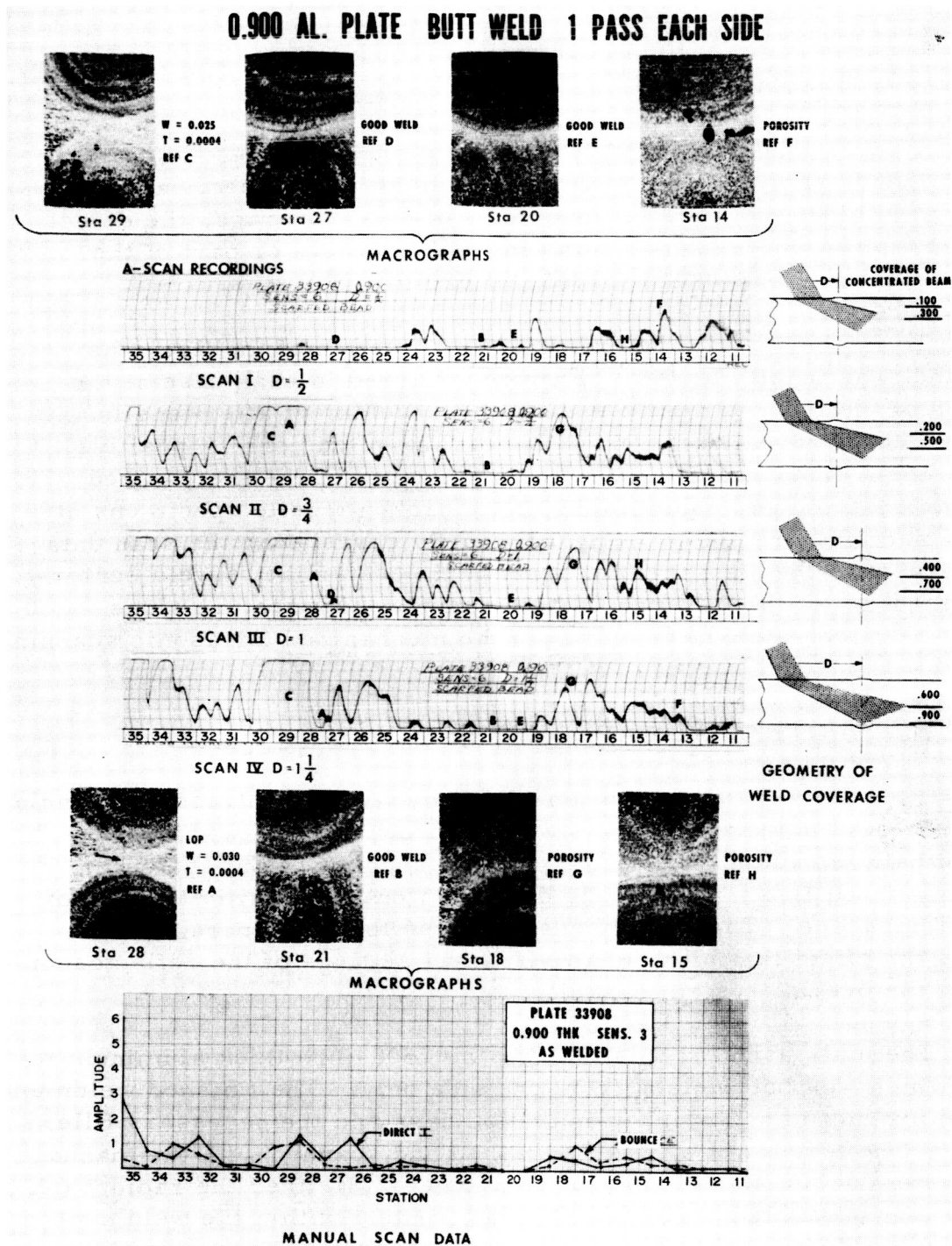


Figure 39.   Test Data for Lack-of-Penetration, Panel No. 3

47

| Distance (D) | Indication |
|---|---|
| 1 inch | Slight indications. |
| 1 1/2 inch | Definite indication obtained; based on geometry of weld coverage, the defect was located in the lower part of the weld, 0.600 to 0.800 inch. |

To further verify the existence and location of the flaw, the test panel was tensile tested. Failure occurred in each case at the location of the flaw. An examination of the weldment after tensile testing clearly revealed the existence of lack-of-fusion. A positive X-ray, the A-scan recording for the fourth scan of the mechanized scanning system, and photographs of the broken tensile specimens at certain sections are shown in figure 40. By correlating the scan data with respect to the distance (D), from beam centerline to weld centerline, the depth of the flaw can be determined. This feature alone greatly enhances the practicability of the mechanized ultrasonic scanning system.

## D.    POTENTIAL CAPABILITIES

During the evaluation of the mechanized ultrasonic scanning system, it was noted that the system's indications of flaw thicknesses and widths were subject to variation. The success of the system in detecting small flaws was largely dependent on the sensitivity level of the reflectoscope. The data discussed in the following paragraphs reveals the effect that high sensitivity level settings of the reflectoscope have on the overall system capabilities.

The plate used for this test was a 0.500-inch thick aluminum test plate, which was butt welded from one side only. The finished weldment was the product of a through-penetration pass and the necessary filler passes. The test panel was radiographed and scanned with the manual scan system at the standard sensitivity levels. Neither the radiograph nor the manual system revealed any flaw content within the weldment. When the plate was scanned with the mechanized system, no definite flaw indications were noted, even when the sensitivity level was varied, because flaw definition was masked by the bead effect. However, after scarfing and grinding the weld bead flush with the plate surface, further scanning with the mechanized system did reveal flaw indications. These flaw indications became more pronounced at high sensitivity levels,

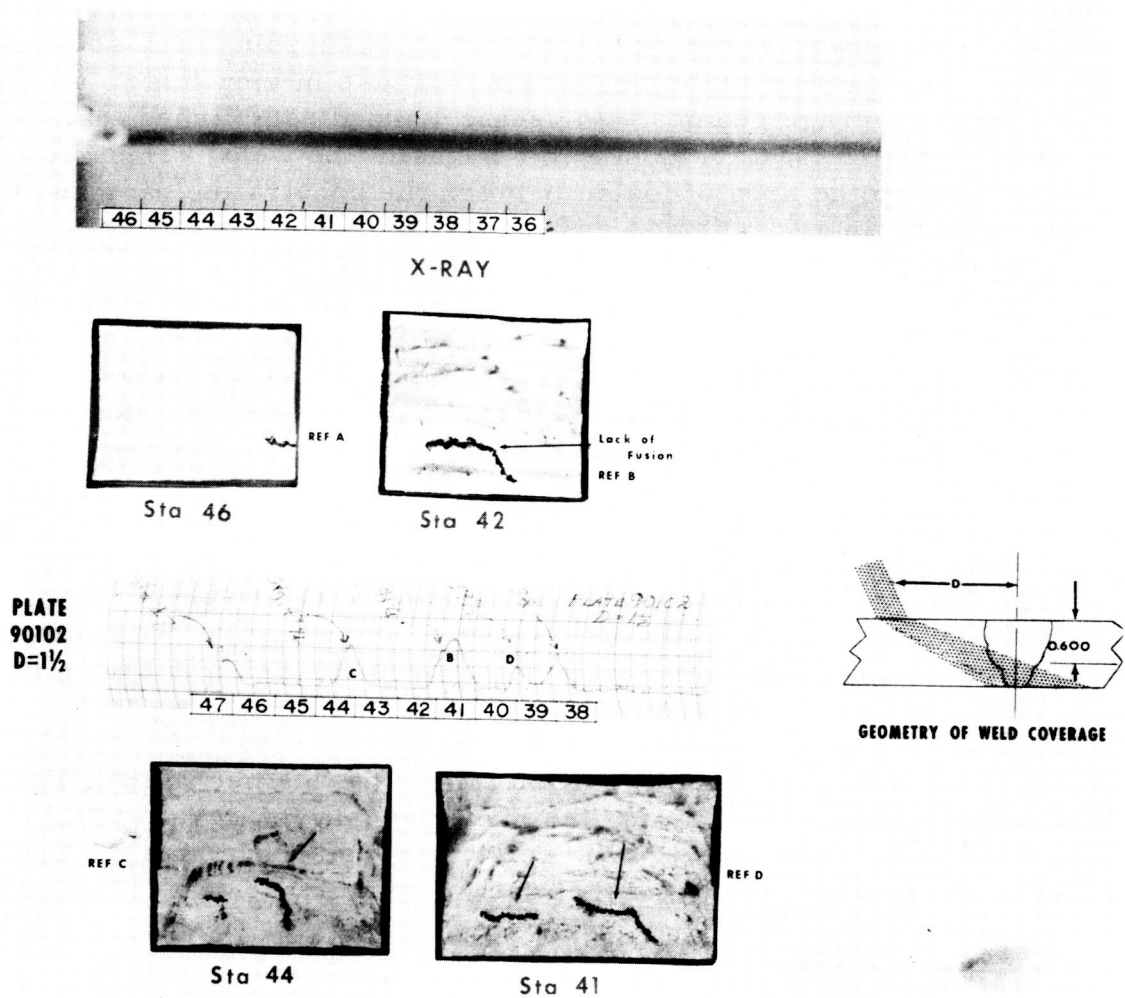# 0.800 AL. PLATE BUTT WELD U JOINT ALL PASSES SAME SIDE



X-RAY



Sta 46

Sta 42

Lack of Fusion

REF A

REF B

PLATE
90102
D=1½



47 46 45 44 43 42 41 40 39 38



GEOMETRY OF WELD COVERAGE

REF C

REF D

Sta 44

Sta 41

Figure 40.   Test Data for Lack-of-Fusion Panel

49

i.e., any level above the recommended sensitivity level of the reflecto-
scope for normal testing. The test panel was dissected at the areas
where the mechanized scanning system indicated flaw content. These
areas were then metallographically polished, etched, and then examined
under 50-power magnification. Evidence of microporosity and lack-of-
fusion were visible. Photomicrographs of these areas definitely show
the flaws to exist in the weldment. The positive X-ray, the three A-scan
recordings, and the photomicrographs are shown in figure 41.

At station 15 in figure 41, the A-scan recordings for scans I and
II clearly show a flaw indication by the increase in amplitude. Analysis
of the weld coverage geometry for scans I and II established that the
flaw at station 15 is in the upper two-thirds of the weld. This area
corresponds to the area of fusion between the penetrating pass and the
filler passes.

The lower third of the weld was covered by scan III. At station
15 of scan III, no flaw indication was noted. At station 22 of scan I, an
indication of a small flaw was noted. The panel was dissected at this
station and prepared for further study. The study revealed that the flaw
was microporosity as shown in the photomicrograph in figure 41.

Scan II, from station 15 through station 22, shows several small
amplitude variations. Since these variations did not appear in scan I
or scan III, they were not investigated. However, at station 25, a
definite flaw indication was noted in scan II and scan III. Investigation
of this area showed the flaw to be microporosity, which is shown in the
photomicrograph in figure 41.

The detection of microporosity flaws by the mechanized ultra-
sonic scanning system utilizing the higher sensitivity level setting
(above recommended level) of the reflectoscope, illustrates the detection
potential available when using the mechanized ultrasonic scanning system.

E.    SYSTEM VARIABLES AND LIMITATIONS

There are many factors affecting the system's capability
and reliability. The most significant variables and limitations are
summarized as follows:

(1)    The setting of the angle of incidence for the water
column probe is very critical; this setting determines
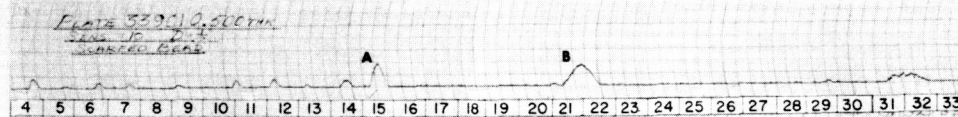the angle of refraction of the sound beam in the
material.

50

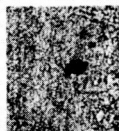# 0.500 AL. PLATE BUTT WELD 2 PASSES 1 SIDE
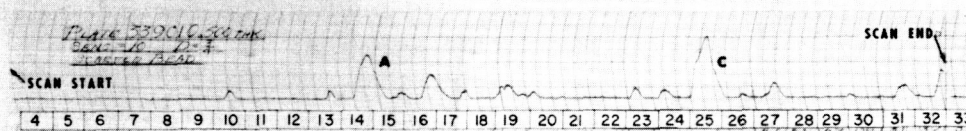


X RAY WELD (UNSCARFED)

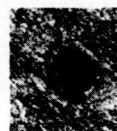**A-SCAN RECORDINGS**



SCAN I D=$\frac{1}{2}$

Lack Of Fusion (400X) 1micron x 0.100 Long (approx.)

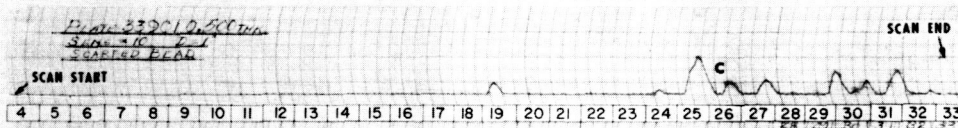Porosity (100X) 0.0001 (approx)



SCAN II D=$\frac{3}{4}$

Porosity (100X) 0.0008 (approx)



SCAN III D=1

GEOMETRY OF WELD COVERAGE

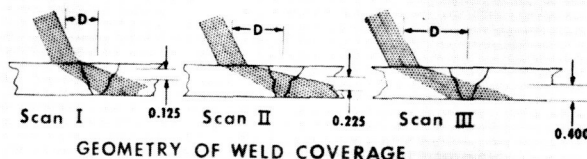Scan I  0.125  Scan II  0.225  Scan III  0.400

Figure 41. Test Data from Higher Sensitivity Level

51

(2)    The distance from the weld centerline to the sound beam centerline, as the sound beam exits from the probe, is critical because this is one factor in determining the depth of weld coverage. It is imperative that this distance remain the same throughout the entire scan to insure complete coverage of the weld at the specified depth.

(3)    The alignment of the probe at right angles to the weld is a very important factor; this alignment holds the sound beam in the best possible position for the optimum detection of flaw content in the weld.

(4)    The pressure on the probe tip is another important factor because variations will change the distance between the transducer and the material being inspected. If equal pressure is not maintained throughout both the setup and the testing, some flaw content in the weld may not be recorded due to the electronic gate settings.

(5)    A layer of couplant must be constantly maintained on the surface of the material during testing. If there is an insufficient amount of couplant on the material, the ultrasonic beam cannot enter the material being inspected.

(6)    The flaw may lie in a plane parallel to the sound beam. If this is the case, then the flaw would be rendered virtually invisible to the ultrasonic beam.


SECTION V. PRODUCTION APPLICATIONS


A.    EVALUATION OF PROTOTYPE SYSTEM

Special tooling, utilizing the radiographic mechanized equipment, was designed to hold and position the water column probe. Inasmuch as the radiographic boom was mechanized, the adaptation consisted primarily of removing the film reel unit and mounting the

special tooling for the probe. Thus, a prototype mechanized ultrasonic scanning system was readily provided. Prototype tooling units were fabricated for two separate applications to weld inspection on the S-IC propellant tanks.

1. Gore-to-Gore Weld Evaluation. The radiographic boom with the special tooling shown in figure 42 was used to evaluate the problems that would be encountered in a production system. Several gore-to-gore welds were inspected utilizing the prototype mechanized scanning system. In each case, the data recorded from the prototype mechanized system was compared with the radiographic data and in some areas flaw indications were noted where the radiographs indicated nothing or a clear weld. These flaw indications were then scanned by the production manual scanning group. Flaw content indicated by the mechanized system was, in each instance, confirmed by the manual scanning group. Some of the problems encountered in using the prototype tooling were as follows:

(1)  Probe positioning in relation to the weld bead was not maintained as required because of the inflexibility of the prototype tooling; the causes were as follows:

● The binding of the springs on the guide pins prevented the angular movement necessary for the wheels to follow the contour of the gore.

● The wheels for contour following were located an excessive distance from the probe tip, which prevented a true plane from being established at the probe tip. This would cause the probe tip to either bind on the surface at times or be at the wrong angle for properly inspecting the weld.

(2)  There was no way to apply a uniform layer of couplant. As a result, there was excessive couplant in some areas and insufficient couplant in others. The problem was remedied by a spray nozzle provision in the production system design. (Reference section II, paragraph C.)

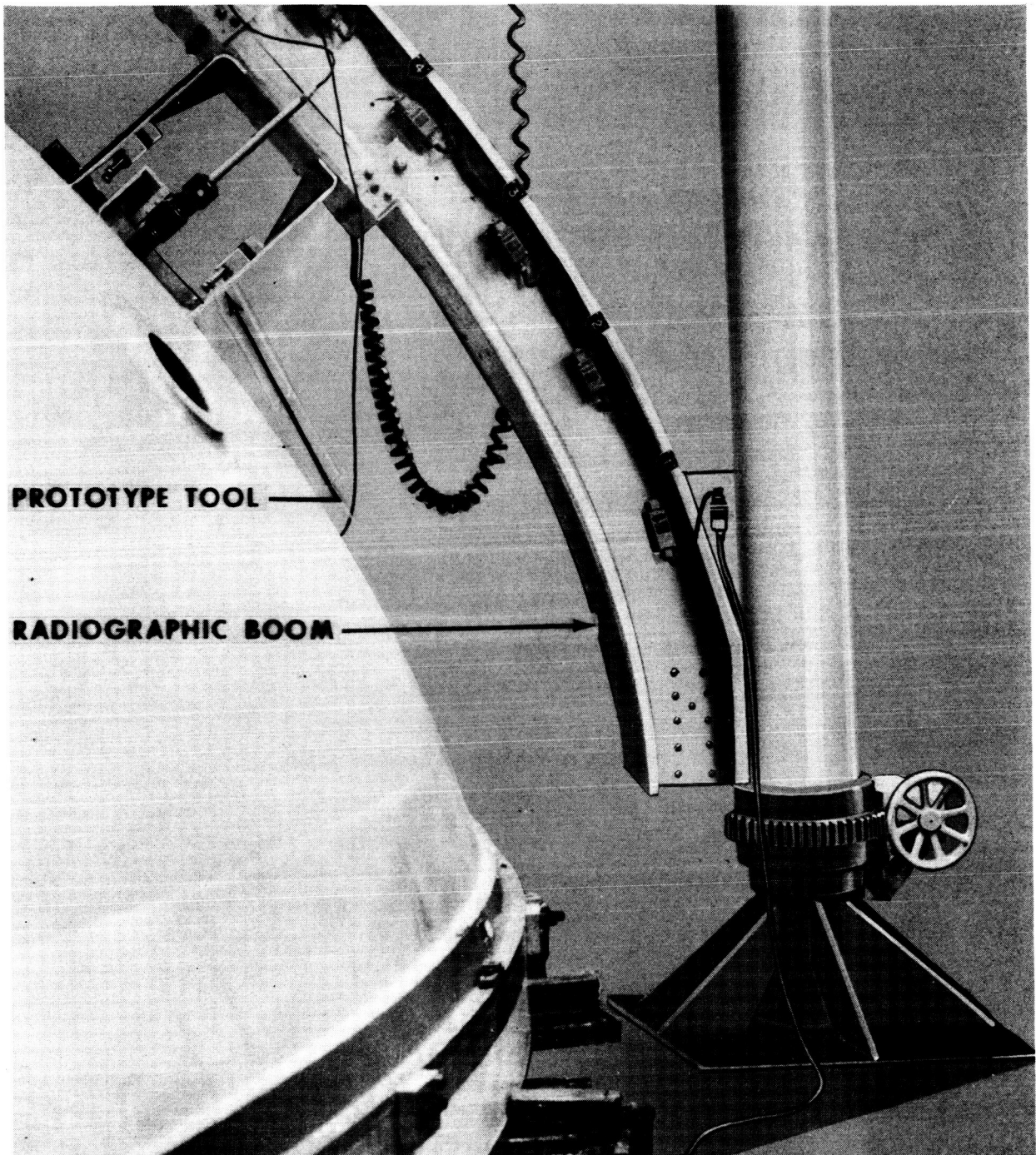**PROTOTYPE TOOL**

**RADIOGRAPHIC BOOM**

Figure 42.   Prototype Tooling for Gore-to-Gore Weld Evaluation

2.    Y-Ring to Bulkhead Weld Evaluation. The radiographic elevator was used to mount the special tooling (prototype tool) as shown in figure 43. This setup permitted analyzation of the problems that were encountered in the production system, which was used to inspect the Y-ring-to-bulkhead, Y-ring-to-skin, and the skin-to-skin welds. Satisfactory performance was obtained with this setup, except for one problem: the difficulty of maintaining uniform couplant due to the type of couplant applicator.

Several production welds were inspected with the prototype system. In each case the data from the prototype mechanized ultrasonic scanning system was compared with the radiographic data. In some areas, flaw indications were noted where the radiographs indicated nothing or a clear weld. These flaw indications were then scanned by the production manual scanning group. Flaw content indicated by the mechanized system was, in each case, confirmed by the manual scanning group.

## B.    PRODUCTION SYSTEM

The final production system has been designed, but was completed too late for use during S-IC propellant tank fabrication at MSFC. All of the problems and system variables that were encountered in the prototype tooling were given consideration during final design of the production system. The final production system utilizes the improved water column probe. Section II, System Description, and figures 17, 18, and 19 of this report provide a description of the production system design.

## SECTION VI.   WATER COLUMN PROBE IMPROVEMENTS

During the evaluation of the system, erroneous signals were noted. These indications fell in the usable range of the pulse echo returned from the material and were believed to be wave-refracted pulses that were reflected from the diaphragm. Therefore, further study was made to improve the water column probe performance. An acoustic absorber and the near field were the objects of this study.

## A.    ACOUSTIC ABSORBER

1.    Selection of Material. Before designing an acoustic absorber, it was necessary to select a material that would best eliminate the extraneous echoes in the water column probe. After a literature

PROTOTYPE TOOL

RADIOGRAPHIC
ELEVATOR

Figure 43. Prototype Tooling for Y-Ring-to-Bulkhead Weld Evaluation

56

search, it was found that neoprene has an attenuation of 22 db/cm* at
a frequency of 2.25 mc while dry air has an attenuation of only 11 db/cm*.

In addition, foam rubber was suggested as a material which would
possibly eliminate the echoes. Therefore, it was decided that abosrbers
of both neoprene and foam rubber would be fabricated in order to select
an absorber.

2.     Design.  The beam divergence was calculated in
order to determine the maximum beam diameter when passing through
the polyurethene rubber diaphragm.  The formula* for computing the
beam divergence as the beam travels through water is given below.
The divergence angle ($\emptyset$) is shown in figure 44.

$$\text{Sin } \emptyset = \frac{1.22\lambda}{D} = \frac{1.22v}{fD}$$

Where:     $\lambda$ = Wavelength - v/f
           f = Frequency in cycles
           D = Diameter of transducer face
           v = Acoustic velocity

By Substituting:     D = 0.75 in. (1.9 cm)
(For water            f = 2,250,000 cps
column probe)         v = 149,000 cm/sec in water

Therefore:     Sin $\emptyset$ = 0.0425
               $\emptyset$ = 2.5°

The geometry of the water column probe was then studied to
determine the necessary length of absorber that would be required to
absorb  the reflected echos that were returning from the rubber dia-
phragm as shown in figure 44.  The necessary length was determined
geometrically by using the laws of incidence and reflection.  It was
calculated that, when the transducer was at a maximum distance of 8
inches away from the probe tip center, the average length of absorber
necessary to stop extraneous echoes was 1.71 inches.  This means that
when the absorber was installed, the transducer and probe center tip
could be no closer than 1.71 inches.  However, since this region was
in the near field, no loss in performance should be noted.

*McMaster, Robert C., Nondestructive Testing Handbook, Ronald
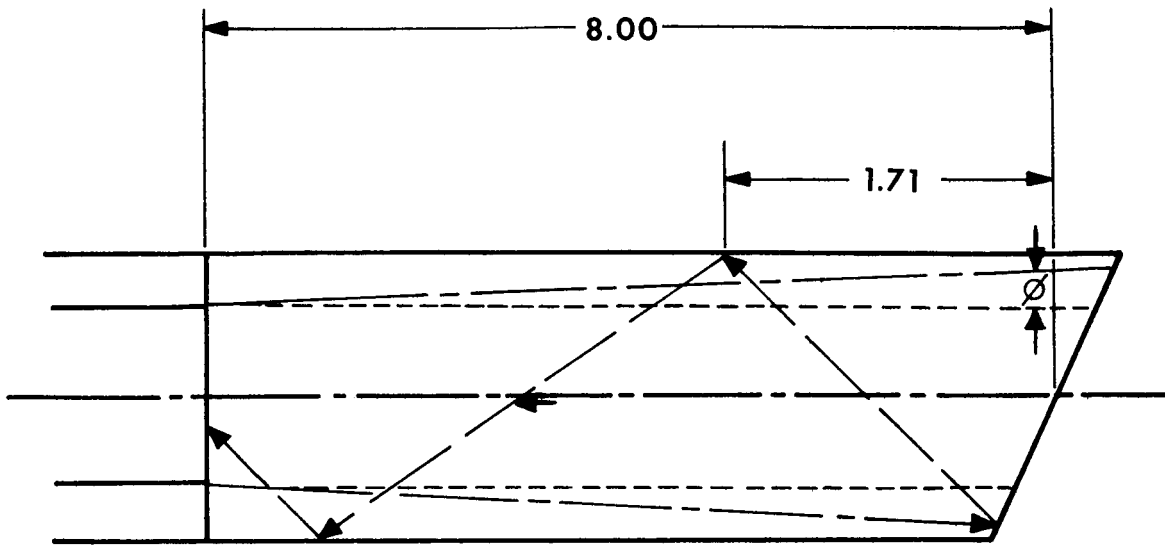  Press Company, New York, New York, 1959.

57

Figure 44. Sound Beam Divergence

3.    Fabrication.   Neoprene (Redstone Arsenal No.
RA24160 NE) with a Brinell hardness of 60 was obtained in thicknesses
of 1/16 and 1/8 inch.   Three absorbers of 1/16-inch thicknesses were
fabricated, each with different surface finish.   One absorber was made
so that the exposed surface was smooth (mold finish).   A second was
molded and the interior surface was roughed with a wire brush and num-
ber 60 sandpaper.   The third absorber was fabricated with the interior
surface very rough (lacerated the entire width with slashes 0.010 to
0.020-inch deep at distances of 1/32-inch apart and then roughed with
a wire brush and number 60 sandpaper).

    One absorber of 1/8-inch thickness was made with a smooth sur-
face (mold finish) and a second absorber was fabricated with the surface
very rough (lacerated the entire width with slashes 0.010 to 0.020-inch
deep at distances of 1/32-inch apart and then roughed with a wire brush
and number 60 sandpaper).

    An absorber was also made to simulate a 3/16-inch thick neo-
prene absorber.   A 1/18-inch thickness was used as an outside lining
and a 1/16-inch thick layer of smooth (mold finish) neoprene was used
as a sleeve inside the thicker absorber.   This lamination was necessary
because the 3/16-inch thick neoprene was too rigid for easy insertion
into the probe.

58

All of the noeprene absorbers were fabricated with a centerline length of 1.71 inches and were cut so as to completely line the inner surface of the probe without overlapping. However, the foam rubber absorber was cut to a maximum circumferential length of 2 inches, which only partially covered the inner surface. From the geometry of the probe, it appeared that this width would be adequate to absorb the echos. It was later determined, through testing, that an absorber which extended around the entire inner surface of the probe eliminated more echos than did one that partially covered the surface.

4.    Testing. Acoustic absorber tests were conducted using the water column probe and a Sperry UR reflectoscope. The probe was positioned on the 0.800-inch thick reference plate for beam size (figure 8) so that the reflectoscope displayed the echo pulse of the 0.062-inch diameter flat-bottom hole. The water column probe was then secured by C-clamps so that the probe could be removed and replaced by means of a slider without affecting the angle of incidence. The controls on the reflectoscope were adjusted with a sensitivity setting of 3. The control settings and test setup are shown in figure 45. Once adjusted, the settings were maintained throughout the tests.

Each acoustic absorber was placed in the probe and the pulse return display was obtained on the reflectoscope. Figures 46 through 53 show photographs of the pulse return display for each absorber.

5.    Evaluation. From the previous photographs, it was determined that the smooth surfaced neoprene more effectively eliminates the echo than does the rougher surface neoprene. When the 1/8-inch thick and the 1/16-inch thick neoprene were combined, simulating a 3/16-inch thickness, the extraneous echoes were virtually eliminated. The foam rubber was found to be ineffective toward the elimination of echos.

Once it was established that the simulated 3/16-inch thick smooth neoprene was the best absorber, the probe was set up, as shown in figure 45, on the 0.800-inch thick reference plate for beam size (figure 8). The photographs in figures 54 and 55 were taken of the pulse return display on the reflectoscope. Separate photographs were taken both with and without the acoustic absorber. Comparison of the photographs revealed that the absorber eliminated the extraneous echoes for any useful flaw echo signal.
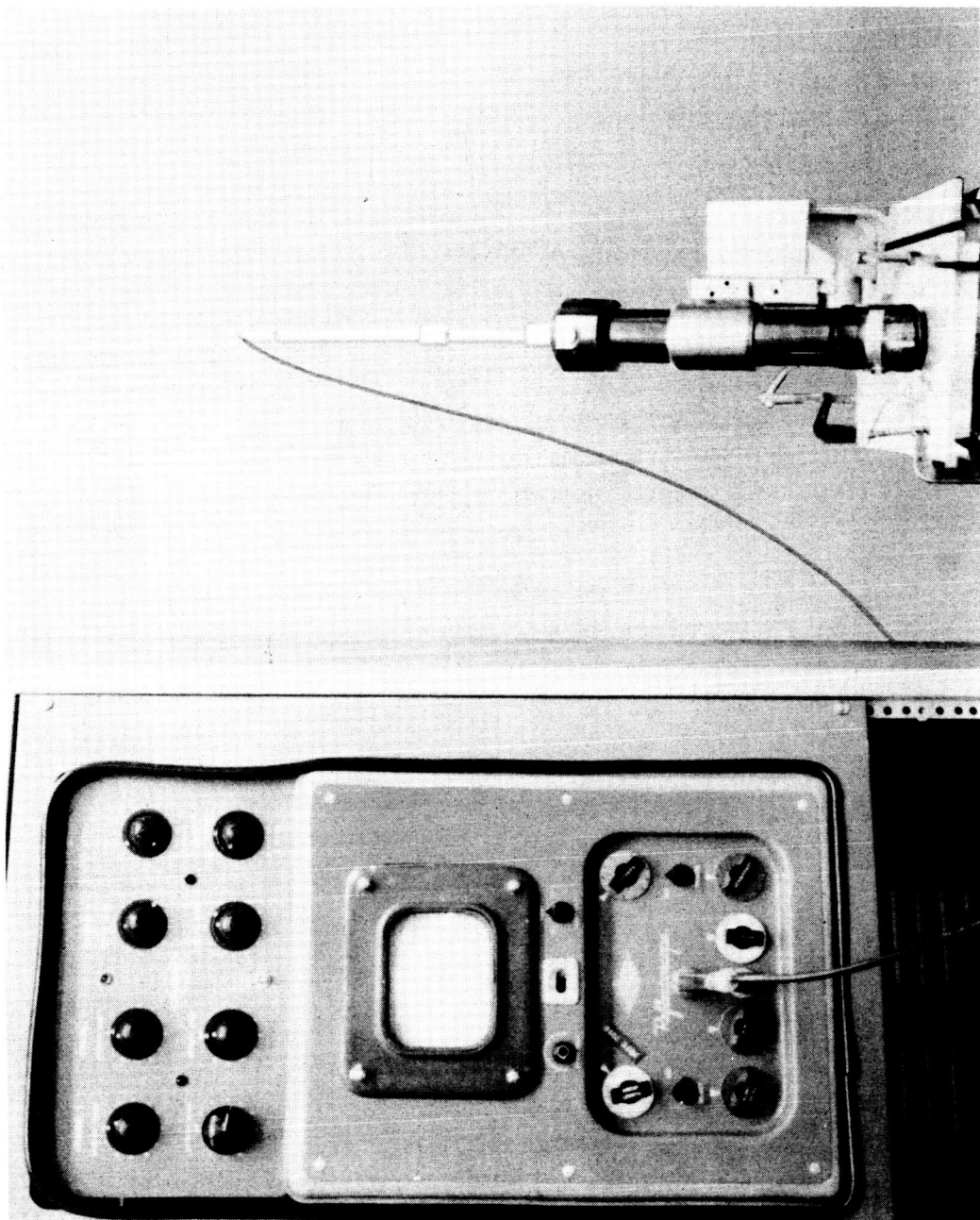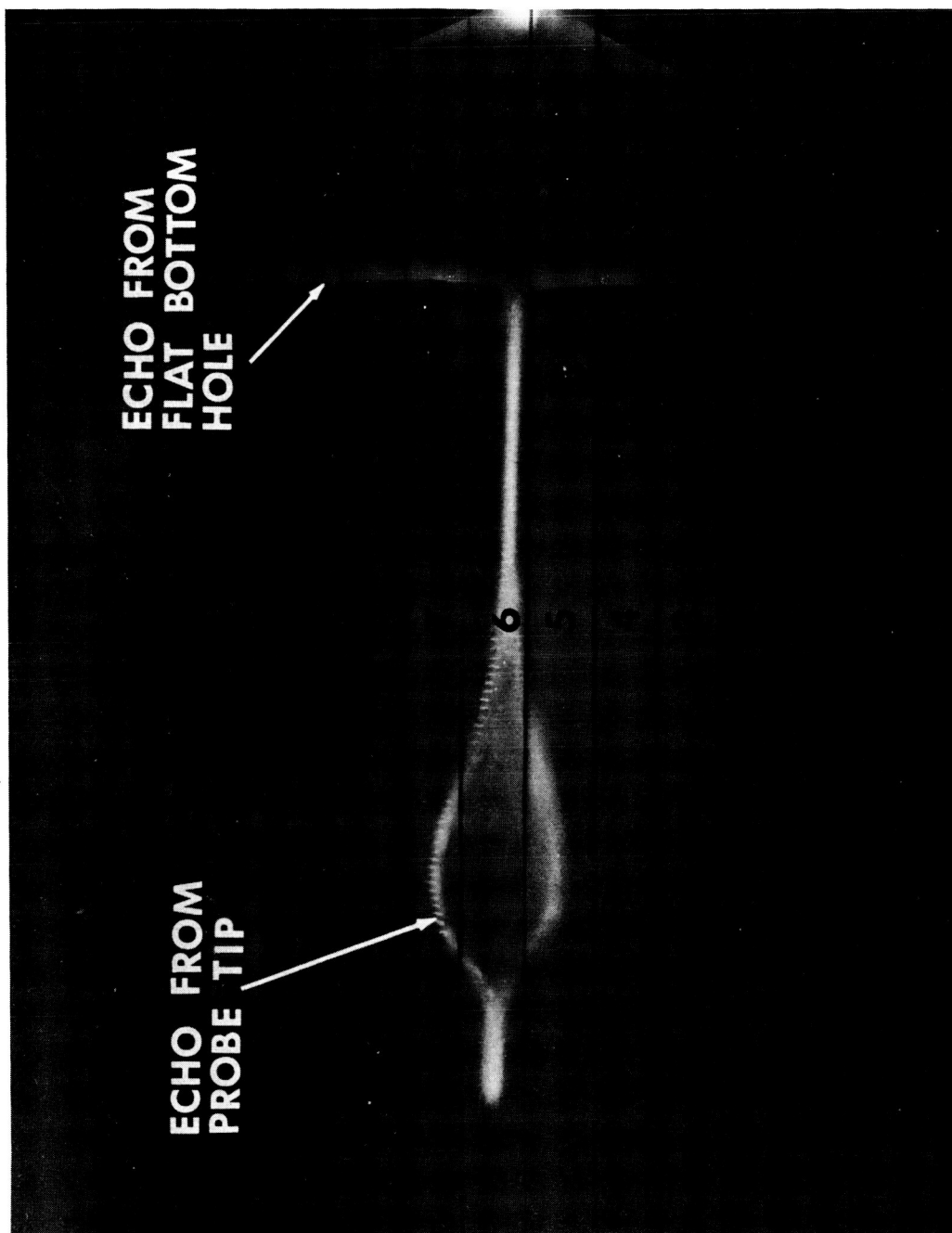
Figure 45.  Equipment Setup for Acoustic Absorber Test

Figure 46. Reflectoscope Display for No Acoustic Absorber

ECHO FROM FLAT BOTTOM HOLE

ECHO FROM PROBE TIP

ECHO FROM
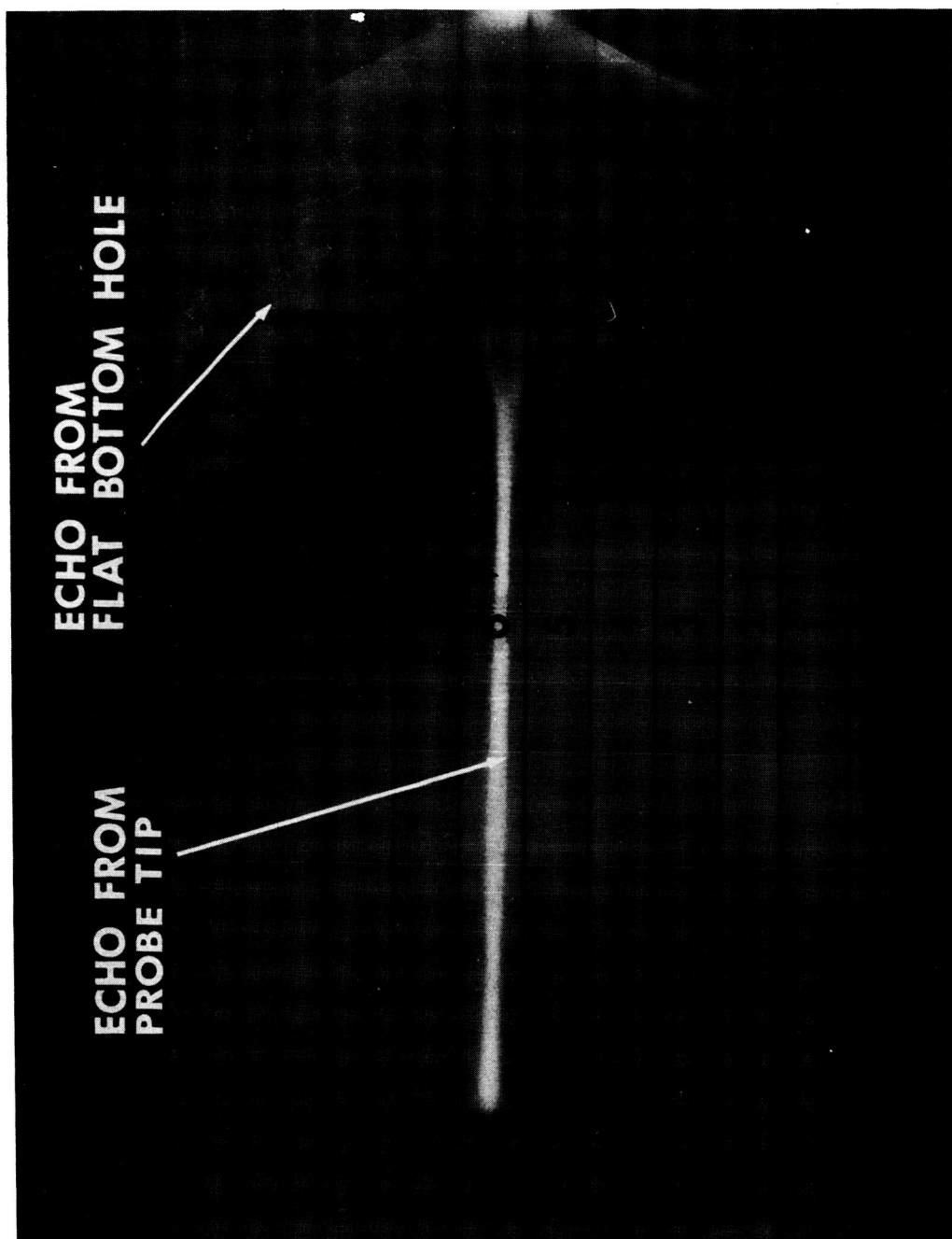FLAT BOTTOM HOLE

ECHO FROM
PROBE TIP

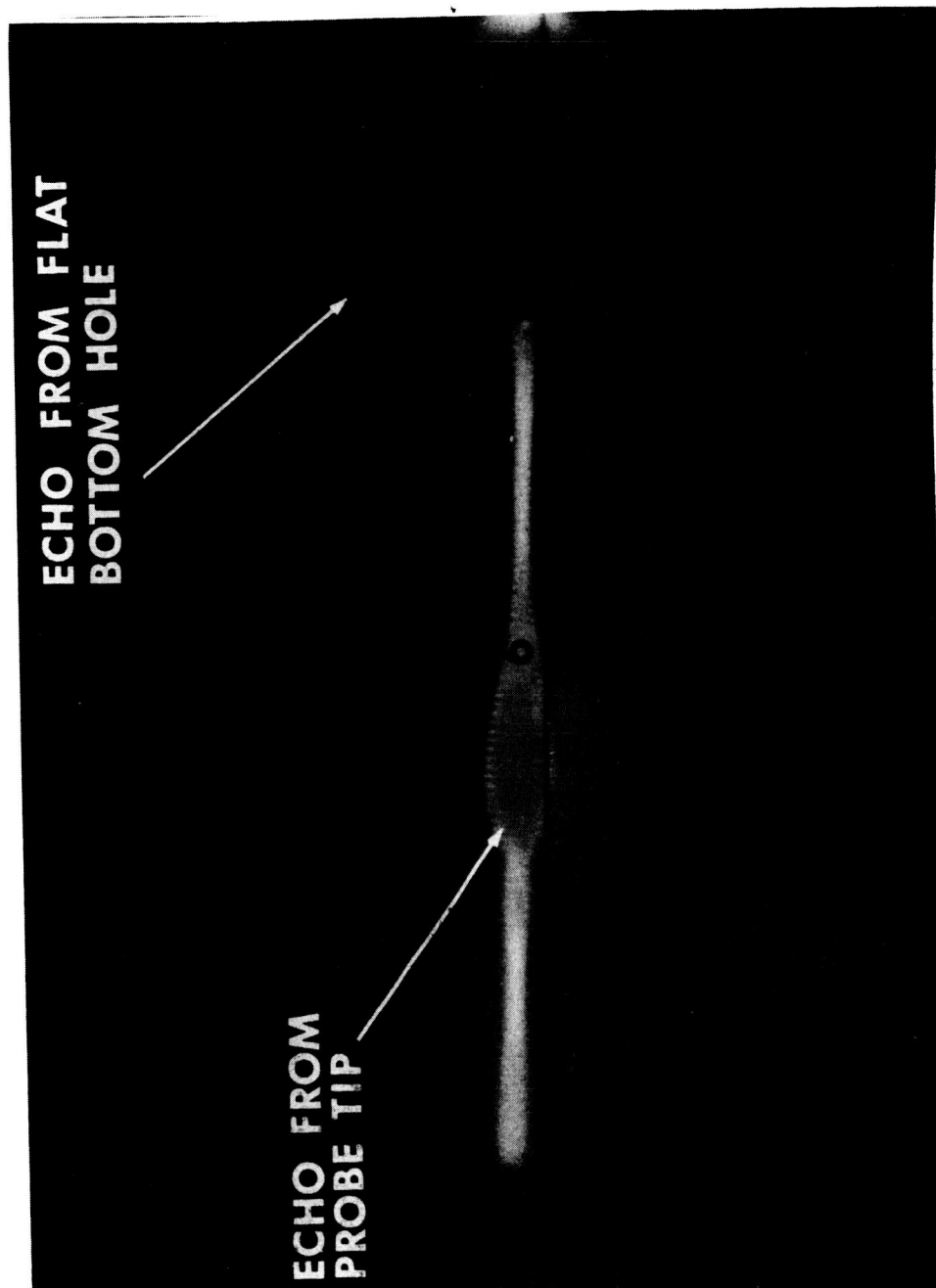Figure 47. Reflectoscope Display for 1/16-Inch Smooth Neoprene as Acoustic Absorber

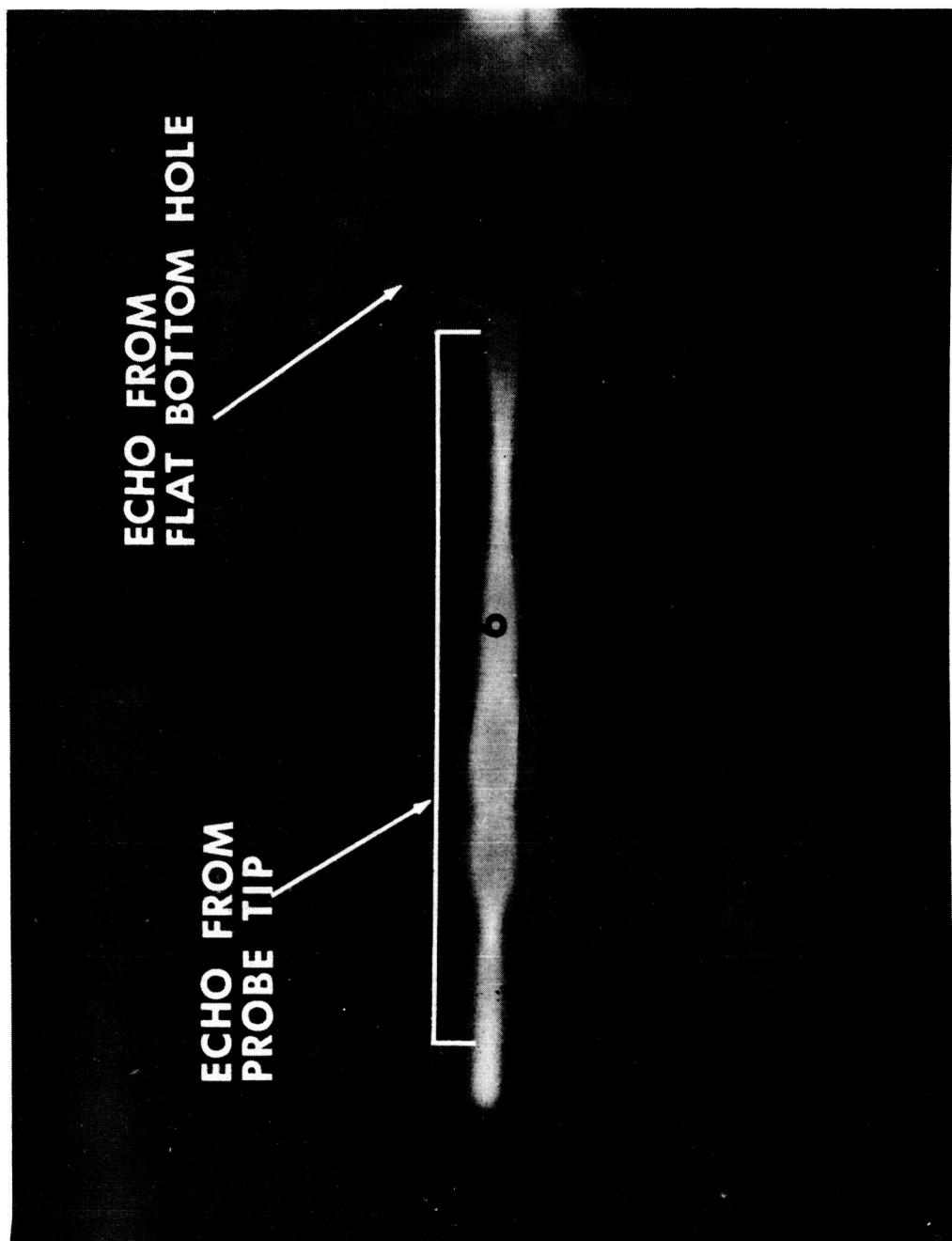Figure 48. Reflectoscope Display for 1/16-Inch Thick Rough Neoprene as Acoustic Absorber

63

Figure 49. Reflectoscope Display for 1/16-Inch Thick Very Rough Neoprene as Acoustic Absorber
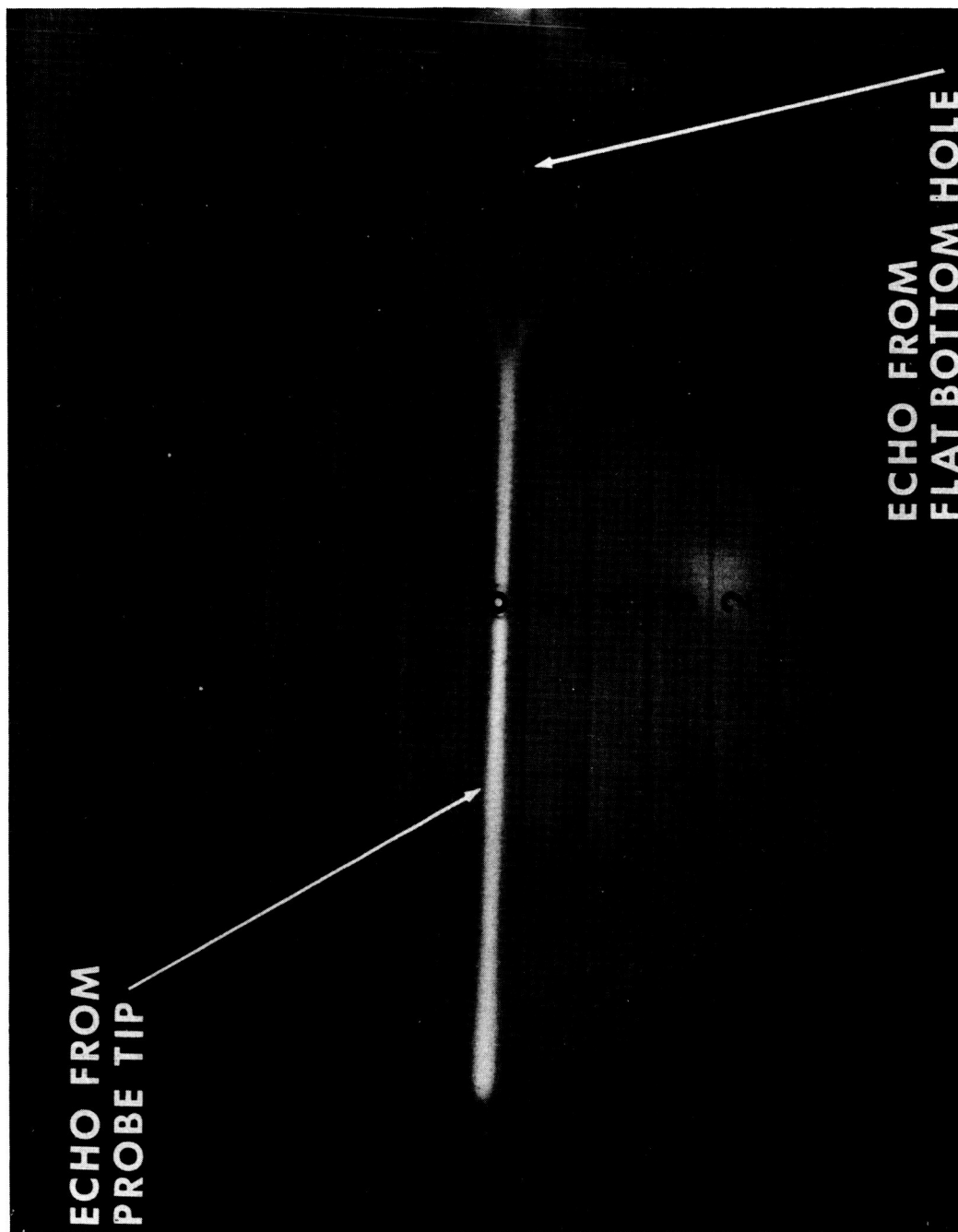
64

Figure 50. Reflectoscope Display for 1/8-Inch Thick Smooth Neoprene as Acoustic Absorber
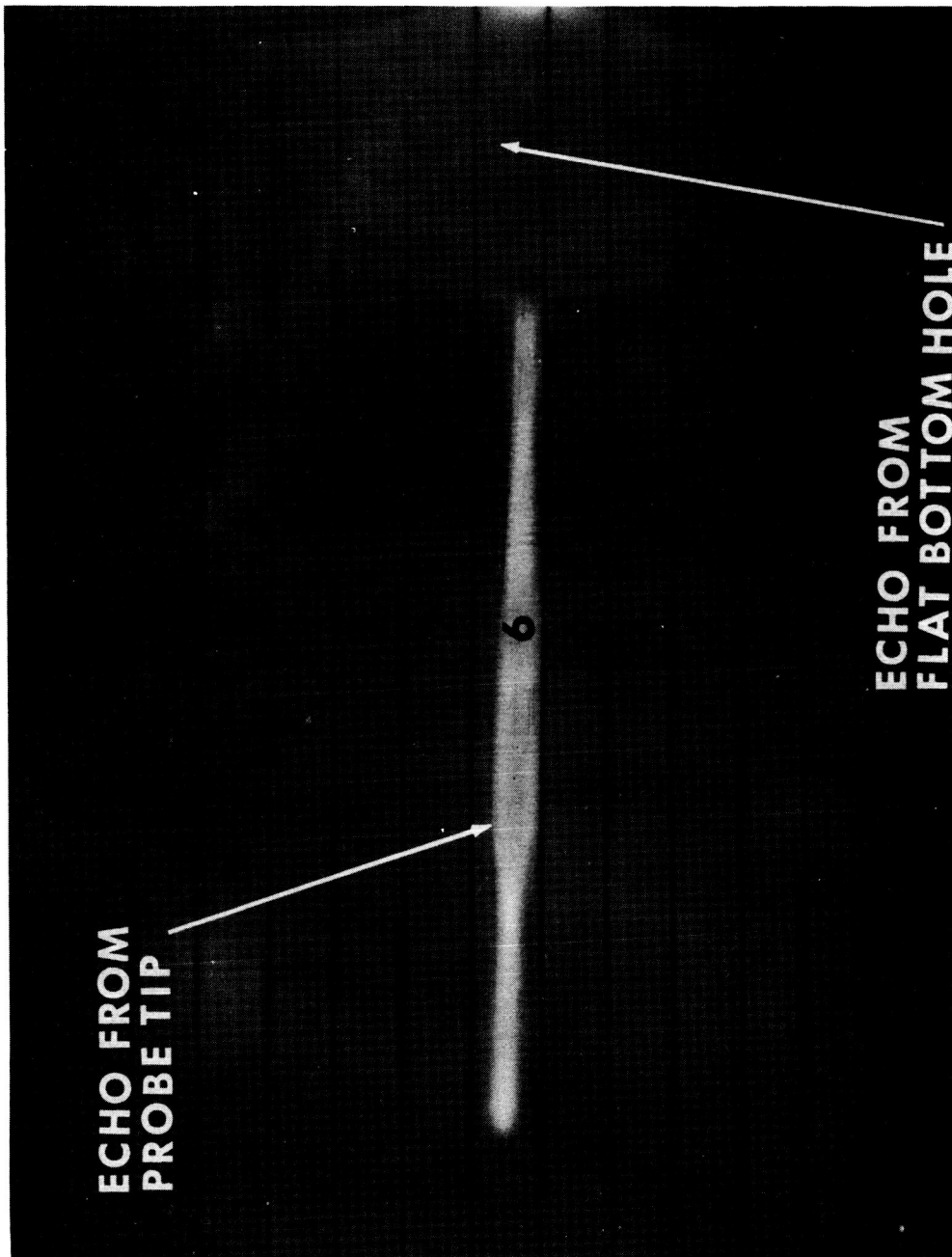
65

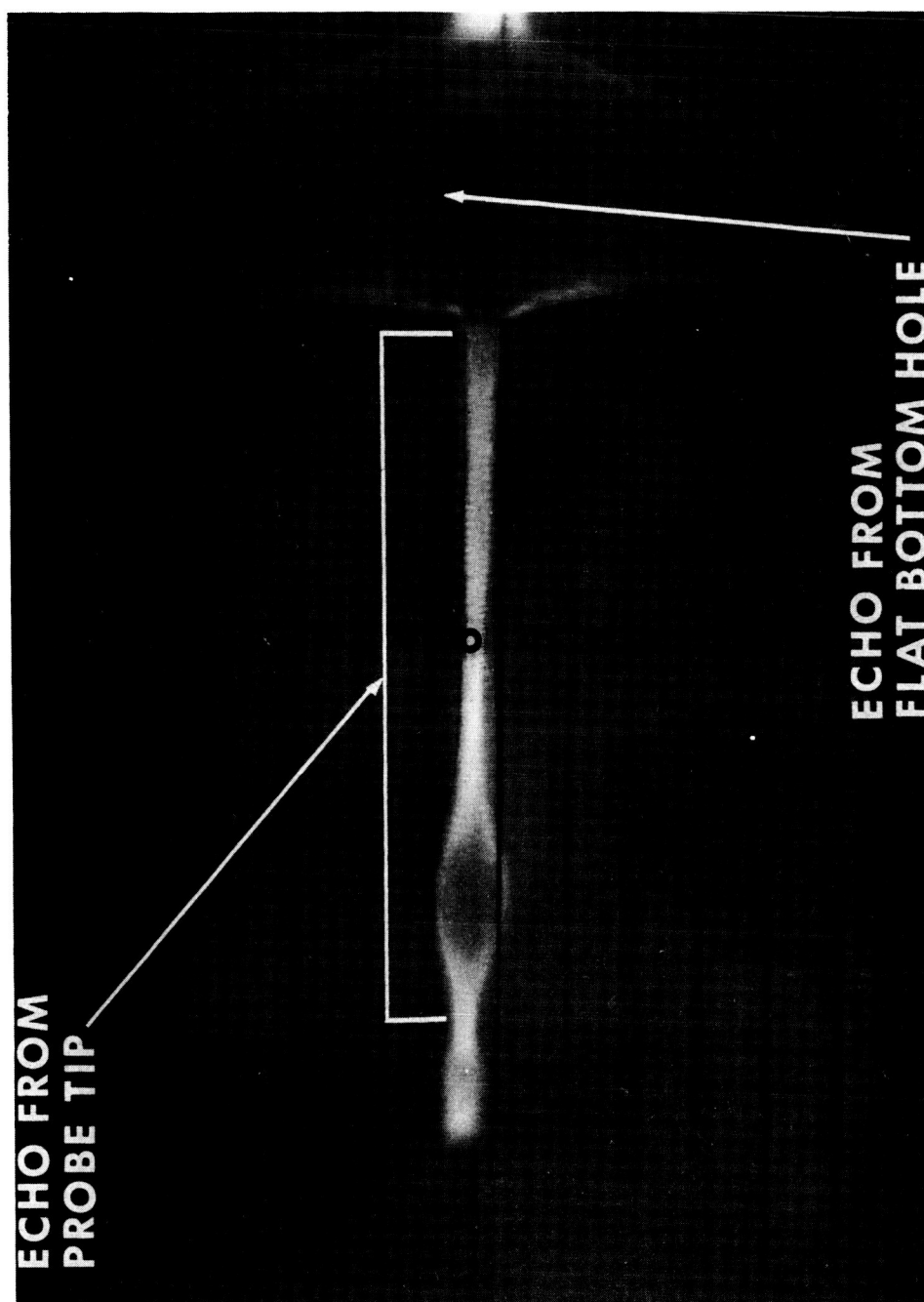Figure 51. Reflectoscope Display for 1/8-Inch Thick Very Rough Neoprene as Acoustic Absorber

ECHO FROM
PROBE TIP

ECHO FROM
FLAT BOTTOM HOLE

Figure 52. Reflectoscope Display for 1/8-Inch Thick Foam Rubber as Acoustic Absorber

67

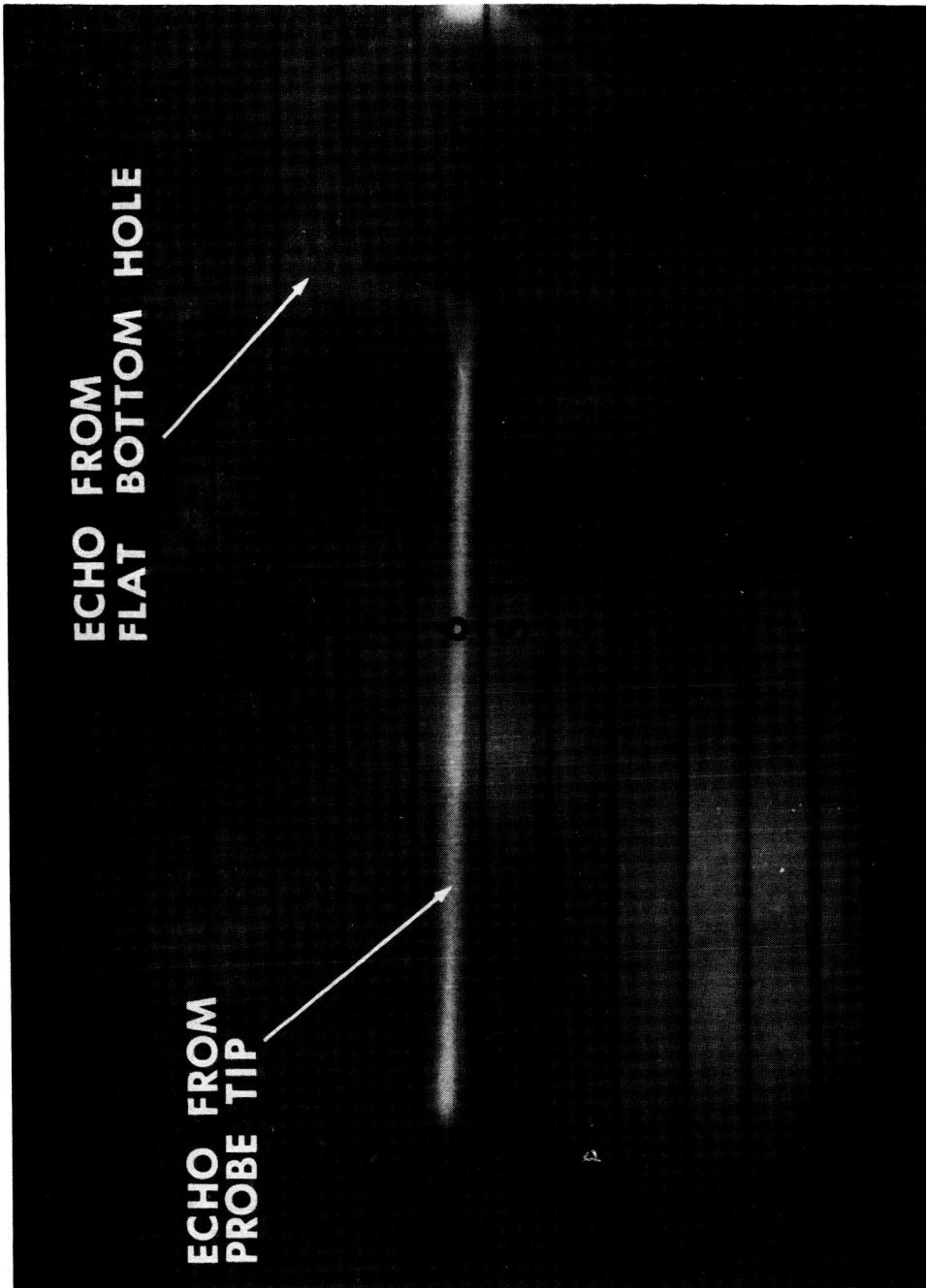ECHO FROM
FLAT BOTTOM HOLE

ECHO FROM
PROBE TIP

Figure 53. Reflectoscope Display for 3/16-Inch (1/8-Inch plus 1/16-Inch) Thick Smooth Neoprene as Acoustic Absorber
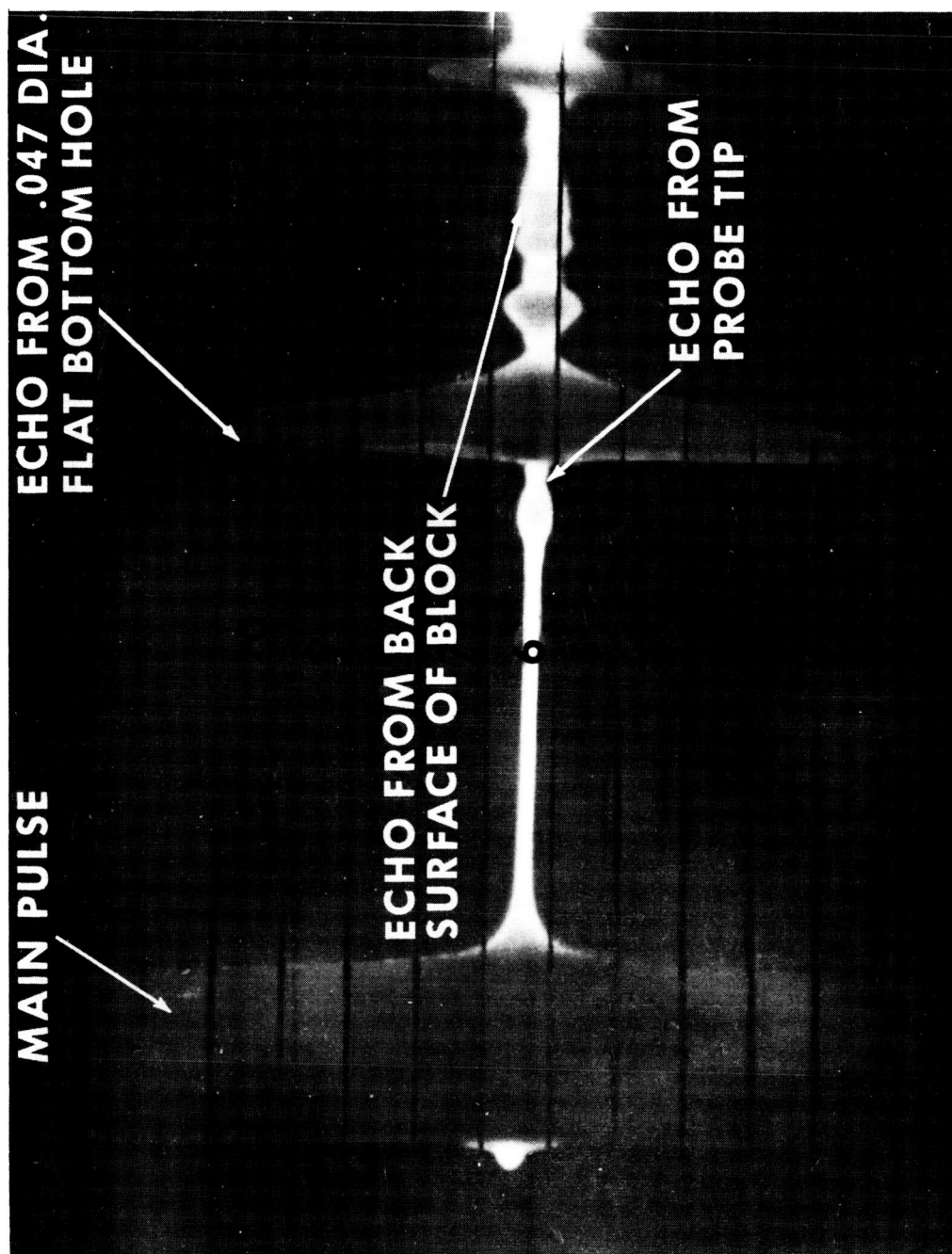
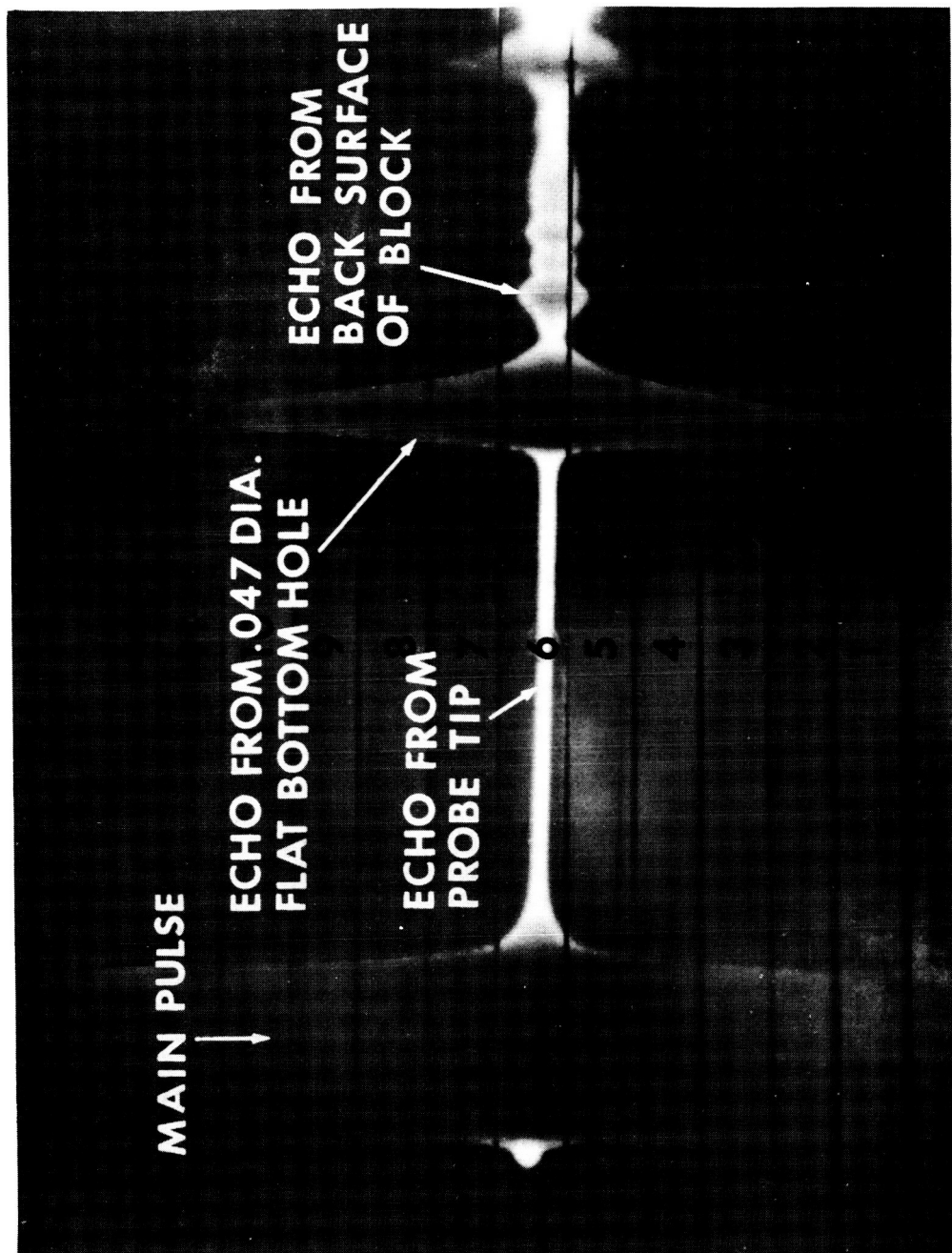Figure 54. Reflectoscope Display for No Acoustic Absorber with Near Field in Metal

Figure 55. Reflectoscope Display for 3/16-Inch (1/8-Inch plus 1/16-Inch) Thick Smooth Neoprene as Acoustic Absorber with Near Field in Metal

70

## B. NEAR FIELD IN WATER COLUMN

It was noted during previous tests that when the transducer probe tip distance was increased a small echo appeared. Although this was not aniticpated by the theoretical analysis (paragraph A, 2), it could have created problems when examining thin materials where the transducer probe tip center distance must be greater than 1.71 inches to be out of the near field. An absorber was then made to simulate a 3/16-inch thick smooth neoprene absorber. This consisted of a 1/8-inch thickness of neoprene as an outside lining and a 1/16-inch thickness of smooth (mold finish) neoprene as the inside lining. The length of the absorber was made with the transducer to probe tip center distance equal to 5.4 inches so that the near field would be confined entirely within the water column probe.

The probe was set up for sensitivity level testing, as shown in figure 45, on the standard angle beam reference plate (figure 33). The photographs shown in figures 56 and 57 were taken of the pulse return display on the reflectoscope. Figure 57 was taken with the absorber installed and figure 56 was taken without the absorber installed in the probe. Comparison of these pulse return displays revealed that the absorber eliminated the extraneous echoes for any useful flaw signal.

The conclusion was reached that in order to eliminate the extraneous echoes, when the transducer to probe tip distance increases, the length of the absorber must also be increased. However, no significant problems are created since the distance is seldom varied and the absorbers are easily fabricated.

## C. COLLIMATION OF BEAM

As observed during testing, the absorber appears to collimate the sound beam rather than absorb it. It is established that use of the absorber causes an increase in amplitude of the reflected pulse. This may be explained by considering the relatively small angle of incidence of the ultrasonic beam to the surface of the absorber. Apparently, the sound waves do not significantly shift from a longitudinal wave, thereby tending to stop the divergence of the beam, and thus collimate the beam. This would tend to make the beam cylindrical in shape rather than conical as would be expected. The minimizing of the beam divergence would then explain the increase in amplitude of the return pulse. A measure of power transmitted in a cylinder of smaller area would result in a stronger signal generated than the same amount of power transmitted
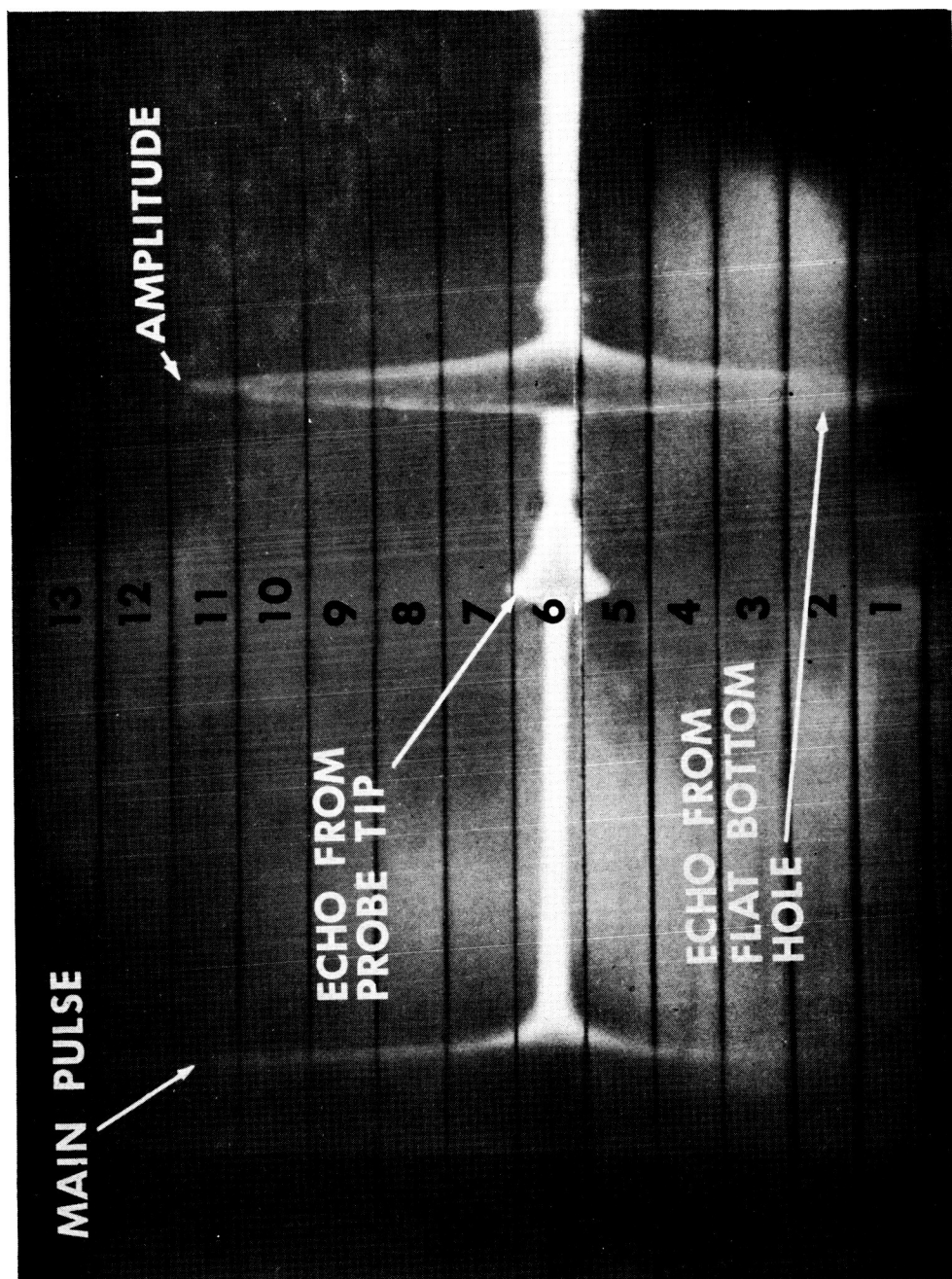
71

Figure 56. Reflectoscope Display for No Acoustic Absorber with Near Field Confined Entirely in Water Column Probe
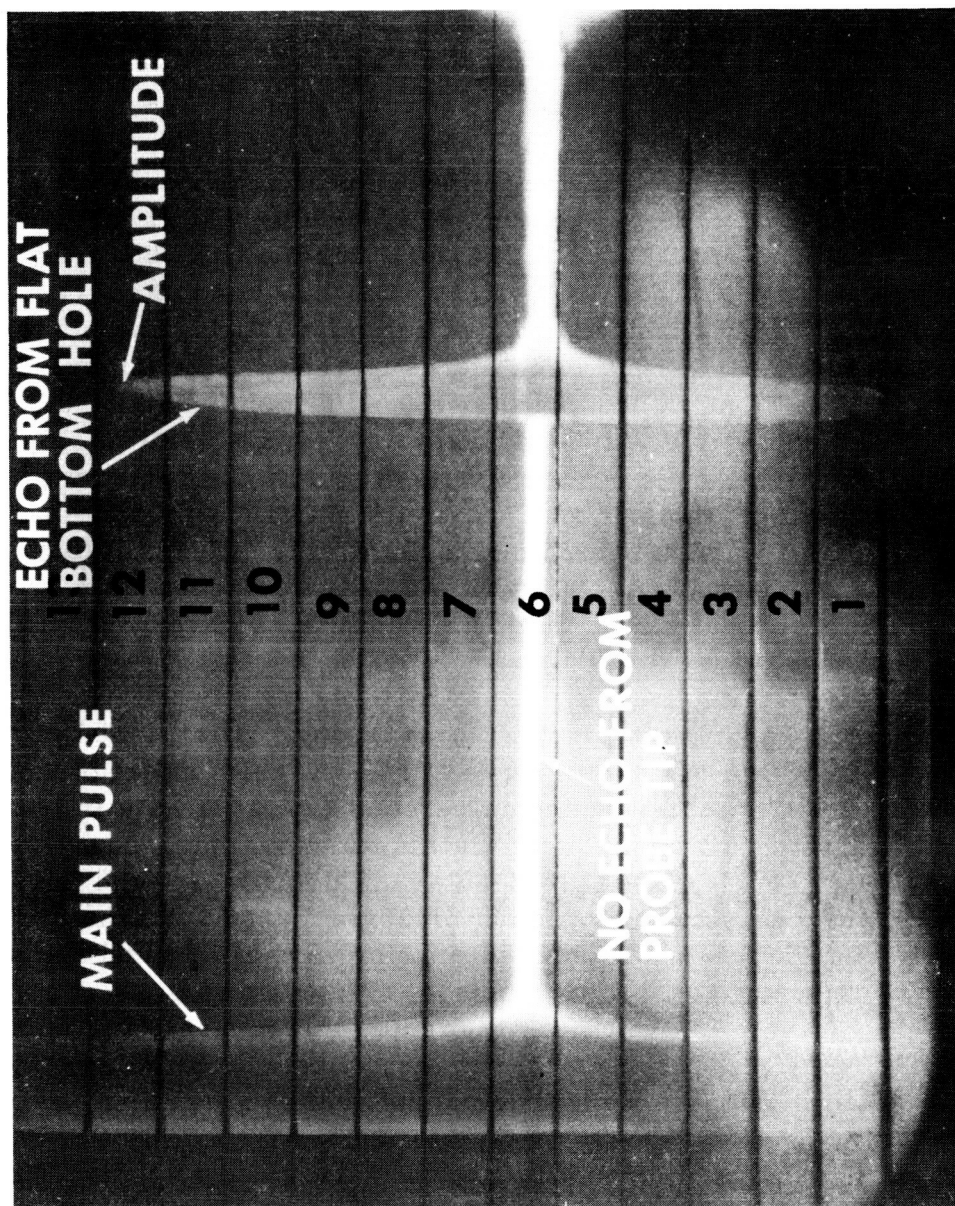
Figure 57.  Reflectoscope Display for 3/16-Inch (1/8-Inch plus 1/16-Inch) Thick Smooth Neoprene as Acoustic Absorber with Near Field Confined Entirely in Water Column Probe

in a cone of larger area. By applying this hypothesis, the conclusion may then be reached that the acoustic absorber, lining the lower portion of the water column probe, has collimated the ultrasonic beam; thus, stronger indications from defects may be obtained.

## D.  BEAM CHARACTERISTICS

1.  <u>General.</u>  The addition of an acoustic absorber did not in any way change the centerline of the beam in the material being tested. However, a variation was noted in the beam size versus depth in the material. Tests to determine the beam size with the acoustic absorber installed are presented in the following paragraphs.

2.  <u>Ultrasonic Beam Size.</u>  To determine the beam size, the setup shown in figure 26 was used. All tests were conducted with the near field confined entirely within the water column probe. The beam size was determined by using reference plates for beam size (figure 8) of different thicknesses; one 0.224-inch, one 0.410-inch, and one 0.608-inch thick. Plate movement was in an X-axis and Y-axis relationship to the probe. All tests for X-axis measurements were conducted with the beam centered over the hole in the Y-axis direction so that the beam width in the X direction was at a maximum. Similarly, all tests for Y-axis measurements were conducted with the beam centered over the hole in the X-axis direction so that the beam width in the Y direction was at a maximum.

By turning the handwheel (figure 26, reference 1) lathe bed travel was effected and the plate was moved in the X-axis direction while observing the CRT display of the pulse echo from the hole in the plate. The readings for full beam width in table 4 were obtained by setting the dial indicator (reference 2) to zero at the point where the pulse echo on the CRT was two small divisions, or 10 percent of the maximum, above the baseline. The plate was moved in the X direction until the pulse reached a maximum and was then returned to the starting level. The distance traveled, as shown by the dial indicator, represents the width of the beam. The readings for the width of the concentrated portion of the beam were taken in the same manner except that the starting and ending points were 10 percent below the maximum pulse amplitude shown on the CRT display.

74

Table 4. Beam Size Versus Depth Test Data Using Improved Probe

| TEST NUMBER | BEAM DEPTH IN MATERIAL | BEAM SIZE | | | |
|---|---|---|---|---|---|
| | | X-AXIS | | Y-AXIS | |
| | | FULL BEAM | CONCEN-TRATED BEAM | FULL BEAM | CONCEN-TRATED BEAM |
| 1 | 0.224 | 0.772 | 0.477 | 0.284 | 0.144 |
| 2 | 0.224 | 0.772 | 0.477 | 0.284 | 0.144 |
| 1 | 0.410 | 0.603 | 0.243 | 0.260 | 0.123 |
| 2 | 0.410 | 0.603 | 0.243 | 0.260 | 0.123 |
| 1 | 0.608 | 0.620 | 0.290 | 0.271 | 0.134 |
| 2 | 0.608 | 0.620 | 0.290 | 0.271 | 0.134 |
| DIMENSIONS IN INCHES | | | | | |

For the Y-axis full beam widths, as shown in table 4, the plate was moved in the same manner as for the X-axis readings except that the lathe crossfeed handwheel (figure 26; reference 3) was used to move the plate. The readings for the width of the concentrated portion of the beam were obtained in the same manner as the X-axis readings.

A plot of the data in table 4, shown in figure 58, shows that both the X-axis and Y-axis beam dimensions decrease in size to a certain depth and then gradually increase in size as the beam depth increases.

3. Weld Coverage by The Ultrasonic Beam with Improved Probe. It is necessary to determine the number of scans required to completely cover the weld in a given thickness of material. Utilizing the size of the beam at a specified depth, the portion of the weld covered by each scan can be determined and a distance (D) from the weld centerline can be specified, as shown in table 3. Figure 59 depicts the number of scans required versus the weld thickness.
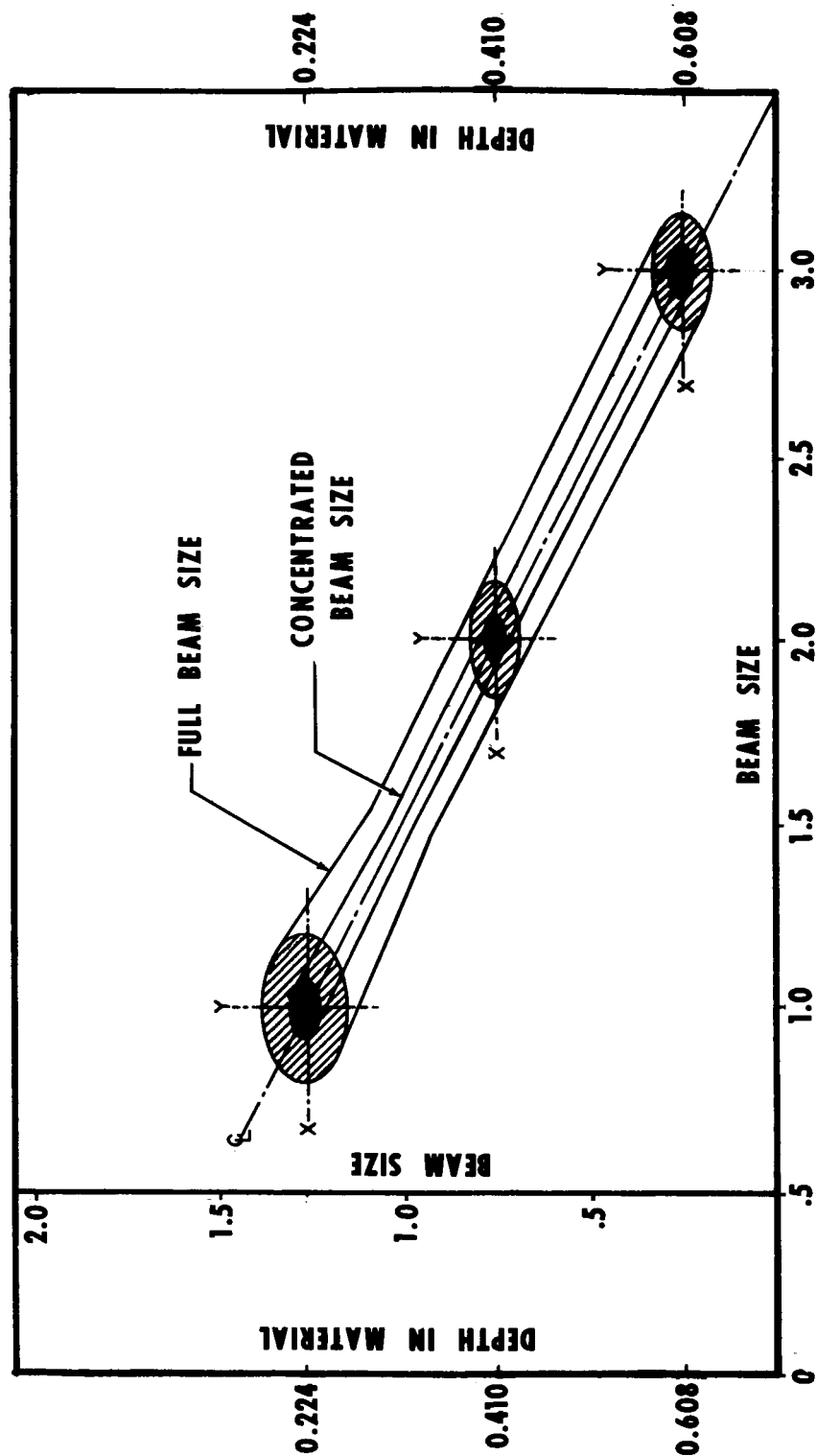
Figure 58.  Beam Size Versus Depth in Material for Improved Probe
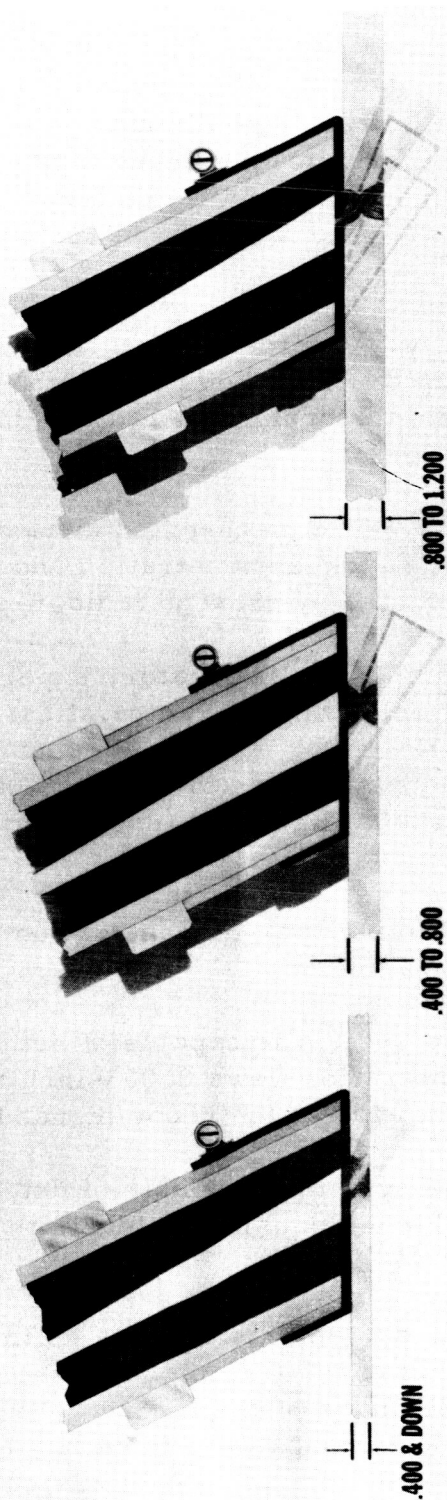
76

ANGLE OF INCIDENCE 26°
ANGLE OF REFRACTION 65°

.400 & DOWN

.400 TO .800

.800 TO 1.200

Figure 59.  Thickness of Material Versus Number of Scans

77

# SECTION VII. CONCLUSIONS AND RECOMMENDATIONS

## A.  CONCLUSIONS

The mechanized ultrasonic scanning system has been evaluated with respect to its performance in the detection of weld flaws, especially lack-of-penetration and lack-of-fusion, in butt-welded aluminum. The following conclusions are given relative to overall performance.

1.  <u>Feasibility</u>.  The mechanized ultrasonic scanning system, employing a simulated immersion pulse-echo technique, is a feasible and economic system to supplement radiography in testing butt-welded aluminum.

2.  <u>Capability</u>.  The mechanized ultrasonic scanning system is capable of detecting lack-of-penetration and lack-of-fusion flaws not presently being detected by present radiographic methods.

3.  <u>Characteristics</u>.  Laboratory experimentation with the system has indicated the following characteristics:

(1)  The system can provide the capability for 100 percent ultrasonic inspection of butt welds.

(2)  The system will increase the capability for detecting lack-of-penetration and lack-of-fusion flaws.

(3)  The system is capable of detecting lack-of-penetration flaws 0.003-inch thick by 0.015-inch wide at the recommended level of sensitivity.

(4)  The system is capable of detecting small flaws at higher sensitivity levels than the recommended level.

(5)  The system has shown a definite relationship between the flaw type and the recorded amplitude shape of the return echo pulse. A lack-of-penetration flaw is normally a flat-topped indication whereas lack-of-fusion is normally a sharp spike and porosity is normally a rounded spike.

## B. RECOMMENDATIONS

The mechanized ultrasonic production scanning system should be utilized to inspect butt-welded aluminum structures on an in-house production basis and at all contractor plants on a production basis.

Techniques and methods for applying the mechanized ultrasonic scanning system for the inspection of welds in materials other than aluminum should be investigated.

Adaptation of a computer system for recording and analyzing the ultrasonic data from the mechanized ultrasonic scanning system should be considered.

Continued investigation should be performed to define the limits of the minimum flaw size detectable, at the higher sensitivity levels, without interference from the granular structure of the material.

# REFERENCES

1. Condon, E. U. and Hugh Odishaw, *Handbook of Physics*, McGraw Hill Book Company, Inc., New York, New York, 1959.

2. Huzfeld, Karl F. and Theodore A. Litovitz, *Absorption and Dispersion of Ultrasonic Waves*, Academic Press, New York, New York, 1959.

3. Jenkins, Francis A. and Harvey E. White, *Fundamentals of Optics*, McGraw Hill Book Company, Inc., New York, New York, 1959.

4. McGonnagle, Warren J., *Nondestructive Testing*, McGraw Hill Book Company, Inc., New York, New York, 1961.

5. McMaster, Robert C., *Nondestructive Testing Handbook*, Ronald Press Company, New York, New York, 1959.

6. Marks, Lionel, *Marks Mechanical Engineering Handbook*, McGraw Hill Book Company, Inc., New York, New York, 1959.

7. Richardson, E. G., *Ultrasonic Physics*, Elsevier Publishing Company, Amsterdam, 1952.

8. Stanford, E. G., and J. H. Fearon, *Progress in Nondestructive Testing*, Volumes 1 and 2, The MacMillan Company, New York, New York, 1960.
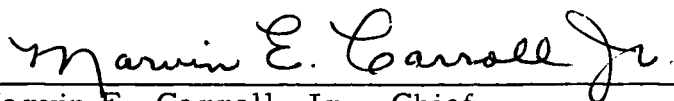
## APPROVAL

## DEVELOPMENT OF MECHANIZED
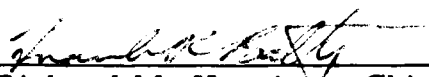## ULTRASONIC SCANNING SYSTEM

By

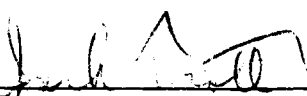Raymond Evans
and
J. A. MacDonald

The information in this report has been reviewed for security classification.  Review of any information concerning Department of Defense or Atomic Energy Commission programs has been made by the MSFC Security Classification Officer.  This report, in its entirety, has been determined to be unclassified.

This document has also been reviewed and approved for technical accuracy.

_____
Marvin E. Carroll, Jr., Chief
Methods and Research Section

_____
Evan S. Hendricks, Chief
Mechanical Analysis Branch

_____
Richard M. Henritze, Chief
Analytical Operations Division

_____
Dieter Grau, Director
Quality and Reliability Assurance Laboratory

81

# DISTRIBUTION

MS-ID, Mr. Garrett

MS-IP, Mr. Ziak

MS-T, Mr. Wiggins (6)
        Mr. Bulette (14)

R-P&VE-MRE, Mr. Hoop

R-P&VE-ME, Mr. Kingsbury

R-P&VE-MM, Mr. Clotfelter

R-P&VE-S, Mr. Verble


R-QUAL-DIR, Mr. Grau

R-QUAL-A, Mr. Batty
            Mr. Henritze

R-QUAL-AE, Mr. Neuschaefer

R-QUAL-AM, Mr. Hendricks

R-QUAL-AMR, Mr. Carroll
            Mr. Johnston
            Mr. Kurtz (3)
            Mr. Beal
            Mr. Barnes (SPACO) (3)

R-QUAL-AMS, Mr. Tillery

R-QUAL-AV, Mr. Allen

R-QUAL-T, Mr. Davis

R-QUAL-J, Mr. Klauss (5)

R-QUAL-OCP, Mr. Krone (3)

R-QUAL-OT, Mr. Phillips

R-QUAL-T, Mr. Smith


R-RP-R, Mr. Miles

MS-H

CC-P

MS-IL (8)

Scientific and Technical Information Facility (25)
P. O. Box 33
College Park, Maryland 20540
Attn: NASA Rep. (SAK-RKT)

Mr. J. Patrick
Chrysler Corp., Space Div.,
P.O. Box 29200
New Orleans, La. 70129

Mr. W. Reaser
Douglas Missile & Space Systems
Div., /Space Systems Center
5301 Bolsa Avenue
Huntington Beach, Calif 92646

Mr. W. Ahern
North American Aviation, Inc.
Space & Information Sys. Div.
11214 South Lakewood Blvd.
Downey, Calif. 90241

Mr. C. Musser
The Boeing Company
Michoud Assembly Facility
Mail Stop LE-43
P.O. Box 29100

Mr. W. Ramminger
Dept. 373, IBM Building #2
150 Sparkman Drive
Huntsville, Alabama 35805

Mr. T. C. Jenkins
Lockheed-Georgia Co.
Quality Engineering
Marietta, Georgia 30061